UNIVERSITY OF CALIFORNIA SAN DIEGO

SAN DIEGO STATE UNIVERSITY

Factors that contribute to Group B *Streptococcus* colonization and disease states

A dissertation submitted in partial satisfaction of the requirements for the degree
Doctor of Philosophy

in

Biology

by

Liwen Deng

Committee in charge:

University of California San Diego

Professor Victor Nizet
Professor Joseph Pogliano

San Diego State University

Professor Scott Kelly, Chair
Professor Kelly Doran, Co-chair
Professor Greg Harris
Professor Roland Wolkowicz

2019

This Dissertation of Liwen Deng is approved, and is acceptable in quality and form for publication on microfilm and electronically:

Co-chair

Chair

University of California San Diego

San Diego State University

2019

DEDICATION

This dissertation is dedicated to my family and friends who have supported me in every way. Thank you.

TABLE OF CONTENTS

LIST OF FIGURES

LIST OF TABLES

LIST OF SUPPLEMENTAL FILES

ACKNOWLEDGEMENTS

First I would like to acknowledge Professor Kelly Doran for her mentorship and guidance during the past 5 years. Thank you for teaching me how to do science and so much more. I have learned more than I ever thought I could.

I would also like to thank my dissertation committee members Dr. Kelley, Dr. Wolkowicz, Dr. Harris, Dr. Nizet, and Dr. Pogliano for their help and advice in my dissertation project.

I would like to thank every member of the Doran lab that I have worked with during my tenure, especially Rong, Thomas, Kati, Brady, Josh, Lindsey, and Paige.

I also have to thank Professor Alex Horswill and members of his lab Katrin, Kuba, Jeff, and Heidi.

I am so grateful to the administrative staff at SDSU, Gina and Patti, for being endlessly helpful and supportive.

Lastly, I would like to thank Jon for his patience, encouragement, and humor. You are the kindest, smartest, and most loving person I know. I couldn't have done it without you.

Chapter 2, in full, is a reprint of the material as it appears in: Deng L, Spencer BL, Holmes JA, Mu R, Rego S, Weston TA, Hu Y, Sanches GF, Yoon S, Park N, Nagao PE, Jenkinson HF, Thornton JA, Seo KS, Nobbs AH, Doran KS. The Group B streptococcal surface antigen I/II protein, BspC, interacts with host vimentin to promote adherence to brain endothelium and inflammation during the pathogenesis of meningitis. *PLoS Pathog*. 15(6). 2019. The dissertation author was the primary investigator and author of this paper.

Chapter 3, in full, is a reprint of the material as it appears in: Deng L, Mu R, Weston TA, Spencer BL, Liles RP, Doran KS. Characterization of a two-component system transcriptional

regulator, LtdR, that impacts Group B streptococcal colonization and disease. *Infect Immun*. 86(7). 2018. The dissertation author was the primary investigator and author of this paper.

Chapter 4, in full, is currently in submission to *mBio*, 2019. Deng L, Schilcher K, Burcham LR, Kwiecinski JM, Johnson PM, Head SR, Heinrichs DE, Horswill AR, Doran KS. Identification of key determinants of *Staphylococcus aureus* vaginal colonization. The dissertation author was the primary investigator and author of this paper.

VITA

2010 Bachelor of Science, University of California San Diego

2019 Doctor of Philosophy, University of California San Diego and San Diego State University

PUBLICATIONS

Deng L, Schilcher K, Burcham LR, Kwiecinski JM, Johnson PM, Head SR, Heinrichs DE, Horswill AR, Doran KS. Importance of fibrinogen binding and iron acquisition to *Staphylococcus aureus* vaginal colonization. Submitted (2019)

Kim BJ, MacDonagh MA, **Deng L**, Gastfriend BD, Schubert-Unkmeir A, Doran KS, Shusta EV. *Streptococcus agalactiae* disrupts P-glycoprotein function in brain endothelial cells. *Fluids Barriers CNS* (2019)

Spencer BL, **Deng L**, Patras KA, Burcham ZM, Sanches GF, Nagao PE, Doran KS. Cas9 contributes to Group B streptococcal colonization and disease. *Front Microbiol* (2019)

Deng L, Spencer BL, Holmes JA, Mu R, Rego S, Weston TA, Hu Y, Sanches GF, Yoon S, Park N, Nagao PE, Jenkinson HF, Thornton JA, Seo KS, Nobbs AH, Doran KS. The Group B Streptococcal surface antigen I/II protein, BspC, interacts with host vimentin to promote adherence to brain endothelium and inflammation during the pathogenesis of meningitis. *PLoS Pathog* (2019)

Deng L, Mu R, Weston TA, Spencer BL, Liles R, Doran KS. Characterization of a two-component system transcriptional regulator LtdR that impacts Group B Streptococcal colonization and disease. *Infect Immun* (2018)

***Deng L**, * Feng Y, *Ma X, Yao B, Xiong Y, We Y, Wang L, Ma Q, Ma F. Role of selectins and their ligands in human implantation stage. *Glycobiology* (2017)

*these authors contributed equally

Ma F, **Deng L**, Secrest P, Shi L, Zhao J, Gagneux P. A mouse model for dietary xenosialitis: antibodies to xenoglycan can reduce fertility. *J Biol Chem* (2016)

Fong JJ, Sreedhara K, **Deng L**, Varki NM, Angata T, Liu Q, Nizet V, Varki A. Immunomodulatory activity of extracellular Hsp70 is mediated via paired receptors Siglec-5 and Siglec-14. *Embo J* (2015)

Gordts PL, Foley EM, Lawrence R, Sinha R, Lameda-Diaz C, **Deng L**, Nock R, Glass CK Erbilgin A, Lusis AJ, Witztum JL, Esko JD. Reducing macrophage proteoglycan sulfation increases atherosclerosis and obesity through enhance type I interferon signaling. *Cell Metab* (2014)

Laubli H, Alisson-Silva F, Stanczak MA, Siddiqui SS, **Deng L**, Verhagen A, Varki NM, Varki A. Lectin galactoside-binding soluble 3 binding protein (LGALS3BP) is a tumor-associated immunomodulatory ligand for CD33-related Siglecs. *J Biol Chem* (2014)

Laubli H, Pearce OMT, Schwarz F, Siddiqui SS, Deng L, Stanczak MA, **Deng L**, Verhagen A, Secrest P, Lusk C, Schwarz AG, Varki NM, Bui JD, Varki A. Engagement of myelomonocytic Siglecs by tumor-associated ligands modulates the innate immune response to cancer. *Proc Natl Acad Sci* (2014)

Ma F, Wu D, **Deng L**, Secrest P, Zhao J, Varki NM, Lindheim S, Gagneux P. Sialidases on mammalian sperm mediate deciduous sialylation during capacitation. *J Biol Chem* (2012)

Wang X, Mitra N, Cruz P, **Deng L**, DISC Comparative Sequencing Program, Varki NM, Angata T, Green E, Mullikin J, Hayakawa T, Varki A. Evolution of Siglec-11 and Siglec-16 genes in hominins. *Mol Biol Evol* (2012)

Wang X, Chow R, **Deng L**, Anderson D, Weidner N, Goldwin AK, Bewtra C, Zlotnik A, Bui JD, Varki A, Varki NM. Expression of Siglec-11 by human and chimpanzee ovarian stromal cells with uniquely human ligands: implications for human ovarian physiology and pathology. *Glycobiology* (2011)

ABSTRACT OF THE DISSERTATION

Factors that influence Group B streptococcal colonization and disease states

by

Liwen Deng

Doctor of Philosophy in Biology

University of California San Diego, 2019

San Diego State University, 2019

Professor Scott Kelley, Chair

Professor Kelly S. Doran, Co-chair

Streptococcus agalactiae (Group B *Streptococcus* [GBS]) is an opportunistic pathogen that normally colonizes healthy adults asymptomatically and is a frequent inhabitant of the vaginal tract in women. However, GBS can cause severe disease when transmitted to newborns. Despite widespread antibiotic prophylaxis administration to colonized mothers, GBS remains a leading cause of neonatal meningitis. Bacterial meningitis is a life-threatening infection of the central nervous system (CNS) and is marked by GBS gaining access to the blood and further by penetration of GBS across the blood-brain barrier (BBB) and activation of host inflammatory responses. Although several GBS surface proteins have been shown to impact bacterial adhesion to endothelium, a direct interaction between a GBS factor and a host endothelial ligand had not been described. Additionally, while it is known that the bacterium tightly regulates its expression of virulence factors in order to occupy various host niches, there are currently many uncharacterized GBS transcriptional regulators. Also, GBS likely competes or cooperates with other resident microbes in the vaginal tract during colonization, however little work has been done to model polymicrobial interactions within this host niche. For this PhD dissertation, I investigated how this bacterium is able to persist in the vagina, transition to an invasive pathogen, disrupt host barriers, and ultimately penetrate into the brain to cause meningitis. I examined a GBS adhesin which promoted bacterial attachment to the brain endothelium and discovered the endothelial receptor for this GBS factor. I also characterized a GBS transcriptional regulator that influenced meningitis as well as GBS vaginal carriage by impacting host immune signaling. Lastly, I developed an *in vivo* vaginal colonization model for another common opportunistic pathogen, *Staphylococcus aureus*, which likely interacts with GBS within this host niche. Using this model, I showed that bacterial interactions with fibrinogen as well as iron uptake are key determinants of vaginal persistence. Taken together, this dissertation furthers our understanding of how GBS

adapts to different host niches in order to transition from asymptomatic colonization to causing invasive inflammatory disease and provides novel insights into GBS disease pathogenesis and treatment strategies to prevent colonization and invasive CNS disease.

Chapter 1

INTRODUCTION

Group B *Streptococcus*

Streptococcus agalactiae (Group B *Streptococcus* [GBS]) is an encapsulated, Gram-positive, chain forming bacterium that commonly colonizes the lower gastrointestinal tract and female reproductive tract in humans (1). GBS was categorized by Rebecca Lancefield as possessing the "Group B" carbohydrate antigen and was originally described as causing mastitis in dairy cows (2, 3). More recently, GBS has emerged as a major cause of invasive infections in humans, especially newborns and immune-compromised individuals (4). Since the 1970s, GBS has been the leading cause bacterial disease in neonates, who can acquire this pathogen through vertical transmission (4-7). GBS infections in newborns are classified as either Early Onset Disease (EOD) or Late Onset Disease (LOD). EOD occurs within the first week of life and is characterized by pneumonia and sepsis, while symptoms of LOD appear a week to six months post birth and the disease more frequently progresses to meningitis (8).

Despite many efforts to develop immunization strategies which target either the GBS capsular polysaccharides or conserved protein antigens, an approved vaccine against GBS does not exist (9-11). In the United States, to reduce the risk of GBS transmission to the newborn, pregnant women are routinely screened for GBS carriage between the 35^{th} and 37^{th} weeks of pregnancy and those who are positive receive intrapartum antibiotic treatment (12). Widespread implementation of antibiotic prophylaxis has drastically reduced the incidence of EOD, from 1.73 per 1000 live births in 1990 to 0.37 per 1000 live births in 2006, however the rates of LOD and meningitis have remained stable (13). Additionally, as pneumococcal meningitis cases have declined rapidly since the introduction of the 13-valent vaccine against *Streptococcus pneumoniae*

in 2010 (14), GBS is currently the most common cause of pediatric bacterial meningitis in the United States, affecting 0.32 per 1000 live births (13, 15).

GBS meningitis disease.

GBS meningitis occurs when bacteria present within the blood spreads into the meninges, which are the protective tissues that surround the central nervous system. There are three meningeal layers: the dura, arachnoid, and pia mater. The dura mater is the thickest and most superficial meningeal layer, and is composed of dense connective tissue. The dura is also heavily vascularized and is the only meningeal layer containing lymphatic vessels (16). The deeper arachnoid and pia layers are collectively known as the leptomeninges, which intimately cover the glia limitans, the outer-most layer of brain and spinal cord nervous tissue formed by astrocytic processes. Cerebrospinal fluid (CSF) is contained within the subarachnoid space of the leptomeninges (16, 17). The structures that separate the blood from central nervous system tissues are the blood-brain barrier (BBB) and the blood-CSF barrier (BCSFB). These barriers are maintained by highly specialized microvascular endothelial cells which possess tight junctions, have high trans-endothelial electrical resistance, lack fenestrations, and function to restrict passage of substances from the blood through to the brain and spinal cord (18-22).

In order to disseminate from the blood into the meningeal and nervous tissues, GBS must first interact with BBB and BCSFB microvascular endothelial cells. An early electron microscopy study showed that GBS can attach to the surface of human brain microvascular endothelial cells (BMEC), invade into these cells, and survive inside the cells contained within vacuoles. In this study, the observation of intracellular GBS inside membrane-bound vacuoles suggested that the bacterium induced endocytic uptake by host cells (23). Subsequent research has identified

numerous GBS virulence factors, including adhesins and invasins, that are important for GBS interactions with BMEC and characterized their effect on host signaling pathways.

Many GBS surface factors are known to interact specifically with extracellular matrix (ECM) components which are present on the surface of BMEC (24). The GBS pilus protein PilA can bind to collagen to promote GBS attachment to BMEC and subsequent uptake into host cells (25, 26). Both the plasminogen-binding surface protein (PbsP) and phosphoglycerate kinase (PGK) are expressed on the GBS cell surface and can engage plasminogen to promote dissemination of the bacterium into the brain (27, 28). Glyceraldehyde 3-phosphate dehydrogenase (GAPDH) is a key enzyme of the glycolytic pathway but is also a GBS surface adhesin. It has been demonstrated to bind to a variety of ECM components including plasminogen, fibrinogen, and laminin (29, 30). Streptococcal fibronectin-binding protein A (SfbA) interacts with fibronectin to promote GBS invasion into BMEC *in vitro* and contributes to meningitis progression *in vivo* (31). Numerous other GBS surface factors, including the serine-rich repeat proteins (Srr1 and Srr2) and the fibrinogen-binding surface proteins (FbsA, FbsB, and FbsC) can adhere to fibrinogen to promote virulence (32-35). The Srr1/2 proteins are similar in structure to *Staphylococcus aureus* clumping factor B (ClfB) and likely engage fibrinogen via a similar "dock, lock, and latch" mechanism (32, 36, 37). Interestingly, while numerous GBS adhesins and invasins have been shown to be important for penetration of the brain endothelial barriers in experimental meningitis models, their identified ligands are all ECM components which can function to bridge a connection between the bacterium and the endothelial cell (38). A direct interaction between a GBS factor and an endothelium specific surface protein has not yet been described.

The host immune response to GBS attachment to and invasion of brain endothelial barriers is a major contributor to neuronal injury and the pathogenesis of meningitis (39). Brain endothelial

cells, microglia, astrocytes, and infiltrating immune cells can all release inflammatory factors and exacerbate neuronal injury beyond direct damage caused by the bacteria (40). Several studies have focused specifically on the immune response of BBB endothelial cells since GBS interacts with this barrier before gaining access to underlying nervous system cells. One microarray analysis of the expression profile of BMEC during GBS infection revealed high induction of genes which promote neutrophil activation such as the cytokines within the CXC family of chemokines like IL-8, the pro-inflammatory cytokine IL-6, and NF-κB pathway components (41). Several GBS virulence factors, such as pili and the beta-hemolysin/cytolysin (β-H/C), have been shown to increase neutrophil recruitment to the meninges and this increase in neutrophil infiltration was associated with worse disease outcome in *in vivo* meningitis models (25, 41).

Vaginal colonization by GBS.

Maternal vaginal carriage of GBS is a major risk factor for transmission to the newborn. In order to successfully colonize the vaginal tract, GBS has to adhere to the epithelial surface, evade clearance by the host immune system, and compete or cooperate with other resident microbes. Many GBS surface factors have been shown to be important for interactions with epithelial cells *in vitro* and/or persistence in *in vivo* animal models of vaginal colonization. These include FbsA and FbsB, Srr1 and Srr2, PilA, the alpha-like proteins, bacterial surface adhesion of GBS (BsaB), BibA, and PbsP (42-48). The expression of these are controlled by various transcriptional regulators, and there is evidence that some of these virulence factors are differentially expressed during persistence in the vagina compared to invasive disease. For example, the expression of BibA is dependent on pH; it is upregulated in neutral environments and repressed in acidic conditions (49). This observation would indicate that BibA is present on the

GBS cell surface during infection of blood or tissues, but may not be highly expressed during vaginal colonization as pH can be low in that host niche.

There have been many studies examining the host immune response to vaginal colonization by GBS. Various innate immune cells have been shown to be activated to promote GBS clearance such as neutrophils, macrophages, and mast cells (50-52). The neutrophil response in particular has been well-characterized and it is influenced by the expression of β-H/C (51, 53). In addition to stimulating the innate immune system, GBS vaginal colonization can also produce an adaptive immune response. Previous work from our group demonstrated that IL-17, a pro-inflammatory cytokine produced by T helper 17 (T_H17) cells, is increased in a mouse model of GBS vaginal colonization and that treatment with recombinant IL-17 promoted GBS clearance. The results of these earlier studies indicate that the ultimate outcome of vaginal colonization by GBS is dependent on both bacterial and host factors.

Polymicrobial interactions likely also influence GBS vaginal carriage, however there are fewer mechanistic studies on this topic. Another notable bacterial inhabitant of the vaginal tract is *Staphylococcus aureus*, which colonizes the vagina in up to 22% of pregnant women. Epidemiological studies indicate that there may be an association between *S. aureus* and GBS during vaginal colonization, with several reports demonstrating the *S. aureus* colonization was more frequent in GBS-positive women than women not colonized by GBS (54-56). Although GBS and *S. aureus* are both commonly found in the lower female reproductive tract during pregnancy and can be transmitted to the neonate with devastating consequences, it is unclear whether colonization with one organism promotes the acquisition and persistence of the other. Before this dissertation, there have not been any experimental examinations of GBS and *S. aureus* co-colonization of the vagina. Investigating interactions between these two common inhabitants of

the vaginal tract would be a reasonable starting point for studying polymicrobial interactions involving GBS, however, *S. aureus* vaginal colonization has never been previously modeled with an *in vivo* system.

Antigen I/II family adhesins promote Streptococcal adherence to host surfaces and inflammation

Antigen I/II (AgI/II) family polypeptides are multifunctional adhesins which are widely distributed among members of the *Streptococcus* genus. Although AgI/II proteins from different *Streptococcus* species vary in size, members of this family share a similar primary sequence comprised of six distinct regions: the N-terminal region which contains the secretion signal, an alanine-rich repeat (A) region, the variable (V) domain, a proline-rich repeat (P) region, the C-terminal region, and the cell-wall anchor which contains the LP*X*TG motif necessary for sortase-mediated attachment to the bacterial surface. The A and P regions of AgI/II proteins form a stalk which extends the V-domain away from the bacterial cell surface. AgI/II genes are well-conserved and most of the variation in sequences between species are clustered in the V-domain (57, 58). The AgI/II protein of *S. mutans*, SpaP or P1 adhesin, was one of the first cell-wall anchored adhesins to be described in Gram positive bacteria (57, 59). The name of this family of proteins is derived from the original observation that SpaP contains two antigenic regions, the "antigen I" and the "antigen II" (60). Since the initial discovery of SpaP in *S. mutans*, AgI/II proteins have been identified in nearly every member of the viridans family of Streptococci which inhabit the human mouth such as SspA and SspB in *S. gordonii*, SoaA in *S. oralis*, PAg and SpaA in *S. sobrinus*, PAa in *S. cricetus*, and Pas in *S. intermedius* (57, 61-65). The AgI/II proteins of oral streptococci have been extensively characterized as important adhesins for promoting bacterial interactions with the

host as well as other microbes within the mouth. Many of these proteins, including SpaP, SspA, and SspB, have been shown to bind specifically to the host innate immunity scavenger receptor glycoprotein-340 (gp-340), which is present in saliva as well as other mucosal secretions (66, 67). In addition to gp-340, AgI/II proteins have been demonstrated to interact with extracellular matrix components such as fibronectin and collagen, and to promote integrin-mediated internalization of oral Streptococci by host endothelial cells (68-70). AgI/II proteins are also important mediators of inter-bacterial adherence and aggregation within the mouth. SspA and SspB from *S. gordonii* can interact with the anaerobic pathogen *Porphyromonas gingivalis*, SspB can also interact with pathogen *Actinomyces naeslundii*, and SpaP from *S. mutans* promotes biofilm formation by the fungal pathogen *Candida albicans* (71-73). Lastly, the immunostimulatory characteristics of these adhesins have inspired numerous studies focused on utilizing AgI/II proteins to develop vaccine therapies to prevent periodontal disease (57, 58, 74-76).

Interestingly, while many strains of *Streptococcus pyogenes* (Group A *Streptococcus*, [GAS]), including the strains belonging to the virulent M1, M12, and M89 M-serotypes, lack an AgI/II homolog, a subset of M-serotypes contain an integrative and conjugative element (ICE) which encodes the AgI/II protein AspA (77). This ICE likely originated from GBS and was acquired by M2, M4, and M28 serotype GAS strains through horizontal gene transfer (78, 79). These particular M-serotypes are highly associated with puerperal sepsis and invasive neonatal infections, and it has been hypothesized that GBS genes contained within the ICE contribute to the enhanced pathogenicity of M2, M4, and M28 GAS serotypes in pregnant and postpartum women as well as newborns (78, 80). AspA can interact with gp-340 to promote GAS biofilm formation and also plays an important role in colonization of the nasopharynx as well as invasive infection of the lower respiratory tract (77, 81).

Four homologs of the Bsp AgI/II proteins (BspA-D), exist in GBS. One strain, NEM316, contains BspA and BspB while other strains have either BspC or BspD (82). BspD is a truncated AgI/II protein which lacks the secretion signal necessary for targeting to the cell membrane by the Sec pathway (82, 83). Previous work has examined the role of the Bsp AgI/II proteins in impacting GBS vaginal colonization. BspA has been shown to bind to gp-340, promote biofilm formation and attachment to vaginal epithelium, and interact with *C. albicans* (82, 84). A subsequent study demonstrated that both BspA and BspC bind to the hypha-specific adhesin Als3 of *C. albicans* and this interaction promotes co-association of both microbes with vaginal epithelial cells *in vitro* (85). However, no studies have investigated the role of GBS AgI/II proteins using *in vivo* infection models. Also, although AgI/II proteins are known to be immunogenic and meningitis disease progression is driven by excessive inflammation, there have not been any investigations on the potential importance of the Bsp proteins on promoting meningitis.

Signaling through two-component systems impacts GBS virulence

Over the course of its disease cycle, GBS has to adapt to very different host microenvironments. In bacteria, the ability to monitor and respond to environmental signals is commonly mediated by signaling through two-component regulatory systems (TCSs) (86, 87). Bacterial TCSs consist of a membrane-bound histidine kinase sensor (HK) and a cognate cytoplasmic response regulator (RR). HKs can sense a variety of signals such as temperature, pH, and the presence of antimicrobial compounds or nutrients. Upon activation by its specific signal, the HK undergoes autophosphorylation at a conserved histidine site, and then transfers this phosphoryl group to the RR. Phosphorylation of the RR induces a conformational change that

alters the DNA-binding capacity of the regulator, affecting expression of downstream gene targets (88).

GBS possesses up to 21 TCSs, a few of which have been well characterized and are known to impact GBS virulence (89, 90). The RgfA/C TCS regulates the expression of FbsA and FbsB to mediate GBS interactions with extracellular matrix components (91). The LiaR transcriptional regulator affects the expression of genes involved in cell wall synthesis in response to the presence of cell wall-active antimicrobial agents (92). The CiaR regulator has been shown to promote GBS survival within brain endothelial cells as well as phagocytic cells, such a neutrophils and macrophages (93). CovR/S (control of virulence regulator/sensor) is the best studied TCS in GBS and has been shown to impact the expression of a many of virulence factors that are important for GBS pathogenesis, such as pili, FbsA, and FbsB, which promote GBS attachment to host surfaces, *cylE*, which impacts the expression of β-H/C, and genes involved in iron uptake, which is important for survival within the host (94-96). The CovR/S system represses expression of these virulence factors, and hypervirulent clinical isolates of GBS containing CovR/S mutations have been identified (97). However, overexpression of virulence factors, especially the β-H/C, has also been associated with decreased persistence during vaginal colonization (53). These findings highlight the importance of TCS regulation in impacting GBS virulence in different host niches.

SPECIFIC AIMS

The purpose of this dissertation is to identify bacterial factors which influence bacterial vaginal colonization as well as the transition to disease states. *I hypothesize that GBS expresses surface factors which promote bacterial interaction with host surfaces, and that the bacterium must tightly regulate these factors in order to successfully colonize the host and to cause disease.*

Specifically, I will assess the ability of the GBS AgI/II protein, BspC, to facilitate GBS interactions with cerebral microvascular endothelial cells during the progression of meningitis. Additionally, I will examine the role of the previously uncharacterized LtdR TCS RR in affecting both GBS meningitis disease and vaginal colonization. Lastly, I will investigate the molecular mechanisms that govern *S. aureus* vaginal colonization. Developing and characterizing an *in vivo* model for *S. aureus* vaginal carriage will be a necessary first step to examining GBS-*S. aureus* interactions within this host niche. To better understand how bacteria can cause invasive disease as well as successfully colonize the female reproductive tract asymptomatically, I will use *in vitro* and murine models to address the following aims:

Aim 1: Characterize the contribution of the cell surface adhesin BspC to inflammation and meningitis.

a. Examine the role of BspC in promoting bacterial adherence to endothelial cells and infiltration into brain tissue.
b. Assess the impact of BspC on the host immune response during meningitis.
c. Identify an endothelial receptor for BspC and characterize the interaction between BspC and its host receptor.

Aim 2: Investigate the role of the LtdR transcriptional regulator in the transition between colonization and disease states.

a. Characterize the impact of LtdR signaling in *in vivo* models of meningitis and vaginal colonization.
b. Determine the effect of LtdR bacterial adherence to and invasion into endothelial and epithelial cells.
c. Identify LtdR-regulated genes that contribute to GBS pathogenicity.

Aim 3: Examine vaginal colonization by *Staphylococcus aureus*.

a. Develop a murine model of *S. aureus* vaginal colonization.

b. Determine the importance of *S. aureus* interactions with host fibrinogen in promoting vaginal persistence.

c. Identify novel determinants of *S. aureus* vaginal colonization.

REFERENCES

1. **Doran KS, Nizet V.** 2004. Molecular pathogenesis of neonatal group B streptococcal infection: no longer in its infancy. Mol Microbiol **54:**23-31.

2. **Lancefield RC.** 1933. A Serological Differentiation of Human and Other Groups of Hemolytic Streptococci. J Exp Med **57:**571-595.

3. **Keefe GP.** 1997. Streptococcus agalactiae mastitis: a review. Can Vet J **38:**429-437.

4. **Raabe VN, Shane AL.** 2019. Group B Streptococcus (Streptococcus agalactiae). Microbiol Spectr **7**.

5. **Stoll BJ, Hansen NI, Sanchez PJ, Faix RG, Poindexter BB, Van Meurs KP, Bizzarro MJ, Goldberg RN, Frantz ID, 3rd, Hale EC, Shankaran S, Kennedy K, Carlo WA, Watterberg KL, Bell EF, Walsh MC, Schibler K, Laptook AR, Shane AL, Schrag SJ, Das A, Higgins RD, Eunice Kennedy Shriver National Institute of Child H, Human Development Neonatal Research N.** 2011. Early onset neonatal sepsis: the burden of group B Streptococcal and E. coli disease continues. Pediatrics **127:**817-826.

6. **Simonsen KA, Anderson-Berry AL, Delair SF, Davies HD.** 2014. Early-onset neonatal sepsis. Clin Microbiol Rev **27:**21-47.

7. **Verani JR, McGee L, Schrag SJ, Division of Bacterial Diseases NCfI, Respiratory Diseases CfDC, Prevention.** 2010. Prevention of perinatal group B streptococcal disease--revised guidelines from CDC, 2010. MMWR Recomm Rep **59:**1-36.

8. **Remington JS, Klein JO.** 2001. Infectious diseases of the fetus and newborn infant, 5th ed. Saunders, Philadelphia.

9. **Song JY, Lim JH, Lim S, Yong Z, Seo HS.** 2018. Progress toward a group B streptococcal vaccine. Hum Vaccin Immunother **14:**2669-2681.

10. **Soto JA, Diaz-Dinamarca DA, Soto DA, Barrientos MJ, Carrion F, Kalergis AM, Vasquez AE.** 2019. Cellular immune response induced by surface immunogenic protein with AbISCO-100 adjuvant vaccination decreases group B Streptococcus vaginal colonization. Mol Immunol **111:**198-204.

11. **Kobayashi M, Vekemans J, Baker CJ, Ratner AJ, Le Doare K, Schrag SJ.** 2016. Group B Streptococcus vaccine development: present status and future considerations, with emphasis on perspectives for low and middle income countries. F1000Res **5:**2355.

12. **Schrag S, Gorwitz R, Fultz-Butts K, Schuchat A.** 2002. Prevention of perinatal group B streptococcal disease. Revised guidelines from CDC. MMWR Recomm Rep **51:**1-22.

13. **Nanduri SA, Petit S, Smelser C, Apostol M, Alden NB, Harrison LH, Lynfield R, Vagnone PS, Burzlaff K, Spina NL, Dufort EM, Schaffner W, Thomas AR, Farley MM, Jain JH, Pondo T, McGee L, Beall BW, Schrag SJ.** 2019. Epidemiology of Invasive Early-Onset and Late-Onset Group B Streptococcal Disease in the United States, 2006 to 2015: Multistate Laboratory and Population-Based Surveillance. JAMA Pediatr **173:**224-233.

14. **Edwards MS, Baker CJ.** 2019. Group B Streptococcal Disease: Interim Prevention at 50 Years and Counting. Clin Infect Dis doi:10.1093/cid/ciz738.

15. **Berardi A, Rossi C, Lugli L, Creti R, Bacchi Reggiani ML, Lanari M, Memo L, Pedna MF, Venturelli C, Perrone E, Ciccia M, Tridapalli E, Piepoli M, Contiero R, Ferrari F, Gbs Prevention Working Group E-R.** 2013. Group B streptococcus late-onset disease: 2003-2010. Pediatrics **131:**e361-368.

16. **Brochner CB, Holst CB, Mollgard K.** 2015. Outer brain barriers in rat and human development. Front Neurosci **9:**75.

17. **Rascher G, Wolburg H.** 1997. The tight junctions of the leptomeningeal blood-cerebrospinal fluid barrier during development. J Hirnforsch **38:**525-540.

18. **Redzic Z.** 2011. Molecular biology of the blood-brain and the blood-cerebrospinal fluid barriers: similarities and differences. Fluids Barriers CNS **8:**3.

19. **Bernacki J, Dobrowolska A, Nierwinska K, Malecki A.** 2008. Physiology and pharmacological role of the blood-brain barrier. Pharmacol Rep **60:**600-622.

20. **Weksler B, Romero IA, Couraud PO.** 2013. The hCMEC/D3 cell line as a model of the human blood brain barrier. Fluids Barriers CNS **10:**16.

21. **Weksler BB, Subileau EA, Perriere N, Charneau P, Holloway K, Leveque M, Tricoire-Leignel H, Nicotra A, Bourdoulous S, Turowski P, Male DK, Roux F,**

Greenwood J, Romero IA, Couraud PO. 2005. Blood-brain barrier-specific properties of a human adult brain endothelial cell line. FASEB J **19:**1872-1874.

22. **Coureuil M, Lecuyer H, Bourdoulous S, Nassif X.** 2017. A journey into the brain: insight into how bacterial pathogens cross blood-brain barriers. Nat Rev Microbiol **15:**149-159.

23. **Nizet V, Kim KS, Stins M, Jonas M, Chi EY, Nguyen D, Rubens CE.** 1997. Invasion of brain microvascular endothelial cells by group B streptococci. Infect Immun **65:**5074-5081.

24. **Baeten KM, Akassoglou K.** 2011. Extracellular matrix and matrix receptors in blood-brain barrier formation and stroke. Dev Neurobiol **71:**1018-1039.

25. **Banerjee A, Kim BJ, Carmona EM, Cutting AS, Gurney MA, Carlos C, Feuer R, Prasadarao NV, Doran KS.** 2011. Bacterial Pili exploit integrin machinery to promote immune activation and efficient blood-brain barrier penetration. Nat Commun **2:**462.

26. **Maisey HC, Hensler M, Nizet V, Doran KS.** 2007. Group B streptococcal pilus proteins contribute to adherence to and invasion of brain microvascular endothelial cells. J Bacteriol **189:**1464-1467.

27. **Buscetta M, Firon A, Pietrocola G, Biondo C, Mancuso G, Midiri A, Romeo L, Galbo R, Venza M, Venza I, Kaminski PA, Gominet M, Teti G, Speziale P, Trieu-Cuot P, Beninati C.** 2016. PbsP, a cell wall-anchored protein that binds plasminogen to promote hematogenous dissemination of group B Streptococcus. Mol Microbiol **101:**27-41.

28. **Boone TJ, Burnham CA, Tyrrell GJ.** 2011. Binding of group B streptococcal phosphoglycerate kinase to plasminogen and actin. Microb Pathog **51:**255-261.

29. **Seifert KN, McArthur WP, Bleiweis AS, Brady LJ.** 2003. Characterization of group B streptococcal glyceraldehyde-3-phosphate dehydrogenase: surface localization, enzymatic activity, and protein-protein interactions. Can J Microbiol **49:**350-356.

30. **Nagarajan R, Sankar S, Ponnuraj K.** 2019. Crystal structure of GAPDH of Streptococcus agalactiae and characterization of its interaction with extracellular matrix molecules. Microb Pathog **127:**359-367.

31. **Mu R, Kim BJ, Paco C, Del Rosario Y, Courtney HS, Doran KS.** 2014. Identification of a group B streptococcal fibronectin binding protein, SfbA, that contributes to invasion of brain endothelium and development of meningitis. Infect Immun **82:**2276-2286.

32. **Six A, Bellais S, Bouaboud A, Fouet A, Gabriel C, Tazi A, Dramsi S, Trieu-Cuot P, Poyart C.** 2015. Srr2, a multifaceted adhesin expressed by ST-17 hypervirulent Group B Streptococcus involved in binding to both fibrinogen and plasminogen. Mol Microbiol **97:**1209-1222.

33. **Seo HS, Mu R, Kim BJ, Doran KS, Sullam PM.** 2012. Binding of glycoprotein Srr1 of Streptococcus agalactiae to fibrinogen promotes attachment to brain endothelium and the development of meningitis. PLoS Pathog **8:**e1002947.

34. **Rosenau A, Martins K, Amor S, Gannier F, Lanotte P, van der Mee-Marquet N, Mereghetti L, Quentin R.** 2007. Evaluation of the ability of Streptococcus agalactiae strains isolated from genital and neonatal specimens to bind to human fibrinogen and correlation with characteristics of the fbsA and fbsB genes. Infect Immun **75:**1310-1317.

35. **Buscetta M, Papasergi S, Firon A, Pietrocola G, Biondo C, Mancuso G, Midiri A, Romeo L, Teti G, Speziale P, Trieu-Cuot P, Beninati C.** 2014. FbsC, a novel fibrinogen-binding protein, promotes Streptococcus agalactiae-host cell interactions. J Biol Chem **289:**21003-21015.

36. **Seo HS, Xiong YQ, Sullam PM.** 2013. Role of the serine-rich surface glycoprotein Srr1 of Streptococcus agalactiae in the pathogenesis of infective endocarditis. PLoS One **8:**e64204.

37. **Walsh EJ, O'Brien LM, Liang X, Hook M, Foster TJ.** 2004. Clumping factor B, a fibrinogen-binding MSCRAMM (microbial surface components recognizing adhesive matrix molecules) adhesin of Staphylococcus aureus, also binds to the tail region of type I cytokeratin 10. J Biol Chem **279:**50691-50699.

38. **Doran KS, Fulde M, Gratz N, Kim BJ, Nau R, Prasadarao N, Schubert-Unkmeir A, Tuomanen EI, Valentin-Weigand P.** 2016. Host-pathogen interactions in bacterial meningitis. Acta Neuropathol **131:**185-209.

39. **Putz K, Hayani K, Zar FA.** 2013. Meningitis. Prim Care **40:**707-726.

40. **Kim KS.** 2003. Pathogenesis of bacterial meningitis: from bacteraemia to neuronal injury. Nat Rev Neurosci **4:**376-385.

41. **Doran KS, Liu GY, Nizet V.** 2003. Group B streptococcal beta-hemolysin/cytolysin activates neutrophil signaling pathways in brain endothelium and contributes to development of meningitis. J Clin Invest **112:**736-744.

42. **Schubert A, Zakikhany K, Pietrocola G, Meinke A, Speziale P, Eikmanns BJ, Reinscheid DJ.** 2004. The fibrinogen receptor FbsA promotes adherence of Streptococcus agalactiae to human epithelial cells. Infect Immun **72:**6197-6205.

43. **Gutekunst H, Eikmanns BJ, Reinscheid DJ.** 2004. The novel fibrinogen-binding protein FbsB promotes Streptococcus agalactiae invasion into epithelial cells. Infect Immun **72:**3495-3504.

44. **Wang NY, Patras KA, Seo HS, Cavaco CK, Rosler B, Neely MN, Sullam PM, Doran KS.** 2014. Group B streptococcal serine-rich repeat proteins promote interaction with fibrinogen and vaginal colonization. J Infect Dis **210:**982-991.

45. **Bodaszewska-Lubas M, Brzychczy-Wloch M, Adamski P, Gosiewski T, Strus M, Heczko PB.** 2013. Adherence of group B streptococci to human rectal and vaginal epithelial cell lines in relation to capsular polysaccharides as well as alpha-like protein genes - pilot study. Pol J Microbiol **62:**85-90.

46. **Jiang S, Wessels MR.** 2014. BsaB, a novel adherence factor of group B Streptococcus. Infect Immun **82:**1007-1016.

47. **Santi I, Scarselli M, Mariani M, Pezzicoli A, Masignani V, Taddei A, Grandi G, Telford JL, Soriani M.** 2007. BibA: a novel immunogenic bacterial adhesin contributing to group B Streptococcus survival in human blood. Mol Microbiol **63:**754-767.

48. **De Gaetano GV, Pietrocola G, Romeo L, Galbo R, Lentini G, Giardina M, Biondo C, Midiri A, Mancuso G, Venza M, Venza I, Firon A, Trieu-Cuot P, Teti G, Speziale P, Beninati C.** 2018. The Streptococcus agalactiae cell wall-anchored protein PbsP mediates adhesion to and invasion of epithelial cells by exploiting the host vitronectin/alphav integrin axis. Mol Microbiol **110:**82-94.

49. **Santi I, Grifantini R, Jiang SM, Brettoni C, Grandi G, Wessels MR, Soriani M.** 2009. CsrRS regulates group B Streptococcus virulence gene expression in response to environmental pH: a new perspective on vaccine development. J Bacteriol **191:**5387-5397.

50. **Patras KA, Rosler B, Thoman ML, Doran KS.** 2015. Characterization of host immunity during persistent vaginal colonization by Group B Streptococcus. Mucosal Immunol **8:**1339-1348.

51. **Carey AJ, Tan CK, Mirza S, Irving-Rodgers H, Webb RI, Lam A, Ulett GC.** 2014. Infection and cellular defense dynamics in a novel 17beta-estradiol murine model of chronic human group B streptococcus genital tract colonization reveal a role for hemolysin in persistence and neutrophil accumulation. J Immunol **192:**1718-1731.

52. **Gendrin C, Vornhagen J, Ngo L, Whidbey C, Boldenow E, Santana-Ufret V, Clauson M, Burnside K, Galloway DP, Adams Waldorf KM, Piliponsky AM, Rajagopal L.** 2015. Mast cell degranulation by a hemolytic lipid toxin decreases GBS colonization and infection. Sci Adv **1:**e1400225.

53. **Patras KA, Wang NY, Fletcher EM, Cavaco CK, Jimenez A, Garg M, Fierer J, Sheen TR, Rajagopal L, Doran KS.** 2013. Group B Streptococcus CovR regulation modulates host immune signalling pathways to promote vaginal colonization. Cell Microbiol **15:**1154-1167.

54. **Chen KT, Huard RC, Della-Latta P, Saiman L.** 2006. Prevalence of methicillin-sensitive and methicillin-resistant Staphylococcus aureus in pregnant women. Obstet Gynecol **108:**482-487.

55. **Andrews WW, Schelonka R, Waites K, Stamm A, Cliver SP, Moser S.** 2008. Genital tract methicillin-resistant Staphylococcus aureus: risk of vertical transmission in pregnant women. Obstet Gynecol **111:**113-118.

56. **Kubota T, Nojima M, Itoh S.** 2002. Vaginal bacterial flora of pregnant women colonized with group B streptococcus. J Infect Chemother **8:**326-330.

57. **Brady LJ, Maddocks SE, Larson MR, Forsgren N, Persson K, Deivanayagam CC, Jenkinson HF.** 2010. The changing faces of Streptococcus antigen I/II polypeptide family adhesins. Mol Microbiol **77:**276-286.

58. **Jenkinson HF, Demuth DR.** 1997. Structure, function and immunogenicity of streptococcal antigen I/II polypeptides. Mol Microbiol **23:**183-190.

59. **Russell MW, Lehner T.** 1978. Characterisation of antigens extracted from cells and culture fluids of Streptococcus mutans serotype c. Arch Oral Biol **23:**7-15.

60. **Russell MW, Bergmeier LA, Zanders ED, Lehner T.** 1980. Protein antigens of Streptococcus mutans: purification and properties of a double antigen and its protease-resistant component. Infect Immun **28:**486-493.

61. **Demuth DR, Duan Y, Brooks W, Holmes AR, McNab R, Jenkinson HF.** 1996. Tandem genes encode cell-surface polypeptides SspA and SspB which mediate adhesion of the oral bacterium Streptococcus gordonii to human and bacterial receptors. Mol Microbiol **20:**403-413.

62. **Ma JK, Kelly CG, Munro G, Whiley RA, Lehner T.** 1991. Conservation of the gene encoding streptococcal antigen I/II in oral streptococci. Infect Immun **59:**2686-2694.

63. **LaPolla RJ, Haron JA, Kelly CG, Taylor WR, Bohart C, Hendricks M, Pyati JP, Graff RT, Ma JK, Lehner T.** 1991. Sequence and structural analysis of surface protein antigen I/II (SpaA) of Streptococcus sobrinus. Infect Immun **59:**2677-2685.

64. **Tamura H, Kikuchi T, Shirato R, Kato H.** 2001. Cloning and DNA sequencing of the surface protein antigen I/II (PAa) of Streptococcus cricetus. FEMS Microbiol Lett **196:**251-256.

65. **Petersen FC, Pasco S, Ogier J, Klein JP, Assev S, Scheie AA.** 2001. Expression and functional properties of the Streptococcus intermedius surface protein antigen I/II. Infect Immun **69:**4647-4653.

66. **Leito JT, Ligtenberg AJ, Nazmi K, de Blieck-Hogervorst JM, Veerman EC, Nieuw Amerongen AV.** 2008. A common binding motif for various bacteria of the bacteria-binding peptide SRCRP2 of DMBT1/gp-340/salivary agglutinin. Biol Chem **389:**1193-1200.

67. **Loimaranta V, Jakubovics NS, Hytonen J, Finne J, Jenkinson HF, Stromberg N.** 2005. Fluid- or surface-phase human salivary scavenger protein gp340 exposes different bacterial recognition properties. Infect Immun **73:**2245-2252.

68. **Petersen FC, Assev S, van der Mei HC, Busscher HJ, Scheie AA.** 2002. Functional variation of the antigen I/II surface protein in Streptococcus mutans and Streptococcus intermedius. Infect Immun **70:**249-256.

69. **Heddle C, Nobbs AH, Jakubovics NS, Gal M, Mansell JP, Dymock D, Jenkinson HF.** 2003. Host collagen signal induces antigen I/II adhesin and invasin gene expression in oral Streptococcus gordonii. Mol Microbiol **50:**597-607.

70. **Nobbs AH, Shearer BH, Drobni M, Jepson MA, Jenkinson HF.** 2007. Adherence and internalization of Streptococcus gordonii by epithelial cells involves beta1 integrin recognition by SspA and SspB (antigen I/II family) polypeptides. Cell Microbiol **9:**65-83.

71. **Daep CA, James DM, Lamont RJ, Demuth DR.** 2006. Structural characterization of peptide-mediated inhibition of Porphyromonas gingivalis biofilm formation. Infect Immun **74:**5756-5762.

72. **Jakubovics NS, Kerrigan SW, Nobbs AH, Stromberg N, van Dolleweerd CJ, Cox DM, Kelly CG, Jenkinson HF.** 2005. Functions of cell surface-anchored antigen I/II family and Hsa polypeptides in interactions of Streptococcus gordonii with host receptors. Infect Immun **73:**6629-6638.

73. **Yang C, Scoffield J, Wu R, Deivanayagam C, Zou J, Wu H.** 2018. Antigen I/II mediates interactions between Streptococcus mutans and Candida albicans. Mol Oral Microbiol **33:**283-291.

74. **Robinette RA, Heim KP, Oli MW, Crowley PJ, McArthur WP, Brady LJ.** 2014. Alterations in immunodominance of Streptococcus mutans AgI/II: lessons learned from immunomodulatory antibodies. Vaccine **32:**375-382.

75. **Robinette RA, Oli MW, McArthur WP, Brady LJ.** 2011. A therapeutic anti-Streptococcus mutans monoclonal antibody used in human passive protection trials influences the adaptive immune response. Vaccine **29:**6292-6300.

76. **Andrian E, Qi G, Wang J, Halperin SA, Lee SF.** 2012. Role of surface proteins SspA and SspB of Streptococcus gordonii in innate immunity. Microbiology **158:**2099-2106.

77. **Franklin L, Nobbs AH, Bricio-Moreno L, Wright CJ, Maddocks SE, Sahota JS, Ralph J, O'Connor M, Jenkinson HF, Kadioglu A.** 2013. The AgI/II family adhesin AspA is required for respiratory infection by Streptococcus pyogenes. PLoS One **8:**e62433.

78. **Green NM, Zhang S, Porcella SF, Nagiec MJ, Barbian KD, Beres SB, LeFebvre RB, Musser JM.** 2005. Genome sequence of a serotype M28 strain of group a streptococcus: potential new insights into puerperal sepsis and bacterial disease specificity. J Infect Dis **192:**760-770.

79. **Sitkiewicz I, Green NM, Guo N, Mereghetti L, Musser JM.** 2011. Lateral gene transfer of streptococcal ICE element RD2 (region of difference 2) encoding secreted proteins. BMC Microbiol **11:**65.

80. **Areschoug T, Carlsson F, Stalhammar-Carlemalm M, Lindahl G.** 2004. Host-pathogen interactions in Streptococcus pyogenes infections, with special reference to puerperal fever and a comment on vaccine development. Vaccine **22 Suppl 1:**S9-S14.

81. **Maddocks SE, Wright CJ, Nobbs AH, Brittan JL, Franklin L, Stromberg N, Kadioglu A, Jepson MA, Jenkinson HF.** 2011. Streptococcus pyogenes antigen I/II-family polypeptide AspA shows differential ligand-binding properties and mediates biofilm formation. Mol Microbiol **81:**1034-1049.

82. **Chuzeville S, Dramsi S, Madec JY, Haenni M, Payot S.** 2015. Antigen I/II encoded by integrative and conjugative elements of Streptococcus agalactiae and role in biofilm formation. Microb Pathog **88:**1-9.

83. **Schneewind O, Missiakas DM.** 2012. Protein secretion and surface display in Gram-positive bacteria. Philos Trans R Soc Lond B Biol Sci **367:**1123-1139.

84. **Rego S, Heal TJ, Pidwill GR, Till M, Robson A, Lamont RJ, Sessions RB, Jenkinson HF, Race PR, Nobbs AH.** 2016. Structural and Functional Analysis of Cell Wall-anchored Polypeptide Adhesin BspA in Streptococcus agalactiae. J Biol Chem **291:**15985-16000.

85. **Pidwill GR, Rego S, Jenkinson HF, Lamont RJ, Nobbs AH.** 2018. Coassociation between Group B Streptococcus and Candida albicans Promotes Interactions with Vaginal Epithelium. Infect Immun **86**.

86. **Beier D, Gross R.** 2006. Regulation of bacterial virulence by two-component systems. Curr Opin Microbiol **9:**143-152.

87. **Bassler BL, Losick R.** 2006. Bacterially speaking. Cell **125:**237-246.

88. **Zschiedrich CP, Keidel V, Szurmant H.** 2016. Molecular Mechanisms of Two-Component Signal Transduction. J Mol Biol **428:**3752-3775.

89. **Faralla C, Metruccio MM, De Chiara M, Mu R, Patras KA, Muzzi A, Grandi G, Margarit I, Doran KS, Janulczyk R.** 2014. Analysis of two-component systems in group B Streptococcus shows that RgfAC and the novel FspSR modulate virulence and bacterial fitness. MBio **5:**e00870-00814.

90. **Glaser P, Rusniok C, Buchrieser C, Chevalier F, Frangeul L, Msadek T, Zouine M, Couve E, Lalioui L, Poyart C, Trieu-Cuot P, Kunst F.** 2002. Genome sequence of

Streptococcus agalactiae, a pathogen causing invasive neonatal disease. Mol Microbiol **45:**1499-1513.

91. **Al Safadi R, Mereghetti L, Salloum M, Lartigue MF, Virlogeux-Payant I, Quentin R, Rosenau A.** 2011. Two-component system RgfA/C activates the fbsB gene encoding major fibrinogen-binding protein in highly virulent CC17 clone group B Streptococcus. PLoS One **6:**e14658.

92. **Klinzing DC, Ishmael N, Dunning Hotopp JC, Tettelin H, Shields KR, Madoff LC, Puopolo KM.** 2013. The two-component response regulator LiaR regulates cell wall stress responses, pili expression and virulence in group B Streptococcus. Microbiology **159:**1521-1534.

93. **Quach D, van Sorge NM, Kristian SA, Bryan JD, Shelver DW, Doran KS.** 2009. The CiaR response regulator in group B Streptococcus promotes intracellular survival and resistance to innate immune defenses. J Bacteriol **191:**2023-2032.

94. **Lembo A, Gurney MA, Burnside K, Banerjee A, de los Reyes M, Connelly JE, Lin WJ, Jewell KA, Vo A, Renken CW, Doran KS, Rajagopal L.** 2010. Regulation of CovR expression in Group B Streptococcus impacts blood-brain barrier penetration. Mol Microbiol **77:**431-443.

95. **Landwehr-Kenzel S, Henneke P.** 2014. Interaction of Streptococcus agalactiae and Cellular Innate Immunity in Colonization and Disease. Front Immunol **5:**519.

96. **Jiang SM, Cieslewicz MJ, Kasper DL, Wessels MR.** 2005. Regulation of virulence by a two-component system in group B streptococcus. J Bacteriol **187:**1105-1113.

97. **Sendi P, Johansson L, Dahesh S, Van-Sorge NM, Darenberg J, Norgren M, Sjolin J, Nizet V, Norrby-Teglund A.** 2009. Bacterial phenotype variants in group B streptococcal toxic shock syndrome. Emerg Infect Dis **15:**223-232.

Chapter 2

The Group B Streptococcal surface antigen I/II protein, BspC, interacts with host vimentin to promote adherence to brain endothelium and inflammation during the pathogenesis of meningitis

Liwen Deng[1,2], Brady L. Spencer[2], Joshua A. Holmes[2], Rong Mu[1], Sara Rego[3], Thomas A. Weston[1], Yoonsung Hu[4], Glenda F. Sanches[2,5], Sunghyun Yoon[6], Nogi Park[6], Prescilla E. Nagao[5], Howard F. Jenkinson[3], Justin A. Thornton[4], Keun Seok Seo[6], Angela H. Nobbs[3] and Kelly S. Doran[1,2]

[1]Department of Biology, San Diego State University, 5500 Campanile Dr. San Diego, CA, 92182, USA.
[2]Department of Immunology and Microbiology, University of Colorado School of Medicine, Aurora, CO, 80045, USA.
[3]Bristol Dental School, University of Bristol, Lower Maudlin Street, Bristol BS1 2LY, UK.
[4]Department of Biological Sciences, Mississippi State University, Mississippi State, MS, 39762, USA.
[5]Laboratory of Molecular Biology and Physiology of Streptococci, Instituto de Biologia Roberto Alcantara Gomes, Rio de Janeiro State University, Rio de Janeiro, Brazil.
[6]Department of Basic Sciences, College of Veterinary Medicine, Mississippi State University, Mississippi State, MS 39762, USA.

Published in *PLoS Pathogens*

June 2019

Volume 15. Issue 6. e1007848

Short Title: The GBS adhesin BspC interacts with vimentin to promote meningitis

Key words: Group B *Streptococcus*, meningitis, blood-brain barrier, antigen I/II proteins, vimentin, inflammation

ABSTRACT

Streptococcus agalactiae (Group B *Streptococcus*, GBS) normally colonizes healthy adults but can cause invasive disease, such as meningitis, in the newborn. To gain access to the central nervous system, GBS must interact with and penetrate brain or meningeal blood vessels; however, the exact mechanisms are still being elucidated. Here, we investigate the contribution of BspC, an antigen I/II family adhesin, to the pathogenesis of GBS meningitis. Disruption of the *bspC* gene reduced GBS adherence to human cerebral microvascular endothelial cells (hCMEC), while heterologous expression of BspC in non-adherent *Lactococcus lactis* conferred bacterial attachment. In a murine model of hematogenous meningitis, mice infected with Δ*bspC* mutants exhibited lower mortality as well as decreased brain bacterial counts and inflammatory infiltrate compared with mice infected with WT GBS strains. Further, BspC was both necessary and sufficient to induce neutrophil chemokine expression. We determined that BspC interacts with the host cytoskeleton component vimentin, and confirmed this interaction using a bacterial two-hybrid assay, microscale thermophoresis, immunofluorescent staining, and imaging flow cytometry. Vimentin null mice were protected from WT GBS infection and also exhibited less inflammatory cytokine production in brain tissue. These results suggest that BspC and the vimentin interaction is critical for the pathogenesis of GBS meningitis.

AUTHOR SUMMARY

Group B *Streptococcus* (GBS) typically colonizes healthy adults but can cause severe disease in immune compromised individuals, including newborns. Despite wide-spread intrapartum antibiotic prophylaxis given to pregnant women, GBS remains a leading cause of neonatal meningitis. To cause meningitis, GBS must interact with and penetrate the blood-brain

barrier (BBB), which separates bacteria and immune cells in the blood from the brain. In order to develop targeted therapies to treat GBS meningitis, it is important to understand the mechanisms of BBB crossing. Here, we describe the role of the GBS surface factor, BspC, in promoting meningitis and discover the host ligand for BspC, vimentin, which is an intermediate filament protein that is constitutively expressed by endothelial cells. We determined that BspC interacts with the C-terminal domain of cell-surface vimentin to promote bacterial attachment to brain endothelial cells and that purified BspC protein can induce immune signaling pathways. In a mouse model of hematogenous meningitis, we observed that a GBS mutant lacking BspC was less virulent compared to WT GBS and resulted in less inflammatory disease. We also observed that mice lacking vimentin were protected from GBS infection. These results reveal the importance of the BspC-vimentin interaction in the progression of GBS meningitis disease.

INTRODUCTION

Streptococcus agalactiae (Group B *Streptococcus*, GBS) is an opportunistic pathogen that asymptomatically colonizes the vaginal tract of up to 30% of healthy women. However, GBS possesses a variety of virulence factors and can cause severe disease when transmitted to susceptible hosts such as the newborn. Despite widespread intrapartum antibiotic administration to colonized mothers, GBS remains a leading cause of pneumonia, sepsis, and meningitis in neonates (1, 2). Bacterial meningitis is a life-threatening infection of the central nervous system (CNS) and is marked by transit of the bacterium across endothelial barriers, such as the blood-brain barrier (BBB) or the meningeal blood-cerebral spinal fluid barrier (mBCSFB). Both consist of a single layer of specialized endothelial cells that serve to maintain brain homeostasis and generally prevent pathogen entry into the CNS (3-5). Symptoms of bacterial meningitis may be

due to the combined effect of bacterial adherence and brain penetration, direct cellular injury caused by bacterial cytotoxins, and/or activation of host inflammatory pathways that can disrupt brain barrier integrity and damage underlying nervous tissue. (6-8)

Bacterial meningitis typically develops as a result of the pathogen spreading from the blood to the meninges. In order to disseminate from the blood into the brain, GBS must first interact with barrier endothelial cells (9). A number of surface-associated factors that contribute to GBS-brain endothelium interactions have been described such as lipoteichoic acid (LTA) (10), pili (11), serine-rich repeat proteins (Srr) (12), and streptococcal fibronectin-binding protein (SfbA) (13). Pili, the Srr proteins, and SfbA have been shown to interact with extracellular matrix (ECM) components, which may help to bridge to host receptors such as integrins or other ECM receptors. However, a direct interaction between a GBS adhesin and an endothelial cell receptor has not been described.

Antigen I/II family (AgI/II) proteins are multifunctional adhesins that have been well characterized as colonization determinants of oral streptococci (14). These proteins mediate attachment of *Streptococcus mutans* and *Streptococcus gordonii* to tooth surfaces and can stimulate an immune response from the colonized host (14). Genes encoding AgI/II polypeptides are found in streptococcal species indigenous to the human mouth as well as other pathogenic streptococci such as GBS, *S. pyogenes* (Group A *Streptococcus*, GAS), and *S. suis* (14, 15). Intriguingly, the GAS AgI/II protein AspA (Group A *Streptococcus* surface protein) is absent in many GAS M serotypes and is found predominantly among M serotypes implicated in puerperal sepsis and neonatal infections, including M2, M4, and M28. The gene encoding AspA is located within an integrative and conjugative element designated region of difference 2 (RD2), which likely originated in GBS and was acquired by invasive GAS serotypes through horizontal gene

transfer (Fig. 1A). It has been proposed that genes carried within RD2 may contribute to pathogenicity of both GAS and GBS in pregnant women and newborns (16, 17). Supporting this, AspA has been shown to facilitate GAS biofilm formation and virulence in a murine model of GAS respiratory infection (18). Recently, *in silico* analysis has revealed four AgI/II gene homologs in GBS, designated Group B *Streptococcus* surface proteins (BspA-D), that are distributed among GBS of different capsular serotypes and sequence types (15, 19, 20).

Previous work has shown that BspA and BspB, which share 90% sequence identity, are found in GBS strain NEM316. BspA has been demonstrated to be important in biofilm formation as well as adherence to epithelial cells and may play a role in facilitating colonization through its ability to bind to vaginal epithelium as well as interact with the hyphal filaments of *Candida albicans* (15, 20), a frequent fungal colonizer of the lower female reproductive tract. Other GBS strains contain the homolog BspC, or in some cases BspD, which is over 99% identical to BspC, with the major difference being that BspD is missing the leader peptide for targeting to the cell surface by the Sec translocation machinery. While most of the variability between Bsp proteins is in the alanine-rich and proline-rich repeats, the V domain shares 96 to 100% identity across all Bsp homologs (15, 20). To date, there have not been any studies examining the impact of the AgI/II proteins on GBS invasive disease. A previous study by Chuzeville et al. identified 75 GBS genomes which contain an antigen I/II homolog. Of those 75 CDS, only 40 were associated with transcription and translation signals and out of those, 36 were 2952 base pairs in size encoding the full length BspC protein (19). Therefore, we chose to investigate the importance of the BspC antigen I/II homolog in the pathogenesis of meningitis. Using targeted mutagenesis, we show that BspC promotes adherence of bacteria to human cerebral microvascular endothelial cells (hCMEC) and interacts with the host cytoskeleton component, vimentin. Additionally, we found that BspC

and vimentin contribute to the development of GBS meningitis in a mouse infection model. Lastly, we observe that BspC stimulates inflammatory signaling from brain endothelial cells *in vitro* and *in vivo* and that this immune signaling involves the NF-κB pathway.

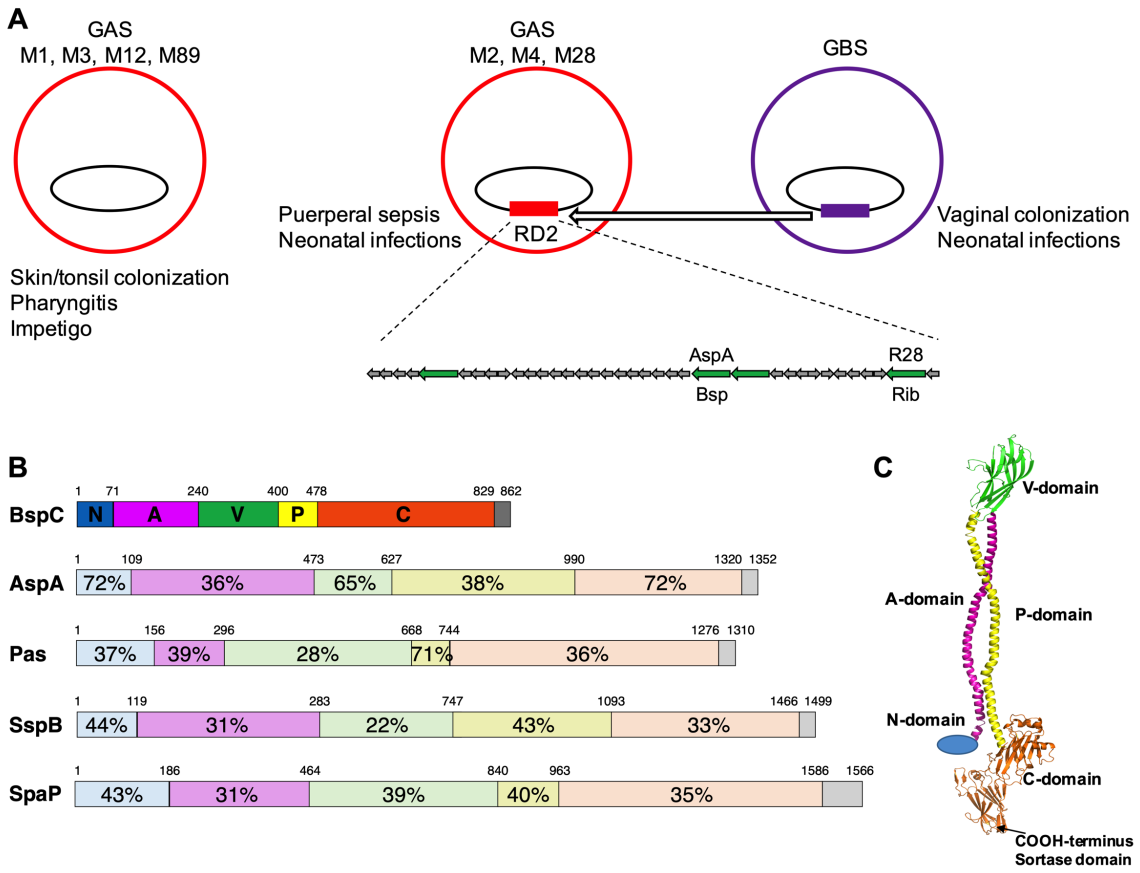

Figure 2.1. Analysis of BspC domain architecture. (A) Diagram of MGAS6180 region of difference 2 (RD2). M2, M4, and M28 strains of Group A *Streptococcus* contain RD2, which was likely acquired from Group B *Streptococcus* through horizontal gene transfer and is absent in other common disease causing GAS *emm*-types. Open reading frames encoding LPXTG cell wall anchor domain-containing proteins are indicated with green arrows. Proteins AspA and R28 in GAS and their respective homologs in GBS, Bsp and Rib, have been previously described. The other two cell wall anchor domain-containing proteins have not been characterized. (B) Schematic of sequence homologies across antigen I/II family proteins from select *Streptococcus* species. Six structural regions are shown: N, N-terminal region; A, alanine-rich repeats; V, variable region; P, proline-rich repeats; C, C-terminal region; and the cell-wall anchor-containing region. Numbers indicate percentage amino acid residue identities to BspC from *S. agalactiae* strain COH1 (NCBI Ref. Seq.: WP_000277676.1). The proteins depicted are the antigen I/II proteins AspA from *S. pyogenes* strain M28 (WP_011285012.1), Pas from *S. intermedius* (WP_049476098.1), SspB from *S. gordonii* (WP_011999747), and SpaP from *S. mutans* (WP_024781655.1). (C) Hypothetical model of BspC generated using PyMOL.

RESULTS

Analysis of BspC domain architecture and construction of a *bspC* deletion strain.

BspC contains all six domains characteristic of the AgI/II protein family, and shares high homology with other streptococcal AgI/II proteins, especially GAS AspA (Fig. 1B). The proposed domain organization of streptococcal AgI/II polypeptides comprises a stalk consisting of the α-helical A (alanine-rich repeats) domain and the polyproline II (PPII) helical P domain, separating the V (variable) domain and the C-terminal domain, which contains the LP*X*TG motif required for cell wall anchorage (14). While the GBS BspC structure is not known, the structure of several regions of the GBS homolog, BspA, has been solved (15). We generated a hypothetical model of full length BspC using PyMOL (The PyMOL Molecular Graphics System, Version 2.1 Schrödinger, LLC) for the purpose of showing the overall domain structure (Fig. 1C). Structures of individual BspC domains were generated using Phyre2 server (21). The V- and C-domains were modeled on the V- and C-domains of BspA (PDB entries 5DZ8 and 5DZA, respectively) (15), and approximately two-thirds of the A-domain sequence was modeled on human fibrinogen (PDB entry 3GHG) (22). It was not possible to generate models for the N- and P-domains, so the N-domain is shown as a sphere and the P-domain shown is a mirror image of the A-domain.

We performed precise in-frame allelic replacement to generate a Δ*bspC* mutant in GBS strain COH1, a hypervirulent GBS clinical isolate that is highly associated with meningitis (sequence type [ST]-17, serotype III) (23, 24), using a method as described previously (10). We further determined the presence of surface BspC expression in the WT and complemented strains compared to the Δ*bspC* mutant by flow cytometry and immunofluorescent staining with specific BspC antibodies (Fig. S1A-G). Growth curve analysis demonstrated that the Δ*bspC* mutant grew

similarly to the WT parental strain under the conditions used here (Fig. S1H). Similarly, we observed no differences in hemolytic activity or capsule abundance between the WT and mutant strains (Fig. S1I-L). High-magnification scanning electron microscopy (SEM) images of COH1 strains showed that the Δ*bspC* deletion strain exhibits similar surface morphology to the isogenic wild type (Fig. 2A and 2B). However, lower-magnification SEM revealed that the Δ*bspC* mutant appeared to exhibit decreased interaction between neighboring cells (Fig. 2C,D).

BspC promotes bacterial adherence to endothelial cells *in vitro*.

Since AgI/II proteins are known to demonstrate adhesive properties in other streptococci (14), we hypothesized that BspC would contribute to GBS interaction with brain endothelium. Thus, we characterized the ability of the Δ*bspC* mutant to attach to and invade hCMEC using our established adherence and invasion assays (10, 25). The Δ*bspC* mutant exhibited a significant decrease in adherence to hCMEC compared to WT GBS, and this defect was complemented when BspC was expressed in the Δ*bspC* mutant strain (Fig. 2E). This resulted in less recovery of intracellular Δ*bspC* mutant (Fig. 2F), but together these results indicate that BspC contributes primarily to bacterial attachment to hCMEC. To determine if BspC was sufficient to confer adhesion, we heterologously expressed the GBS *bspC* gene in the non-adherent, non-pathogenic bacterium *Lactococcus lactis*. Flow cytometric analysis of *L. lactis* confirmed surface expression of BspC protein in the strain containing the pMSP.*bspC* plasmid (Fig. S2). BspC expression resulted in a significant increase in *L. lactis* adherence to hCMEC compared to *L. lactis* containing the control vector, while invasion was not affected (Fig. 2G,H). These results demonstrate that BspC is both necessary and sufficient to confer bacterial adherence to hCMEC.

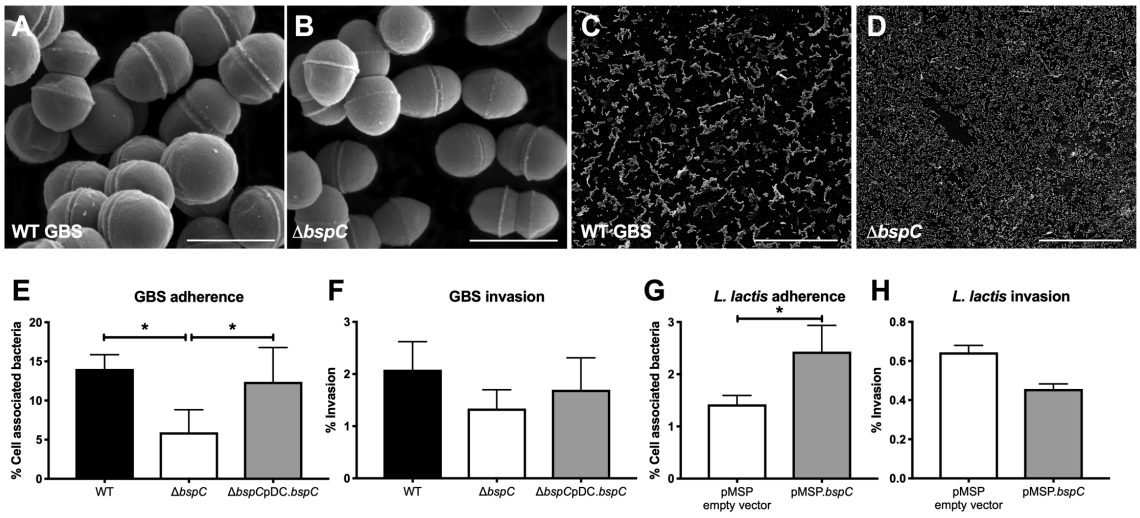

Figure 2.2. BspC bacterial adherence to endothelial cells *in vitro.* (A-D) Scanning electron microscopy images of WT (A and C) and Δ*bspC* mutant (B and D) GBS. Scale bar in high magnification images (A and B) is 1 μM. Scale bar in low magnification images (C and D) is 50 μM. (E) Adherence of WT GBS, the Δ*bspC* mutant, and the Δ*bspC*pDC.*bspC* complemented strain to hCMEC was assessed after a 30 min incubation. Total cell-associated bacteria are shown. (F) Invasion of WT GBS, the Δ*bspC* mutant, and the Δ*bspC*pDC.*bspC* strain was quantified after a 2 h infection. (G) Adherence and (H) invasion of *Lactococcus lactis* containing the pMSP empty vector or pMSP.*bspC* to hCMEC were quantified. Data indicates the percentage of the initial inoculum that was recovered. Experiments were performed three times with each condition in triplicate. Data from one representative experiment are shown and error bars represent the standard deviation. Statistical analysis: (E and F) One-way ANOVA with Tukey's multiple comparisons test. (G and H) Unpaired t test. ∗, $P < 0.05$.

BspC contributes to pathogenesis of GBS meningitis *in vivo*.

Our results thus far suggest a primary role for BspC in GBS adherence to brain endothelium. We hypothesized that these *in vitro* phenotypes would translate into a diminished ability to penetrate the BBB and produce meningitis *in vivo*. Using our standard model of GBS hematogenous meningitis (10, 26, 27), mice were challenged with either WT GBS or the Δ*bspC* mutant as described in the Methods. The WT GBS strain caused significantly higher mortality than the isogenic Δ*bspC* mutant strain (Fig. 3A). By 48 hours, 80% of mice infected with WT COH1 had succumbed to death, while all of the mice infected with the Δ*bspC* mutant survived up to or past the experimental endpoint. In a subsequent experiment mice were infected with a lower dose

of either WT GBS or the Δ*bspC* mutant and were sacrificed at a defined endpoint (48 hrs) to determine bacterial loads in blood, lung, and brain tissue. We recovered similar numbers of the Δ*bspC* mutant strain from mouse blood and lung compared to WT, however we observed a significant decrease in the amounts of the Δ*bspC* mutant recovered from the brain tissue (Fig. 3B). To confirm these results using other GBS strains, we constructed *bspC* gene deletions as described in the Methods in two other GBS strains: GBS 515 (ST-23, serotype Ia) and meningeal isolate 90356 (ST-17, serotype III). Mice infected with these mutant strains were also less susceptible to infection and exhibited decreased bacterial loads in the brain compared to the isogenic parental WT strain (Fig. S2). Interestingly, the Δ*bspC* mutant in the 515 GBS background, which is a different sequence type and serotype from the other two strains, appeared to also exhibit diminished infiltration into the mouse lungs.

As excessive inflammation is associated with CNS injury during meningitis, we performed histological analysis of brains from infected animals. In WT infected mice, we observed leukocyte infiltration and meningeal thickening characteristic of meningitis that was absent in the mice infected with the Δ*bspC* mutant strain (Fig. 3C,D). Representative images from 8 mice, 4 infected with WT (Fig. 3C) and 4 infected with the Δ*bspC* mutant (Fig. 3D) are shown where the major areas of inflammation were observed. In subsequent experiments to quantify the total inflammatory infiltrate, whole brains from uninfected mice and mice infected with either WT GBS or Δ*bspC* mutant GBS were processed and analyzed by flow cytometry as described in the Methods. There was no significant difference in the numbers of CD45 positive cells between the groups of mice, however within the CD11b positive population we observed higher numbers of Ly6C positive and Ly6G positive cells in the brains of animals infected with WT GBS compared to uninfected mice and mice infected with the Δ*bspC* mutant strain (Fig. 3E,F), indicating an

increased population of monocytes and neutrophils. Consistent with these results, we further observed that mice challenged with WT GBS had significantly more of the neutrophil chemokine, KC, as well as the proinflammatory cytokine, IL-1β, in brain homogenates than Δ*bspC* mutant infected animals. (Fig 3G, H)

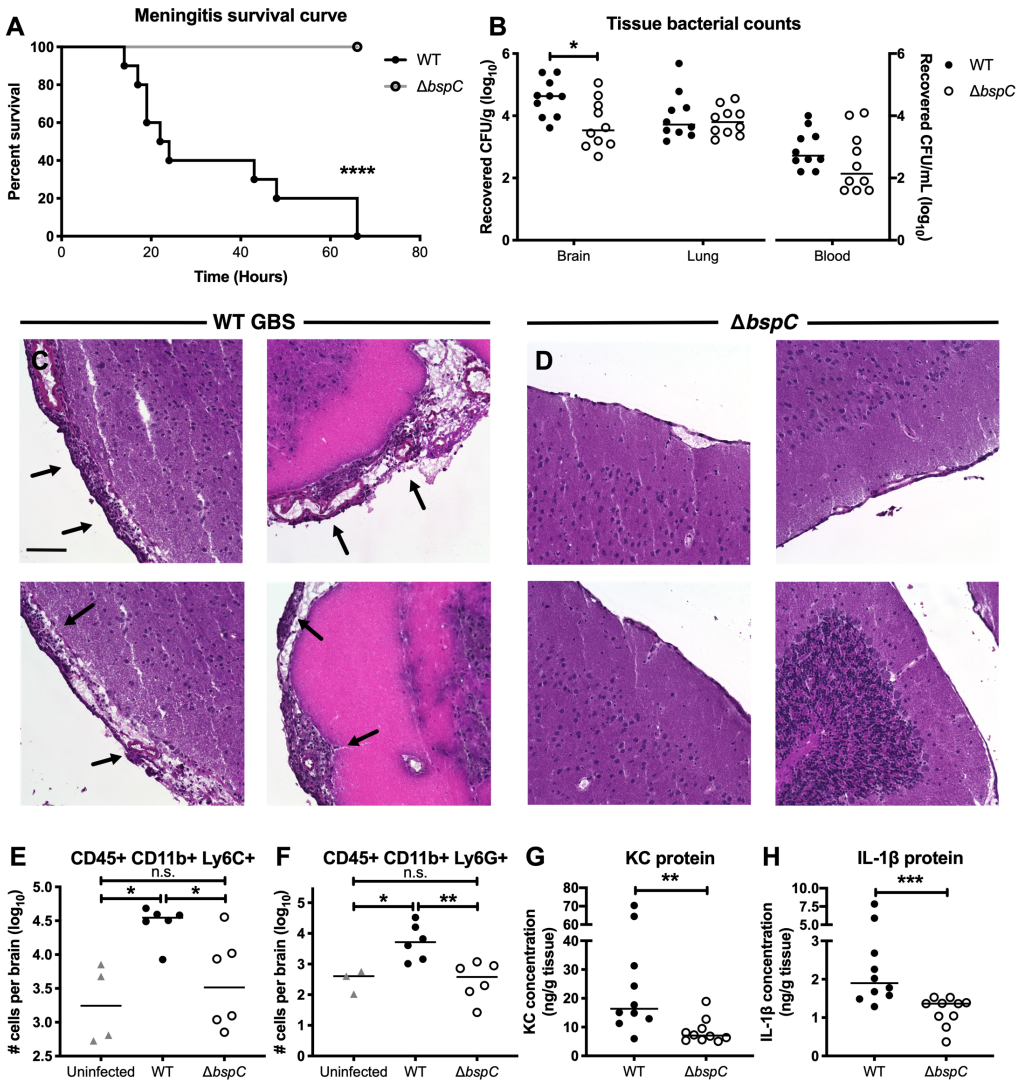

Figure 2.3. BspC contributes to pathogenesis of GBS meningitis *in vivo*. (A) A Kaplan-Meier plot showing survival of CD-1 mice infected with 10^9 CFU of either WT GBS or the Δ*bspC* mutant. (B) 72 h after infection with 10^8 CFU of either WT GBS or the Δ*bspC* mutant, mice were euthanized and bacterial loads in brain, lung, and blood were quantified. Lines indicate statistical median. (C and D) H&E images showing the leptomeninges on the surface of brains from CD-1 mice infected with either WT GBS (C) or the Δ*bspC* mutant (D). Arrows indicate areas of meningeal thickening and leukocyte infiltration. Scale bar is 100 μM. (E and F) Quantification of infiltrating immune cells in the brains of mice infected with WT GBS or the Δ*bspC* mutant. The presence CD45+, CD11b+, Ly6C+ (E), and CD45+, CD11b+, Ly6G+ (F) cells was determined using flow cytometry. (G and H) ELISA was performed on mouse brain tissue homogenates to assess cytokine protein levels. KC (G) and IL-1β (H) were quantified for brains from mice challenged with either WT GBS or the Δ*bspC* mutant. Statistical analysis: (A) Log-rank test. (B) Two-way ANOVA with Sidak's multiple comparisons test. (E and F) One-way ANOVA with Sidak's multiple comparisons test. (G and H) Mann-Whitney test. *, $P < 0.0005$; **, $P < 0.005$; ***, $P < 0.0005$; ****, $P < 0.00005$.

BspC is necessary and sufficient to induce neutrophil chemokine signaling.

To further characterize the role of BspC in stimulating immune signaling pathways we infected hCMEC with WT GBS, the Δ*bspC* mutant, or the complemented strain. After four hours of infection, we collected cells and isolated RNA for RT-qPCR analysis to quantify IL-8 and CXCL-1 transcripts. We focused on the neutrophil chemokines IL-8 and CXCL-1 as these cytokines are highly induced during bacterial meningitis (28) and we observed an increase in neutrophilic infiltrate in brain tissue during the development of GBS meningitis in our mouse model. Cells infected with WT GBS had significantly increases of both transcripts compared to cells infected with the Δ*bspC* mutant. Complementation of the *bspC* mutation restored the ability of the bacteria to stimulate the expression of IL-8 and CXCL-1 (Fig. 4A,B). Additionally, treatment of hCMEC with purified BspC protein resulted in increased transcript abundance (Fig. 4,D) and protein secretion (Fig. 4E,F) for both IL-8 and CXCL-1 compared to untreated cells or treatment with control protein, CshA from *Streptococcus gordonii,* that was similarly purified from *E. coli*.

Nuclear factor-κB (NF-κB) represents a family of inducible transcription factors, which regulates a large array of genes involved in different processes of the immune and inflammatory responses, including IL-8, CXCL-1 and IL-1 (29). To assess whether the NF- κB pathway is activated by BspC, we utilized the Hela-57A NF- κB luciferase reporter cell line as described previously (30). Cells infected with WT GBS had significantly higher luciferase activity than uninfected and Δ*bspC* mutant GBS infected cells, indicating that BspC contributes NF- κB activation (Fig. 4G). Additionally, immunofluorescent staining of hCMEC revealed an increase in

P65 expression, an indicator of NF- κB activation, during infection with WT GBS but not in response to infection with Δ*bspC* mutant GBS (Fig. 4H-J).

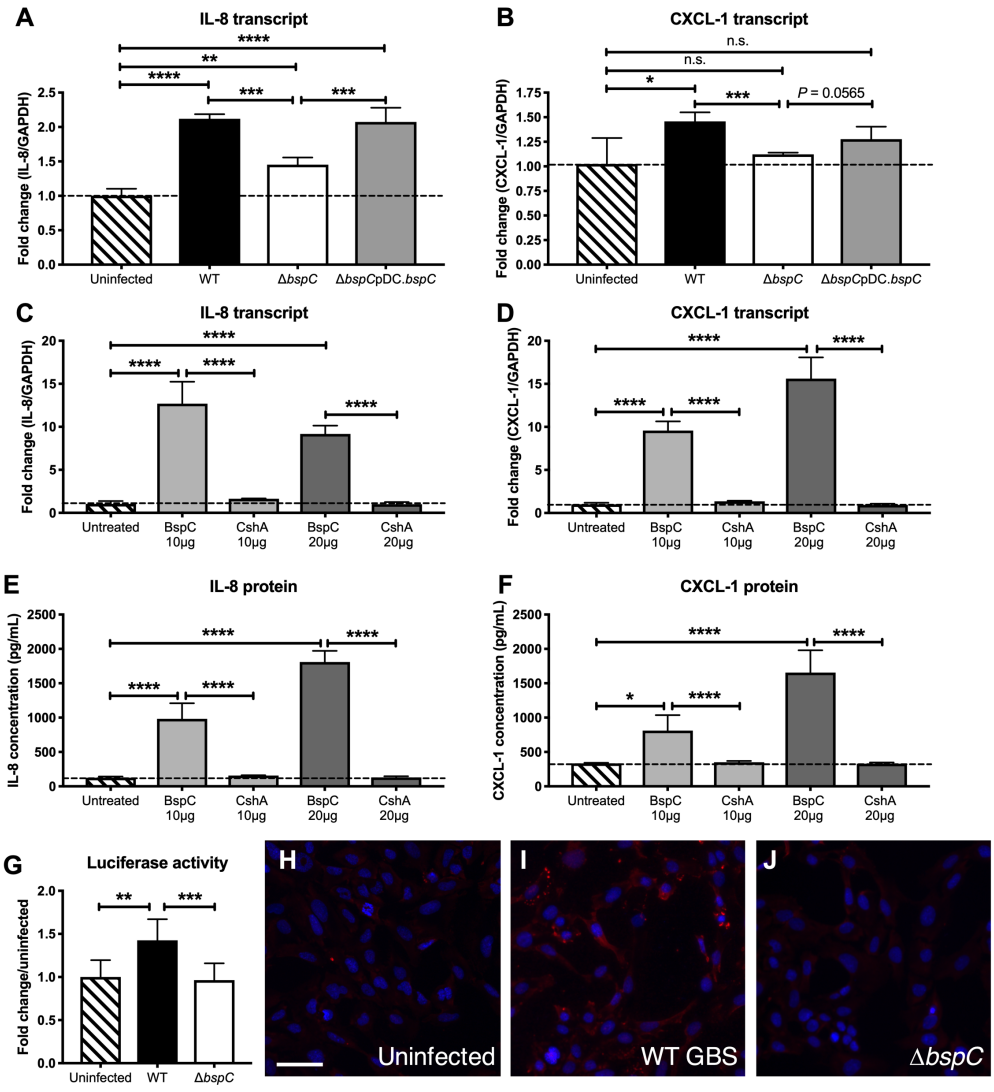

Figure 2.4. BspC is necessary and sufficient to induce neutrophil chemokine signaling. (A and B) RT-qPCR to assess IL-8 (A) and CXCL-1 (B) transcript levels in uninfected hCMEC or hCMEC infected with WT GBS, the Δ*bspC* mutant, or the complemented strain. (C and D) RT-qPCR analysis quantifying IL-8 (C) and CXCL-1 (D) transcripts in hCMEC treated with purified BspC protein or the *S. gordonii* CshA protein. (E and F) ELISA to measure IL-8 (E) and CXCL-1 (F) protein secretion by hCMEC treated with BspC or CshA. (G) Luciferase activity of uninfected Hela-57A cells and cells infected with WT GBS or the Δ*bspC* mutant was assessed. Experiments were performed at least three times with each condition in triplicate. Data from representative experiments are shown and error bars represent the standard deviation of the mean for one experiment. Data were analyzed with One-way ANOVA with Sidak's multiple comparisons test. (H-J) Immunofluorescent staining showing p65 localization in uninfected hCMEC (H), hCMEC infected with WT GBS (I), and hCMEC infected with the Δ*bspC* mutant (J). Following infection, cells were fixed with formaldehyde and incubated with a rabbit antibody to p65. Nuclei were labelled with DAPI. Scale bar is 50 μM. *, $P < 0.05$; **, $P < 0.005$; ***, $P < 0.0005$; ****, $P < 0.00005$.

BspC interacts with the host endothelial cytoskeletal component vimentin.

We next sought to identify the host protein receptor on brain endothelial cells that interacts with BspC. Membrane proteins of hCMEC were separated by 2-dimensional electrophoresis (2-DE), then blotted to a PVDF membrane. Following incubation with biotinylated BspC protein, the PVDF membrane was incubated with a streptavidin antibody conjugated to HRP. While many proteins were detected on the Coomassie stained gel, biotinylated BspC protein specifically interacted predominately with one spot in the PVDF membrane with molecular mass around 50-55 kDa and isoelectric point (pI) around 5 (Fig. 5A,B). The corresponding spot from the Coomassie-stained 2-DE gel was excised and digested with trypsin (Fig. 5C). Resulting peptides were analyzed by liquid chromatography-tandem mass spectrometry. The spectra from the spot yielded 158 peptide sequences which matched to human vimentin. The molecular weight, 53.6 kDa, and calculated pI, 5.12, of vimentin match the values for the spot on the 2-DE gels. This procedure was repeated for membrane proteins from another human brain endothelial cell line (hBMEC) that has been used previously to study GBS interactions (31). Mass spectrometry analysis also determined that BspC interacted with human vimentin (Fig. S3A-C). The control far Western blot with the streptavidin antibody conjugated to HRP did not show any hybridization (Fig. S3D).

To confirm these protein-protein interactions *in vivo*, we employed a bacterial two-hybrid system (BACTH, "Bacterial Adenylate Cyclase-Based Two-Hybrid") (32). This system is based on the interaction-mediated reconstitution of a cyclic adenosine monophosphate (cAMP) signaling cascade in *Escherichia coli*, and has been used successfully to detect and analyze the interactions between a number of different proteins from both prokaryotes and eukaryotes (33). Using a commercially available kit (Euromedex) according to manufacturer's directions and as described

previously (34), vimentin was cloned and fused to the T25 fragment as a N-terminal fusion (T25-Vimentin), using the pKT25 plasmid, and *bspC* was cloned as a c-terminal fusion (BspC-T18) using the pUT18 plasmid. To test for interaction these plasmids were transformed into an *E. coli* strain lacking adenylate cyclase (*cyaA*). We observed blue colonies when grown on LB agar plates containing X-gal, indicating β-galactosidase activity and a positive interaction between Vimentin and BspC compared to the empty vector control (Fig. 5D,E). A leucine zipper that is fused to the T25 and T18 fragments served as the positive control for the system (Fig. 5F). To quantify β-galactosidase activity, cells grown to log phase were permeabilized with 0.1 % SDS and toluene and enzymatic activity measured by adding ONPG as described previously (34). The *E. coli* strain containing both vimentin and BspC expressing plasmids exhibited increased β-galactosidase activity (Miller units) compared to the empty vector control strain (Fig. 5G). We also quantified the interaction between BspC and vimentin by performing microscale thermophoresis (MST) (35) as described in Methods. The dissociation constant (K_d) was 3.39μM as calculated from the fitted curve that plots normalized fluorescence against concentration of vimentin (Fig. S4E). These results demonstrate a direct interaction between BspC and vimentin.

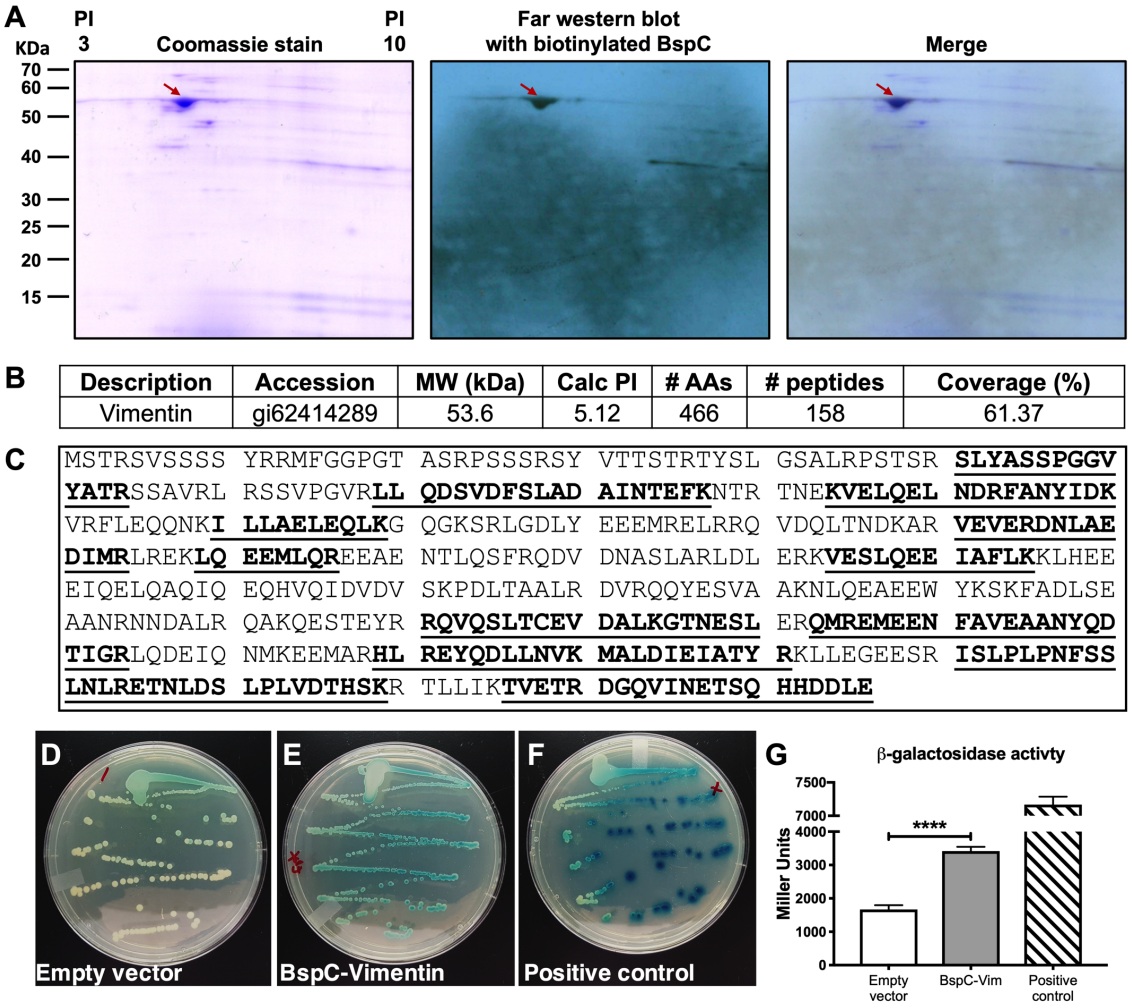

Figure 2.5. BspC interacts with the host endothelial cytoskeletal component vimentin. (A) Far Western blot analysis of hCMEC membrane proteins probed with biotinylated BspC. Membrane proteins were extracted from hCMEC and separated by 2-DE in duplicate. One gel was transferred to a PVDF membrane and probed with biotinylated BspC. The specific interaction of BspC was detected by a streptavidin antibody conjugated to HRP and visualized by x-ray film exposure. The other gel was stained with Coomassie blue. The spot identified from the x-ray film was aligned to the Coomassie stained gel and the corresponding spot was excised and digested with trypsin. (B) Electrospray ionization-tandem mass spectrometry analysis identifies the protein vimentin. (C) Amino acid sequence of human vimentin. Underscored and bolded are the peptide sequences identified from MS analysis. (D-F) Bacterial two-hybrid assay using *E. coli* containing empty vector controls (D), the BspC and vimentin vectors (E), and the positive control vectors (F). (G) β-galactosidase activity of *E. coli* was quantified using a Miller assay. The Miller assay was performed three times with each condition in five replicates. Data from one representative experiment is shown, error bars represent the standard deviation of the mean. Data were analyzed using one-way ANOVA with Dunnett's multiple comparisons test. ****, $P < 0.00005$.

Description	Accession	MW (kDa)	Calc PI	# AAs	# peptides	Coverage (%)
Vimentin	gi62414289	53.6	5.12	466	158	61.37

GBS co-localization with cell-surface vimentin is dependent on BspC.

To visualize the localization of WT GBS and vimentin in brain endothelial cells we performed imaging flow cytometry of uninfected and WT GBS infected hCMEC. Cells were fixed, permeabilized, and incubated with antibodies to vimentin and GBS. We observed that vimentin protein was present throughout the cytoplasm of uninfected hCMEC (Fig. 6A,B), but during infection GBS co-localized with vimentin near the surface of infected cells (Fig. 6C,D). To further characterize the localization of GBS and vimentin, we performed immunofluorescent staining of hCMEC infected with either WT GBS or the Δ*bspC* mutant. Following infection, cells were fixed but not permeabilized to permit labeling of only extracellular bacteria and surface expressed vimentin. We observed that surface vimentin of hCMEC co-localized with WT GBS bacteria, while this was not seen for hCMEC infected with the Δ*bspC* mutant (Fig. 6E-H). To quantify co-localization of GBS with vimentin, the number of bacteria that overlapped with the vimentin signal was divided by the total number of bacteria in each field of view (Fig. 6I). No staining of either GBS or vimentin was observed in IgG controls (Fig 6J-L). Additionally, as a control, we did not observe staining of GBS with the anti-vimentin antibody (data not shown).

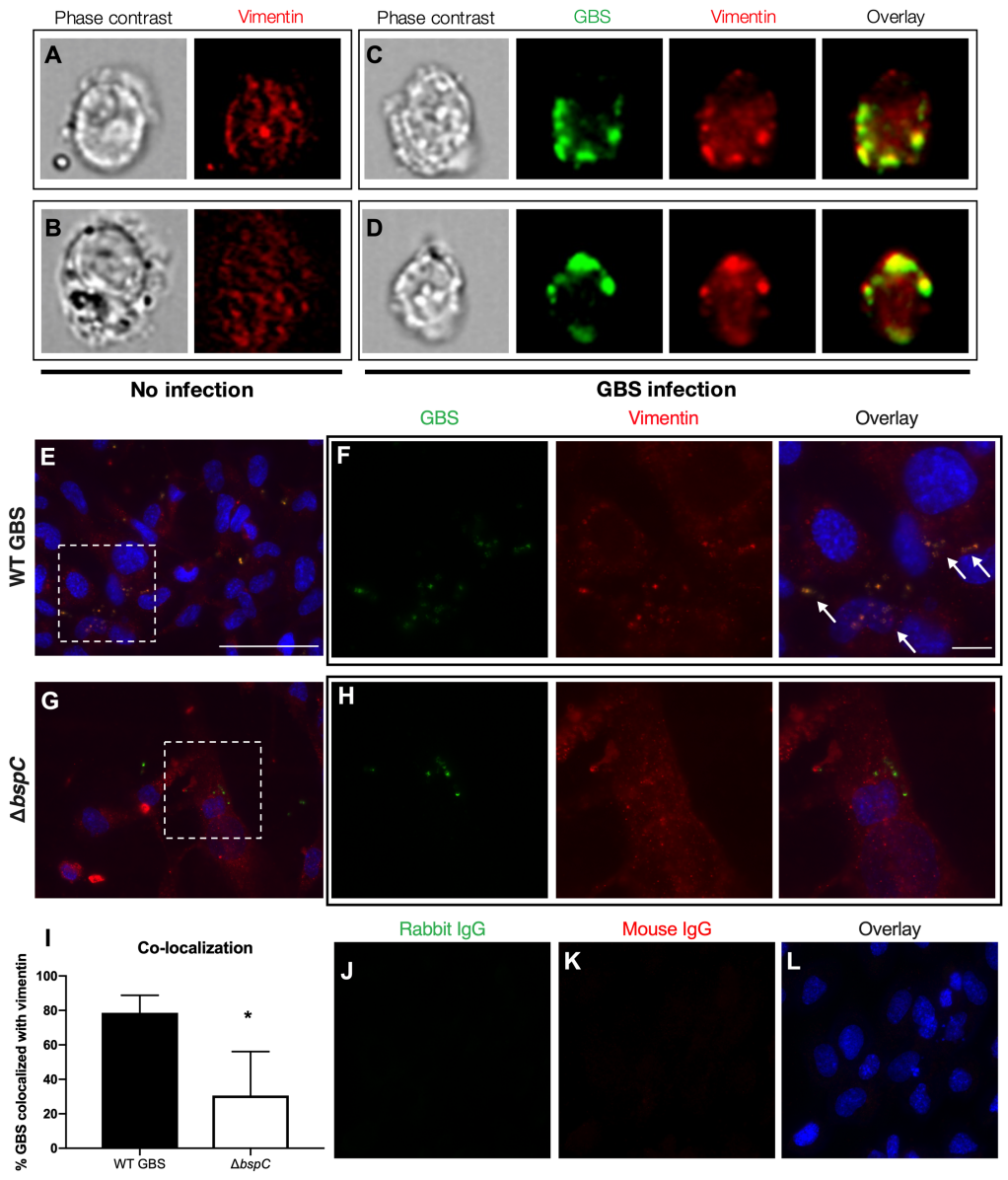

Figure 2.6. GBS co-localization with cell-surface vimentin is dependent on BspC. (A-D) Imaging flow cytometry showing vimentin localization in uninfected hCMEC (A and B) and hCMEC infected with WT GBS (C-D). Cells were fixed and permeabilized prior to staining with antibodies to vimentin and the group B carbohydrate antigen to label cell-associated GBS. (E-H) Immunofluorescent staining of hCMEC monolayers infected with WT GBS (E-F) or the Δ*bspC* mutant (G-H). Following a one-hour infection, hCMEC were washed to remove nonadherent bacteria then fixed and labelled with antibodies to vimentin and GBS. Nuclei were labelled with DAPI. Magnified images of the areas highlighted in (E) and (G) are shown in (F) and (H). Scale bar in (E) is 50 µm. Scale bare in (F) is 10 µm. Arrows indicate GBS co-localizing with vimentin. (I) Quantification of co-localization of GBS and vimentin was performed by dividing the number of GBS that co-localize with vimentin by the total number of GBS. Error bars represent the median. Statistical analysis was performed using and unpaired t test. ∗, $P < 0.05$. (J-L) Negative staining controls of hCMEC monolayers infected with WT GBS.

BspC and vimentin promote GBS attachment to cells *in vitro*.

To first determine if BspC-mediated attachment to cells is dependent on vimentin, we infected HEK293T cells with lentiviruses containing either the vimentin expression plasmid pLenti-VIM or the vector control pLenti-mock. Immunofluorescent staining reveals that HEK293T pLenti-mock cells do not express vimentin while the HEK203T pLenti-VIM clone exhibits strong vimentin labelling (Fig. 7A,B). WT GBS was significantly more adherent to HEK293T cells that express vimentin while the Δ*bspC* mutant showed no difference in attachment to either cell line (Fig. 7C). Next, we assessed the effect of blocking the vimentin-GBS interaction by treating hCMEC with anti-vimentin antibodies prior to infection with GBS (Fig. 7D). Treatment with a vimentin antibody that recognizes the N-terminal epitope (AA31-80), as well as with IgG isotype controls did not alter adherence of the WT or Δ*bspC* mutant strains, however pre-incubation with the mouse V9 antibody (36, 37), which reacts with the C-terminal of vimentin (AA405-466), reduced WT GBS adherence to levels comparable to the adherence of the Δ*bspC* mutant (Fig. 7E,F). These results indicate that the interaction between BspC and cell-surface vimentin is dependent on the C-terminus of vimentin.

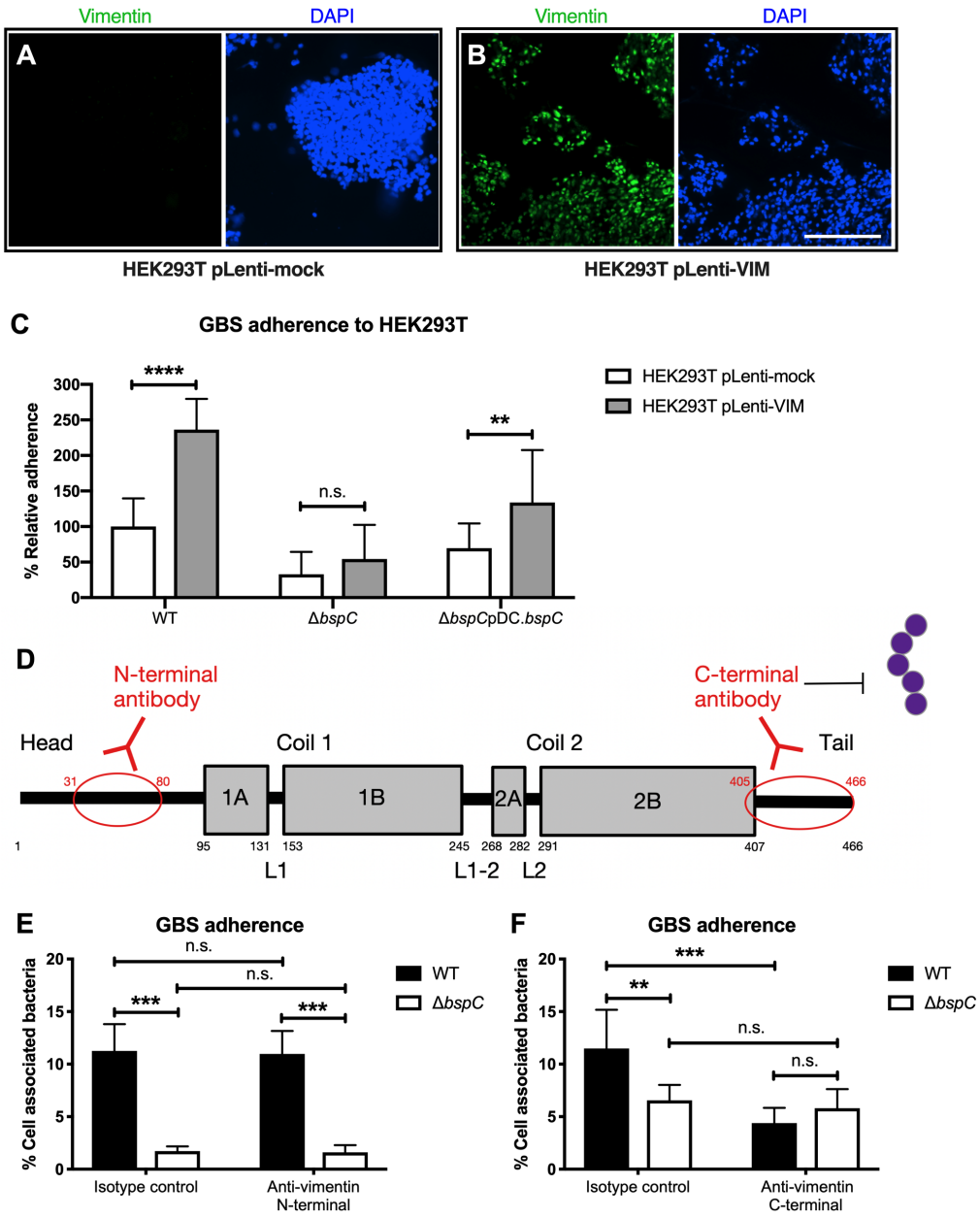

Figure 2.7. GBS adherence to cells is dependent on vimentin. (A and B) Immunofluorescent staining to show vimentin expression of HEK293T pLenti-Mock (A) and HEK293T pLenti-VIM (B) cells. Scale bar is 200 µm. (C) Adherence of WT GBS, the Δ*bspC* mutant, and the complemented strain to transfected HEK293T cells. Data from two independent experiments with each condition in 8 replicates is combined. (D) Schematic showing regions of vimentin recognized by the monoclonal antibodies. (E and F) hCMEC were pre-incubated with antibodies to the N-terminal (E) or the C-terminal (F) of vimentin or with an IgG control prior to a 30 min infection with either WT GBS or the Δ*bspC* mutant. Experiments were performed three times with each condition in triplicate and data from one representative experiment are shown. Error bars represent the standard deviation of the mean. Statistical analysis was performed using a two-way ANOVA with Sidak's multiple comparisons test. **, $P < 0.005$; ***, $P < 0.0005$; ****, $P < 0.00005$.

Vimentin contributes to the pathogenesis of meningitis *in vivo*.

We obtained WT 129 and 129 vimentin KO mice and confirmed the absence of vimentin in the brain endothelium of the KO animals by immunofluorescent staining (Fig. S5A,B). To determine the necessity of vimentin in GBS meningitis disease progression, we infected WT and vimentin KO mice with WT GBS and observed that they were less susceptible to GBS infection and exhibited increased survival compared to WT animals (Fig. 8A). Further, significantly less bacteria were recovered from the tissues of KO mice compared to the tissues of WT mice (Fig. 8B). WT and vimentin KO mice infected with Δ*bspC* mutant GBS showed no difference in survival and tissue bacterial counts (Fig. S6). Additionally, for animals infected with WT GBS, we detected significantly less KC and IL-1β in brain tissues of vimentin KO compared to WT mice, suggesting that vimentin contributes to the initiation of immune signaling pathways during GBS infection (Fig. 8C,D). Taken together these results indicate the importance of vimentin in GBS dissemination into the brain and meningitis disease progression.

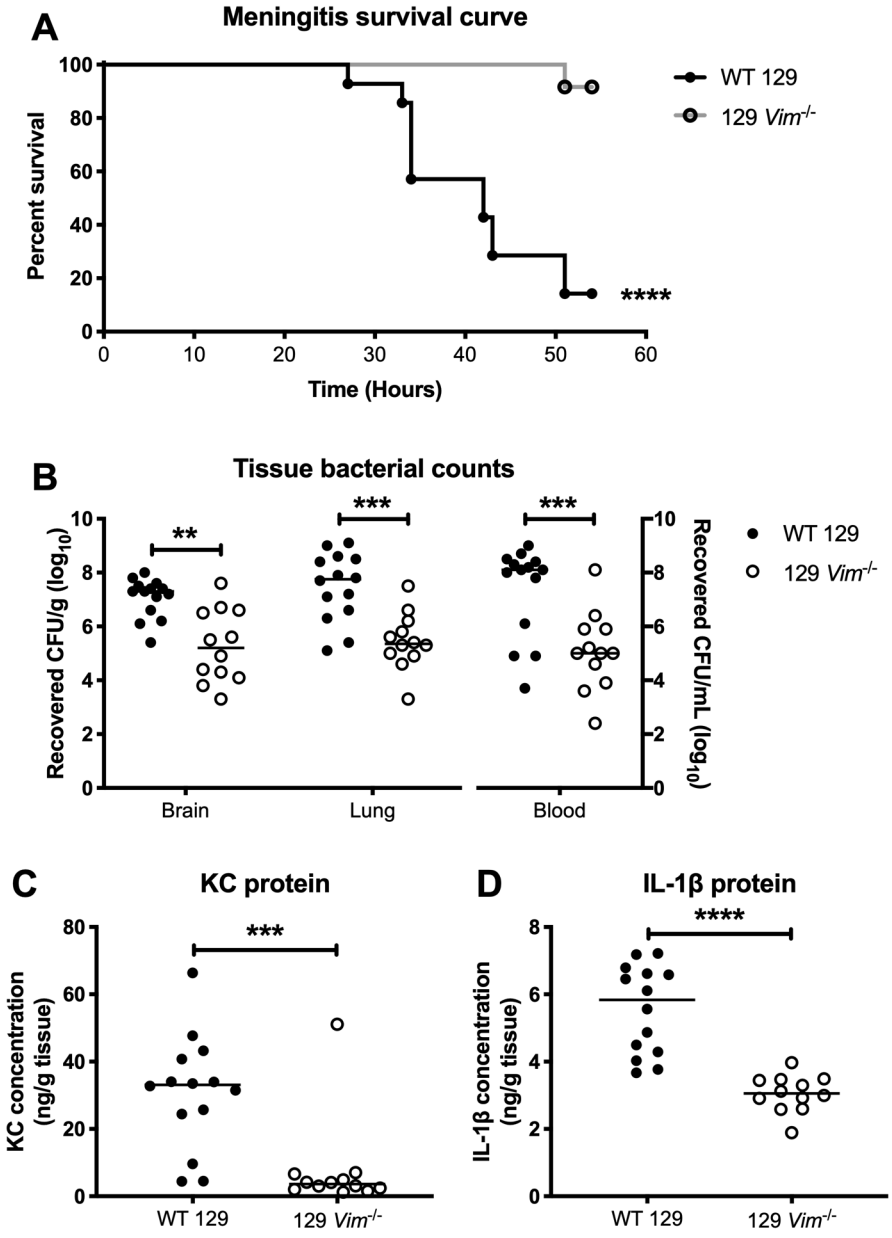

Figure 2.8. Vimentin contributes to the pathogenesis of GBS infection. (A) Kaplan-Meier plot showing survival of WT 129 and 129 *Vim*$^{-/-}$ mice infected with 10^8 CFU of WT GBS. (B) Tissue bacterial counts for WT 129 and 129 *Vim*$^{-/-}$ mice infected with WT GBS. (C and D) ELISA to quantify KC (C) and IL-1β (D) protein in brain tissue homogenates. Statistical analysis: (A) Log-rank test. (B-D) Mann-Whitney test. **, $P < 0.005$; ***, $P < 0.0005$; ****, $P < 0.00005$.

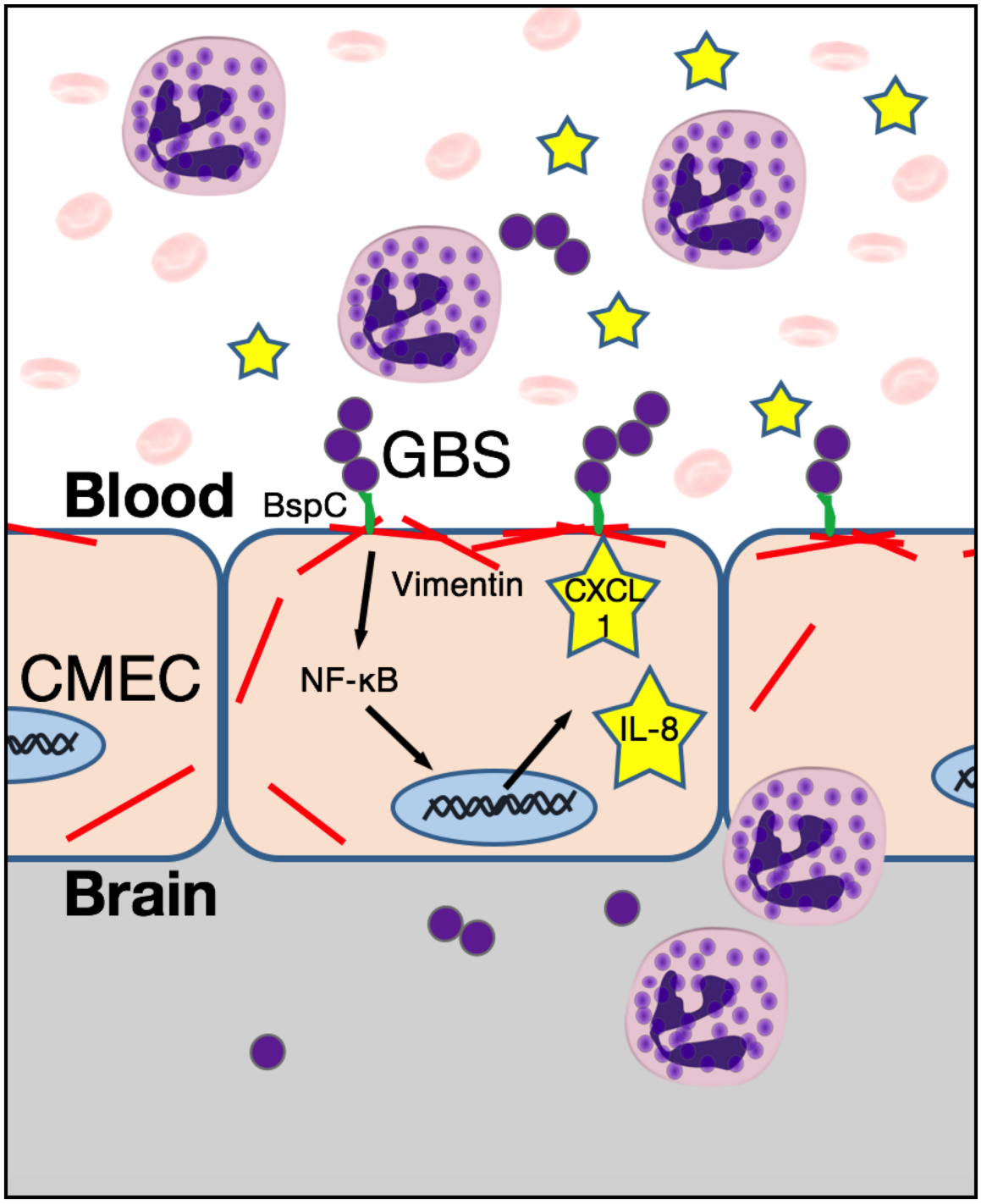

Figure 2.9. Summary of the role of the BspC-vimentin interaction in promoting meningitis. BspC interacts with vimentin on the surface of CMEC to promote GBS attachment and the production of the neutrophil recruiting cytokines IL-8 and CXCL-1 through the NF-κB pathway.

DISCUSSION

Our studies reveal a unique requirement for the Group B streptococcal Antigen I/II protein, BspC, to brain penetration by GBS, the leading agent of neonatal bacterial meningitis. A decreased ability by the GBS Δ*bspC* mutant to attach to brain endothelium and induce neutrophil chemoattractants *in vitro* was correlated with a reduced risk for development of meningitis and markedly diminished lethality *in vivo*. We identified that BspC interacts directly with host vimentin and that blocking this interaction abrogated BspC-mediated attachment to hCMEC. Further, vimentin deficient mice infected with GBS exhibited decreased mortality, bacterial brain loads, and cytokine production in brain tissue. These results corroborate the growing evidence that this intermediate filament protein plays important roles in the pathogenesis of bacterial infections (38), and provide new evidence for the pivotal role of the BspC adhesin in GBS CNS disease (Fig. 8).

The oral streptococcal AgI/II adhesins range in composition from 1310 - 1653 amino acid (AA) residues, while GBS AgI/II proteins are smaller (826-932 AA residues) (39). The primary sequences of AgI/II proteins are comprised of six distinct regions (Fig. 1B), several of which have been shown to mediate the interaction to various host substrates. The *S. mutans* protein SpaP as well as the *S. gordonii* proteins SspA and SspB have been demonstrated to interact specifically with the innate immunity scavenger protein gp-340. (40) Recently, the GAS AgI/II protein AspA, as well as BspA, the AgI/II homolog expressed mainly by the GBS strain NEM316, have also been shown to bind to immobilized gp-340 (15, 18). Gp-340 proteins are involved in various host innate defenses and are present in mucosal secretions, including saliva in the oral cavity and bronchial alveolar fluid in the lung. They can form complexes with other mucosal components such as mucins and function to trap microbes for clearance. However, when gp-340 is immobilized, it can

be used by bacteria as a receptor for adherence to the host surface. (15, 41-44). There is evidence that the Variable (V) regions of SspB, SpaP, AspA and BspA facilitate gp340-binding activity (15, 45-47). AgI/II family adhesins have also been shown to interact with other host factors including fibronectin, collagen, and β1 integrins to promote host colonization (14, 48-50), demonstrating the multifactorial nature of these adhesins. It is unknown if GBS BspC interactions with other host factors are similar to those of the AgI/II proteins from other streptococci, particularly since the respective V-domains of these homologs are distant enough to suggest different binding partners. Previous work by Chuzeville *et al*. suggests that the integrative and conjugative element which contains the *bspC* gene can contribute to bacterial adherence to fibrinogen (19). Our MST experiments reveal the K_d for the interaction between BspC and vimentin to be 3.39 μM. This binding affinity is very similar to that observed for other multifunctional bacterial adhesins and their various host ligands. For example, the K_d for the interaction between fibronectin-binding protein B of *Staphylococcus aureus* and fibrinogen, elastin, and fibronectin has been demonstrated to be 2 μM, 3.2 μM, and 2.5 μM, respectively (51). Whether BspC can promote adherence to other host factors requires further investigation as these interactions may be critical to GBS colonization of mucosal surfaces such as the gut and the vaginal tract.

Here we show that GBS BspC interacts with host vimentin, an important cytoskeletal protein belonging to class III intermediate filaments. Vimentin is located in the cytoplasm and functions as an intracellular scaffolding protein that maintains structural and mechanical cell integrity (52). However, vimentin is also found on the surface of numerous cells such as T cells, platelets, neutrophils, activated macrophages, vascular endothelial cells, skeletal muscle cells and brain microvascular endothelial cells (53-60). Vimentin also mediates a variety of cell processes including cell adhesion, immune signaling, and autophagy (55, 61, 62). Further, the role of cell

surface vimentin as an attachment receptor facilitating bacterial or viral entry, has been previously documented for other pathogens (38, 63-65). The BspC domain that mediates the vimentin interaction is currently under investigation. As the V domain is likely projected from the cell surface and has been implicated in host interactions for other streptococci, we hypothesize that this may be a critical domain for this interaction. Additionally, as the V-domain of other Bsp homologs share 96-100% identity with the V-domain of BspC, we predict that the other Bsp proteins might also interact with vimentin, but this would be a topic for future investigation.

There is a growing body of evidence that various bacteria can interact with vimentin to promote their pathogenesis, including *Escherichia coli* K1, *Salmonella enterica*, *Streptococcus pyogenes*, and *Listeria monocytogenes*. Thus, vimentin has been shown to be important in experimental models of infection at body sites other than the brain (38, 57, 60, 66, 67). Interestingly, previous studies on the meningeal pathogen *E. coli* K1 have demonstrated that the bacterial surface factor, IbeA, interacts with vimentin to promote bacterial uptake into brain endothelial cells (60, 68). Similarly, while our study was underway, it was reported that another bacterium capable of causing meningitis, *L. monocytogenes,* uses InlF to interact with vimentin to promote brain invasion (67). Along with our results presented here, this may suggest a common mechanism for meningeal bacterial pathogens to penetrate the BBB and cause CNS disease. However, our analysis of these three bacteria proteins showed no homology or predicted regions that might commonly interact with vimentin. Furthermore, the interaction between the *E. coli* receptor IbeA and the *L. monocytogenes* receptor InlF with cell-surface vimentin can be blocked by an antibody to the N-terminal region of vimentin (60, 67), while we demonstrate that the interaction between BspC and cell-surface vimentin can be blocked with an antibody to the C-terminal of vimentin. The implications of this unique interaction between a bacterial receptor and

the C-terminal of vimentin remain to be explored.

Neuronal injury during bacterial meningitis involves both microbial and host factors, and subsequent to attachment to the brain endothelium and penetration of the BBB, GBS stimulation of host immune pathways is the next important step in the progression of meningitis. The release of inflammatory factors by brain endothelial cells, microglia, astrocytes, and infiltrating immune cells can exacerbate neuronal injury (9). Our data suggest that, like other streptococcal AgI/II family polypeptides, BspC plays a role in immune stimulation. AgI/II family proteins contain two antigenic regions (the antigens I/II and II) (69) and this ability to elicit an inflammatory response makes SpaP, the *S. mutans* AgI/II protein, an attractive candidate for vaccine development to prevent dental caries (14, 70). In this study we found that BspC can stimulate NF-κB activation and the release of the proinflammatory cytokines IL-8 and CXCL-1 from hCMEC. Both of these chemokines are major neutrophil recruiting chemoattractants and are the most highly induced during GBS infection (27, 71). We observed that mice infected with GBS mutants that lack BspC exhibited lower brain bacterial loads and less meningeal inflammation compared to animals challenged with WT GBS. Interestingly, WT and Δ*bspC* mutant bacterial loads were similar in the blood, indicating that BspC may not influence GBS survival and proliferation in the blood; however further investigation is warranted.

This study demonstrates for the first time the importance of a streptococcal AgI/II protein, BspC, in the progression of bacterial meningitis. Our data demonstrate that BspC, likely in concert with other GBS surface determinants mentioned above (pili, Srr1/2, SfbA), contributes to the critical first step of GBS attachment to brain endothelium. As the other described GBS surface factors have been shown to interact with ECM components, BspC may mediate a more direct interaction with the host cell as it facilitates interaction with vimentin. We have observed a unique

requirement for vimentin to the pathogenesis of CNS disease; vimentin KO mice were markedly less susceptible to GBS infection and exhibited reduced bacterial tissue load and inflammatory signaling. Vimentin is also known to act as a scaffold for important signaling molecules and mediates the activation of a variety of signaling pathways including NOD2 (nucleotide-binding oligomerization domain-containing protein 2) and NLRP3 (nucleotide-binding domain, leucine-rich-containing family pyrin domain-containing-3) that recognize bacterial peptidoglycan and activate inflammatory response via NF-κB signaling (68, 72, 73). Thus, continued investigation into the mechanisms of how BspC-vimentin interactions dually promote bacterial attachment and immune responses, as well as how BspC expression may be regulated and whether known GBS two-component systems are involved, is warranted. These studies will provide important information that may inform future therapeutic strategies to limit GBS disease progression.

MATERIALS AND METHODS

Ethics statement.

Animal experiments were approved by the committee on the use and care of animals at San Diego State University (SDSU) protocol #16-10-021D and at University of Colorado School of Medicine protocol #00316 and performed using accepted veterinary standards. San Diego State University and the University of Colorado School of Medicine are AAALAC accredited; and the facilities meet and adhere to the standards in the "Guide for the Care and Use of Laboratory Animals".

Bacterial strains, growth conditions, proteins, and antibodies.

GBS clinical isolate COH1 (serotype III) (74), 515 (serotype Ia) (20), the recent meningitis isolate 90356 (serotype III) (75) and their isogenic Δ*bspC* mutants were used for the experiments. GBS strains were grown in THB (Hardy Diagnostics) at 37°C, and growth was monitored by measuring the optical density at 600 nm (OD_{600}). *Lactococcus lactis* strains were grown in M17 medium (BD Biosciences) supplemented with 0.5% glucose at 30°C. For antibiotic selection, 2 μg/mL chloramphenicol (Sigma) and 5 μg/mL erythromycin (Sigma) were incorporated into the growth medium. BspC and CshA recombinant proteins, and the BspC antibody were purified as described previously (15, 76). The anti-BspC polyclonal antibody was further adsorbed (as described in (77)) against COH1Δ*bspC* bacteria to remove natural rabbit antibodies that react with bacterial surface antigens. Briefly, anti-BspC antibody was diluted to 2.28 mg/mL in PBS and incubated with COH1Δ*bspC* bacteria overnight at 4ºC, with rotation. Bacteria were pelleted by centrifugation and the supernatant was collected and filtered using 0.22 μM cellulose acetate

SpinX centrifuge tube filters (Costar). A normal rabbit IgG antibody (Invitrogen) was adsorbed as described above, and utilized as a negative isotype control.

Targeted mutagenesis and *complementation* vector construction.

The Δ*bspC* mutant was generated in COH1and 90356 by in-frame allelic replacement with a chloramphenicol resistance cassette by homologous recombination using a method previously described (10). A knockout construct was generated by amplifying up- and down-flanking regions of the *bspC* gene from COH1 genomic DNA using primer pairs of 5'flank-F (GCAGACACCGATTGCACAAGC)/R (GAAGGCGATCTTGCCCTCAA) and 3'flank-F (GTCAGCTATCGGTTTAGCAGG)/R(CTATACACGCCTACAGGTGTC). The chloramphenicol resistance (*cat*) cassette was amplified with primers Cat-F (GAGGGCAAGATCGCCTTCATGGAGAAAAAAATCACTGGAT) and Cat-R (CTGCTAAACCGATAGCTGACTTACGCCCCGCCCTGCCACT). Then the construct of two flanks along with the *cat* cassette was amplified with a pair of nest primers, Nest-xhoI (CCFCTCGAGGATGCTCAAGATGCACTCAC) and Nest-xbaI (GCTCTAGACGAGCCAAATTACCCCTCCT), which was then cloned into the pHY304 vector (78) and propagated in *E. coli* strain DH5α (79) prior to isolation and transformation to COH1 and 90356 GBS. A Δ*bspC* mutant had been generated previously in 515 (20). The complemented strain of Δ*bspC* mutant in COH1 was generated by cloning *bspC* into pDCerm, an *E. coli*-GBS shuttle expression vector. Gene *bspC* was amplified from GBS 515 genomic DNA using primers pDC.*bspC*.F (TGGGTACCAGGAGAAAATATGTATAAAAATCAAAC) and pDC.*bspC*.R (CCGGGAGCTCGCAGGTCCAGCTTCAAATC), designed to encode a *Kpn*I and *Sac*I restriction site at its termini respectively. This *bspC* amplicon was then cloned into pDCerm and

propagated in *E. coli* strain Stellar™ (ClonTech), prior to isolation and transformation into COH1 GBS. A *L. lactis* strain expressing BspC had been generated previously (20).

Hemolysis assay.

GBS strains were grown to an OD_{600} of 0.4, harvested by centrifugation, and resuspended in PBS. A total of 1 x 10^8 CFU was added to fresh sheep blood (VWR) in V-bottom 96-well plates (Corning). The plates were sealed and incubated at 37°C with agitation for 1 h. The plates were centrifuged at 200 x *g* for 10 min, and 100 µl of the supernatant was transferred to a flat-bottom 96-well plate. The absorbance at 541 (A_{541}) was read, and percent hemolysis was calculated by comparing the A_{541} values for GBS-treated wells to the A_{541} values for the wells with blood incubated with water.

GBS BspC and capsule flow cytometry.

Flow cytometry to determine BspC and capsule expression was performed as described in (80). Briefly, bacterial stocks were washed in sterile PBS containing 0.5% bovine serum albumin (BSA) (VWR) then incubated with a purified monoclonal anti-serotype III antibody or a purified monoclonal anti-serotype Ia isotype control at a 1:10,000 dilution, washed via centrifugation, and labeled with a donkey anti-mouse IgM conjugated to AlexaFluor647 (Invitrogen) at a 1:2,000 dilution. All incubations were performed at 4°C with shaking. Samples were washed again then resuspended and read on a FACScalibur flow cytometer (BD Biosciences), and analyzed using FlowJo (v10) software. The monoclonal antibodies were provided by John Kearney at the University of Alabama at Birmingham.

To stain for surface BspC expression, GBS were grown to OD_{600} of 0.25 in EndoGRO-MV culture medium (Millipore) in order to mimic host infection conditions, pelleted by centrifugation, resuspended in PBS and frozen *L. lactis* strain stocks were thawed and washed in buffer. Approximately, 1 x 10^6 CFU of each strain was incubated with either adsorbed anti-BspC antibody or adsorbed anti- rabbit IgG at a 1:50 dilution at 4º C, overnight, with rotation. The next day, bacteria were washed via centrifugation, and labeled with a donkey anti-rabbit IgG conjugated to AlexaFluor488 (Invitrogen) at a 1:2,000 dilution for 45 minutes at room temperature with rotation. Samples were washed again then resuspended and read on a FACScalibur flow cytometer (BD Biosciences), and analyzed using FlowJo (v10) software.

Immunofluorescent staining of GBS.

Bacteria were grown to an OD_{600} of 0.25 in EndoGRO-MV culture medium (Millipore), the bacteria suspension was smeared on charged glass slides (Fisher), and the slides were fixed with 4% paraformaldehyde for 30 min at room temperature. The slides were blocked with 3% BSA for 1 hour, then incubated with rabbit antibodies to BspC or IgG at a 1:50 dilution followed by donkey anti-rabbit conjugated to AlexaFluor488 (Invitrogen). Bacteria were imaged using a BZ-X710 fluorescent microscope (Keyence).

Scanning electron microscopy.

Bacteria were grown to log phase and were then fixed for 10 min using a one-step method with 2.5% glutaraldehyde, 1% osmium tetraoxide, 0.1M sodium cacodylate. Bacteria were collected on 0.4 μM polycarbonate filters by passing the solution through a swinnex device outfitted on a 10 mL syringe. The filters were dehydrated through a series of increasing ethanol

concentrations and then dried in a Tousimis SAMRI-790 critical point drying machine. The dried filters were mounted on SEM sample stubs with double-sided carbon tape, coated with 6nm platinum using a Quorom Q150ts high-resolution coater and imaged with a FEI FEG450 scanning electron microscope.

Cell lines and infection assays.

Cells of the well-characterized human cerebral microvascular endothelial cell line (hCMEC/D3), referred to here as hCMEC were obtained from Millipore and were maintained in an EndoGRO-MV complete medium kit supplemented with 1 ng/ml fibroblast growth factor-2 (FGF-2; Millipore) (81-84). Hela57A were provided by Marijke Keestra-Gounder at the University of Colorado, Anschutz Medical Campus and cultured in DMEM (Corning Cellgro) containing 10% fetal bovine serum (Atlanta Biologicals). HEK293T cells were obtained from Origene and cultured in DMEM containing 10% fetal bovine serum and 2mM L-glutamine (Thermo Fisher). The lentiviral expression plasmid pLenti-C-Myc-DDK harboring the human vimentin gene (NM_003380, pLenti-VIM) was obtained from Origene. To generate lentiviruses, HEK293T cells were transfected with the pLenti-VIM plasmid in combinations with the packaging plasmid psPAX2 and the envelope plasmid pMD2.G (Addgene) using TransIT_293 transfection reagent (Mirus). After an 18 h incubation, the culture supernatant containing lentiviruses was harvested and filtered through a 0.45 μm syringe filter to remove cellular debris. The viral titer was 10^6 to 10^7 transduction units (TU) per mL. 10^5 fresh HEK293T cells were infected with lentiviruses at a MOI of 5 for 24 h in the presence of 10 μg/mL polybrene (Sigma). The empty lentiviral expression plasmid pLenti-mock was used as a vector control. Assays to determine the total number of cell surface-adherent or intracellular bacteria were performed as describe

previously (10). Briefly, bacteria were grown to mid-log phase to infect cell monolayers (1×10^5 CFU, at a multiplicity of infection [MOI] of 1). Total cell-associated GBS and *L. lactis* were recovered following a 30 min incubation, while intracellular GBS were recovered after 2 h infection and 2 h incubation with 100 μg gentamicin (Sigma) and 5 μg penicillin (Sigma) to kill all extracellular bacteria. Cells were detached with 0.1 ml of 0.25% trypsin-EDTA solution and lysed with addition of 0.4 ml of 0.025% Triton X-100 by vigorous pipetting. The lysates were then serially diluted and plated on THB agar to enumerate bacterial CFU. For antibody pre-treatment assays, hCMEC were incubated with 0.3μg/ml antibodies for 30 min prior to infection with GBS. The mouse monoclonal antibody to vimentin, clone V9 (Abcam), the rabbit polyclonal antibody to N-terminal vimentin (Sigma), and the isotype controls (VWR) were used. Total cell-associated GBS were recovered following a 1h incubation. For luciferase assays, Hela57A cells were infected with 1 x 10^6 CFU (MOI, 10) GBS for 90 min. Cells were then lysed and luciferase activity quantified using a luciferase assay system (Promega) according to manufacturer's instructions.

Mouse model of hematogenous GBS meningitis.

We utilized a mouse GBS infection model as described previously (10, 26, 27). Briefly, 8-week old male CD-1 mice (Charles River), 129S WT, or 129S-*Vim*^{tm1Cba}/MesDmarkJ (Vimentin KO) (Jackson Laboratory) were injected intravenously with 1×10^9 CFU of wild-type GBS or the isogenic Δ*bspC* mutant for a high dose challenge, or 1×10^8 CFU for a low dose challenge. At the experimental endpoint mice were euthanized and blood, lung, and brain tissue were collected. The tissue was homogenized, and the brain homogenates and lung homogenates as well as blood were plated on THB agar for enumeration of bacterial CFU.

Histology.

Mouse brain tissue was frozen in OCT compound (Sakura) and sectioned using a CM1950 cryostat (Leica). Sections were stained using hematoxylin and eosin (Sigma) and images were taken using a BZ-X710 microscope (Keyence).

Brain flow cytometry.

At 48 h post-infection with 1×10^8 CFU of GBS, mice were euthanized then perfused to replace blood with PBS. The entire mouse brain was harvested from each animal and the tissue was processed with the Multi-Tissue Dissociation kit #1 following the Adult brain dissociation protocol (Miltenyi Biotec). Cells were resuspended in MACS buffer (Miltenyi Biotec) and incubated with antibodies to Ly6C conjugated to BV421, CD45 conjugated to PE, CD11b conjugated to FITC, and Ly6G conjugated to APC (Invitrogen) at 1:200 dilution, UltraLeaf anti-mouse CD16/CD32 Fc block (Biolegend) at 1:400 dilution, and fixable viability dye conjugated to eFLuor506 (eBioscience) at 1:1000 dilution for 1 h, then fixed (eBioscience). Cells were counted using a Countess automated cell counter (Invitrogen), read on a Fortessa X-20 flow cytometer (BD Biosciences), and analyzed using FlowJo (v10) software. Gates were drawn according to fluorescence minus one (FMO) controls.

RT-qPCR and ELISA.

GBS were grown to mid-log phase and 1×10^6 CFU (MOI, 10) were added to hCMEC monolayers and incubated at 37°C with 5% CO_2 for 4 h. Cell supernatants were collected, the cells were then lysed, total RNA was extracted (Machery-Nagel), and cDNA was synthesized (Quanta Biosciences) according to the manufacturers' instructions. Primers and primer efficiencies for IL-

8, CXCL-1, and GAPDH (glyceraldehyde-3-phosphate dehydrogenase) were utilized as previously described (85). IL-8 and CXCL-1 from hCMEC supernatants, and KC and IL-1β from mouse brain homogenates were detected by enzyme-linked immunosorbent assay according to the manufacturer's instructions (R&D systems).

Immunofluorescent staining of hCMEC and HEK293T cells.

hCMEC were grown to confluency on collagenized coverslips (Fisher). Following a 1 h infection, cells were washed with PBS to remove non-adherent bacteria and fixed with 4% paraformaldehyde (Sigma) for 30 min. For Figure 4, cells were incubated with 1% BSA in PBS with 0.01% Tween-20 (Research Products International) to block non-specific binding for 15 min, then incubated with a rabbit antibody to p65 (Sigma) at a 1:200 dilution overnight at 4°C. Coverslips were then washed with PBS and incubated with donkey anti-rabbit conjugated to Cy3 (Jackson Immunoresearch) at a 1:500 dilution for 1 h at room temperature. For Figure 6, cells were incubated with 1% BSA in PBS for 15 min, then with antibodies to vimentin (Abcam) and GBS (Genetex) at a 1:200 dilution overnight at 4°C. Following washes with PBS and an incubation with donkey anti-mouse conjugated to Cy3 and donkey anti-rabbit conjugated to 488 secondary antibodies (ThermoFisher) at a 1:500 dilution for 1 h at room temperature, coverslips were washed with PBS and mounted onto glass microscopy slides (Fisher) with VECTASHIELD mounting medium containing DAPI (Vector Labs). Cells were imaged using a BZ-X710 fluorescent microscope (Keyence). Quantification of GBS and vimentin co-localization was performed by counting the number of GBS that co-localized with vimentin and dividing by the total number of GBS in each field. For figure 7, HEK293T cells were incubated with the antibody to vimentin

followed by a FITC-conjugated secondary antibody. Cells were imaged using a Cytation 5 fluorescent microplate reader (BioTek).

2-dimensional electrophoresis (2-DE), Far Western blot, and mass spectrometry analysis.

Membrane proteins of hCMEC cells were enriched using a FOCUS membrane protein kit (G Biosciences, St. Louis, MO), dissolved in rehydration buffer (7M urea, 2M thiolurea, 1% TBP, and 0.2% ampholytes 3-10 NL), and quantified using 2D Quant kit (GE Healthcare, Piscataway, NJ). Proteins (100µg) were loaded on 7-cm long immobilized pH gradient (IPG) strips with non-linear (NL) 3-10 pH gradient (GE Healthcare). Isoelectric focusing was carried out in Multiphor II electrophoresis system (GE Healthcare) in three running phase (phase 1: 250V/0.01h, phase 2: 3500V/1.5h, and phase 3: 3500V/ 4.5h). The second dimension SDS-PAGE was carried out using 12.5% acrylamide gels in duplicate. One gel was stained with Coomassie Blue G250 (Bio-Rad, Hercules, CA) for mass spectrometry analysis. The other gel was transferred to a PVDF membrane for far Western blot analysis.

The PVDF membrane was denaturated and renaturated as described in (86), followed by incubation in a blocking solution (5% skim milk in PBS) for 1 h. Recombinant BspC was biotinylated using a EZ-Link Sulfo-NHS-Biotin kit (ThermoFisher Scientific, Waltham, MA). The PVDF membrane was probed with the biotinylated BspC (100µg) in a blocking solution overnight at 4°C. After washing three times with a washing buffer (PBS, 0.05% Tween-20), the PVDF membrane was incubated with an antibody conjugated to streptavidin-horse radish peroxidase (HRP). Interacting proteins were detected by adding enhanced chemiluminescence (ECL) reagents (ThermoFisher Scientific) and visualized by x-ray film exposure. The protein spots from far Western blot were aligned to the corresponding protein spots in the Coomassie stained gel. The

identified spots were excised and digested in gel with trypsin (Worthington, Lakewood, NJ). Peptide mass spectra were collected on MALDI-TOF/TOF, (ABI 4700, AB Systems, Foster City, CA) and protein identification was performed using the automated result dependent analysis (RDA) of ABI GPS Explorer softwareV3.5. Spectra were analyzed by the Mascot search engine using the Swiss protein database.

Bacterial two-hybrid assay.

A bacterial adenylate cyclase two-hybrid assay was performed as in (32) and following manufacturer's instructions (Euromedex). Briefly, plasmids containing T25-Vimentin and BspC-T18 were transformed into *E. coli* lacking *cyaA* and *E. coli* were plated on LB plates containing X-gal (Sigma). To measure β -galactosidase activity, Miller assays were performed according to standard protocols (87). Briefly, *E. coli* were grown in 0.5mM IPTG (Sigma), then permeabilized with 0.1% SDS (Sigma) and toluene (Sigma). ONPG (Research Products International) was added and absorbance was measured at 600, 550, and 420nm.

Microscale thermophoresis.

Three independent MST experiments were performed with His-tagged BspC labelled using the Monolith His-Tag Labeling Kit RED-tris-NTA 2nd Generation (NanoTemper Technologies) according to manufacturer's instructions. The concentration of labelled BspC was kept constant at 10nM. Vimentin was purchased from Novus Biologicals and titrated in 1:1 dilutions to obtain a series of 16 titrations ranging in concentration from 20 μM to 0 μM. Measurements were performed in standard capillaries with a Monolith NT.115 Pico system at 20% excitation power and 40% MST power (NanoTemper Technologies).

Imaging flow cytometry.

Following a 1 h infection with GBS, hCMEC were washed with PBS to remove non-adherent GBS. Cells were collected using a cell scraper (VWR) and resuspended in PBS containing 10% FBS and 1% sodium azide (Sigma). Cells were incubated with primary antibodies to vimentin (Abcam) and GBS (Genetex) at 1:500 dilution for 1 h at 4°C followed by donkey anti-mouse conjugated to Cy3 and donkey anti-rabbit conjugated to 488 (ThermoFisher) secondary antibodies. Cells were then fixed (eBioscience) and analyzed using an ImageStream X imaging flow cytometer (Amnis).

Data analysis.

GraphPad Prism version 7.0 was used for statistical analysis and statistical significance was accepted at P values of <0.05. (*, $P < 0.05$; **, $P < 0.005$; ***, $P < 0.0005$; ****, $P < 0.00005$). Specific tests are indicated in figure legends.

ACKNOWLEDGEMENTS

We thank Dr. Marijke Keestra-Gounder (University of Colorado, Anschutz Medical Campus) for the Hela57A reporter cell line, John Kearney (University of Alabama at Birmingham) for GBS monoclonal antibodies, Tibor Pechan of the Mississippi State University Institute for Genomics, Biocomputing & Biotechnology (IGBB) for assistance with the mass spectrometry, Dr. Felipe Almeida de Pinho-Ribeiro at Harvard Medical School for assistance with brain cell flow cytometry analysis, Jeremy Rakhola at the Rocky Mountain Regional VA Medical Center (RMRVAMC) Flow Core, Shaun Bevers at the University of Colorado Anschutz Medical Campus Biophysics Core, and Catherine Back (University of Bristol, UK) for provision of purified *S gordonii* CshA protein. Also to Katilynn Croom and Jeffrey Kavanaugh for technical support. This study was supported by the Rees Stealy Research Foundation/ SDSU Heart Institute and San Diego Chapter ARCS Scholarships to L.D., the NIH 5T32AI007405-28 to B.L.S., the Coordenação de Aperfeiçoamento de Pessoal de Nível Superior - Brasil (CAPES) - Finance Code 001 to G.F.S., the NIH DE016690 to H.F.J., and the NIH/NINDS R01NS051247 to K.S.D.

Chapter 2, in full, is a reprint of the material as it appears in: Deng L, Spencer BL, Holmes JA, Mu R, Rego S, Weston TA, Hu Y, Sanches GF, Yoon S, Park N, Nagao PE, Jenkinson HF, Thornton JA, Seo KS, Nobbs AH, Doran KS. The Group B streptococcal surface antigen I/II protein, BspC, interacts with host vimentin to promote adherence to brain endothelium and inflammation during the pathogenesis of meningitis. *PLoS Pathog*. 15(6). 2019. The dissertation author was the primary investigator and author of this paper.

SUPPLEMENTAL MATERIALS

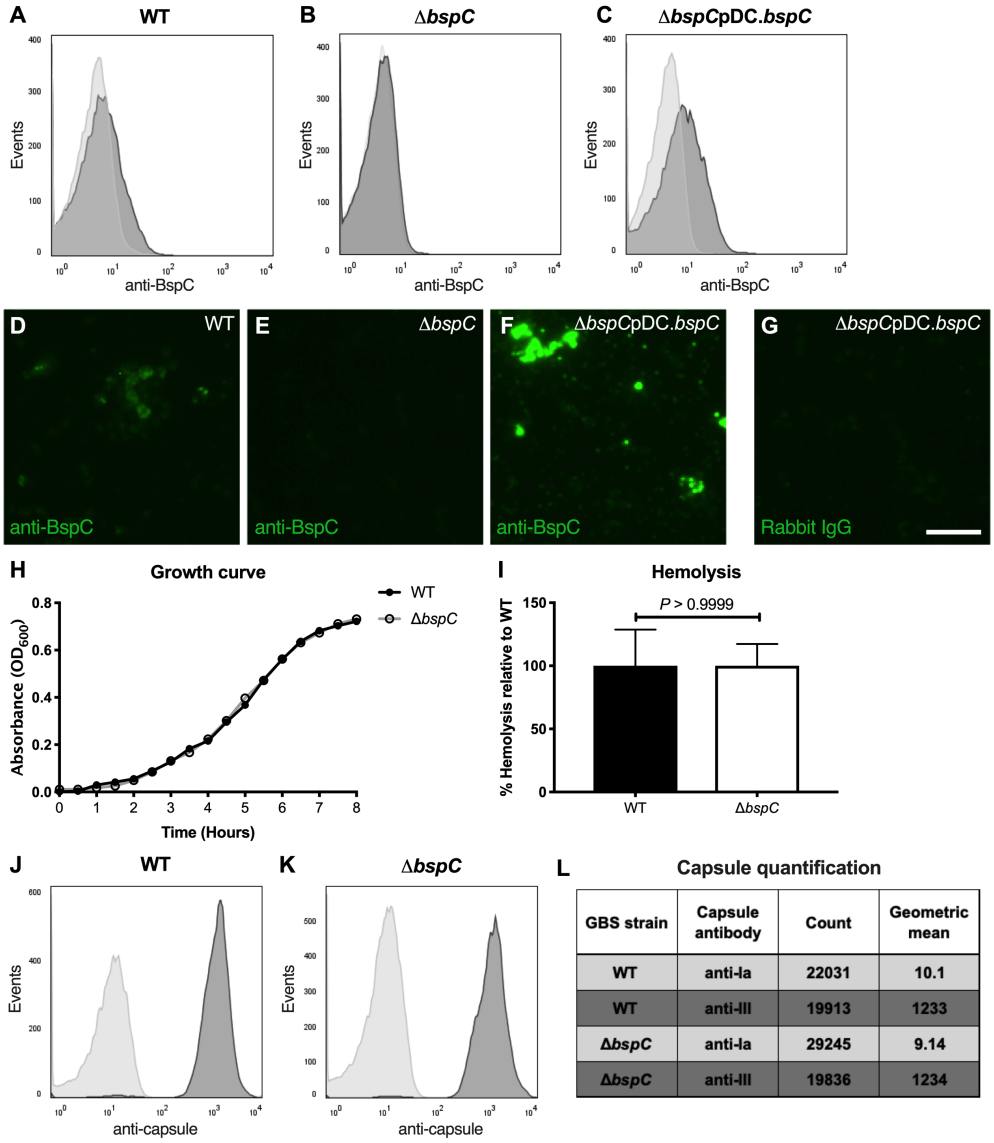

GBS strain	Capsule antibody	Count	Geometric mean
WT	anti-Ia	22031	10.1
WT	anti-III	19913	1233
Δ*bspC*	anti-Ia	29245	9.14
Δ*bspC*	anti-III	19836	1234

Supplemental Figure 2.1. (A-C) Flow cytometry using a polyclonal rabbit antibody to BspC to show expression of BspC in WT COH1 (A), Δ*bspC* mutant (B), and the complemented (C) GBS strains. (D-G) Immunofluorescent staining of WT COH1 (D), Δ*bspC* mutant (E), and the complemented (F) GBS strains using the BspC antibody to show surface localization of BspC protein. (G) Negative staining control. Scale bar is 5 μm. (H) Growth curves for WT GBS and the Δ*bspC* mutant in THB. (I) Hemolysis assay comparing hemolysis of sheep blood by WT GBS and the Δ*bspC* mutant. Representative data of one of at least three independent experiments are shown. Error bars represent the standard deviation of mean in one experiment. Data were analyzed using an unpaired t test. (J and K) Flow cytometry using a monoclonal antibody to the serotype III capsule to determine the presence of capsule in WT GBS (J) and the Δ*bspC* mutant (K) and a monoclonal antibody to the serotype Ia capsule as an isotype control. (L) Quantification of capsule flow cytometry data shown in (J) and (K).

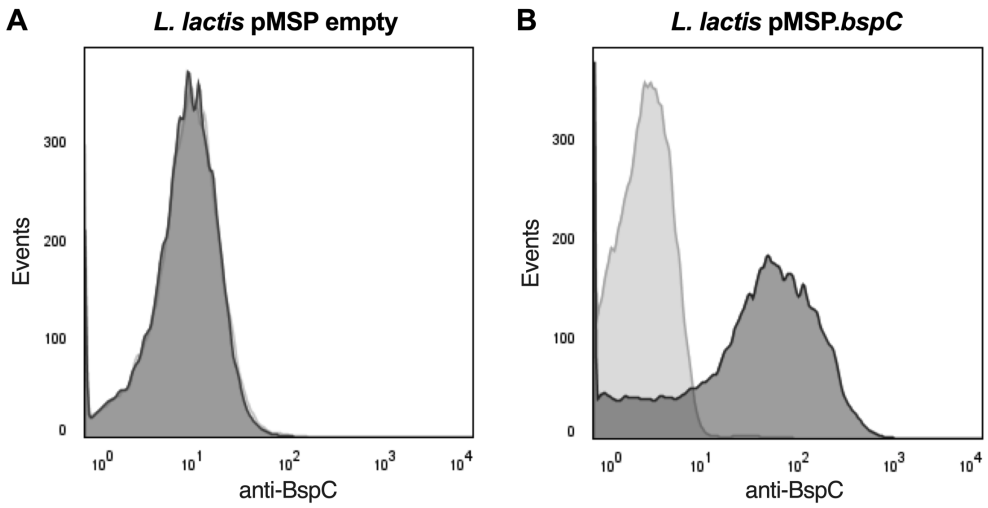

Supplemental Figure 2.2. Flow cytometry to show BspC surface expression in *L. lactis* containing the pMSP empty plasmid (A) and *L. lactis* containing the pMSP.*bspC* vector (B)

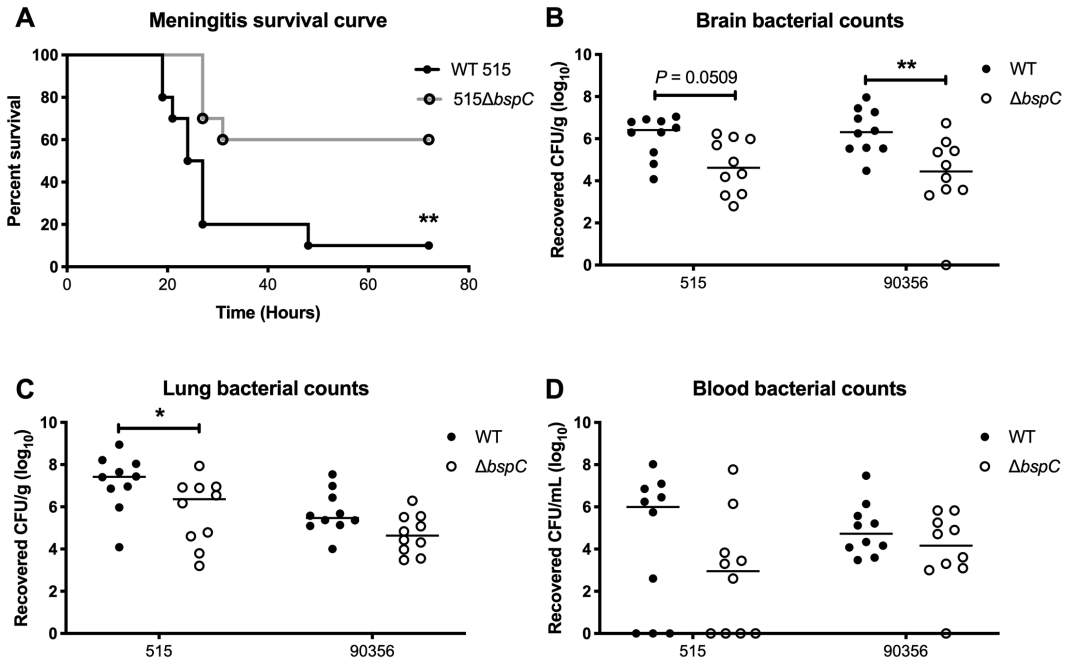

Supplemental Figure 2.3. (A) Kaplan-Meier plot showing survival of mice challenged with either WT 515 GBS or the isogenic Δ*bspC* mutant. (B-D) Tissue bacterial counts for mice infected with WT 515 and 90356 GBS and the isogenic Δ*bspC* mutants. 48h post-infection, mice were sacrificed and bacterial loads in brain (B), lung (C), and blood (D) were quantified. Statistical analysis: (A) Log-rank test. (B-D) Two-way ANOVA with Sidak's multiple comparisons test. ∗, $P < 0.0005$; ∗∗, $P < 0.005$.

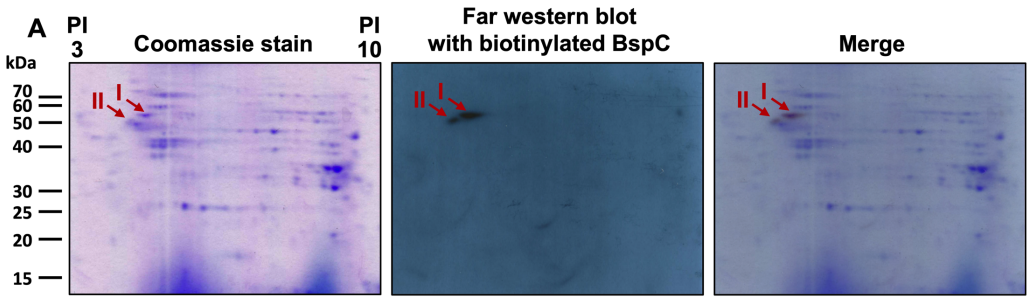

B

Spot	Description	Accession	MW (kDa)	Calc PI	# AAs	# peptides	Coverage (%)
I	Vimentin	gi62414289	53.6	5.12	466	17	29.61
II	Vimentin	gi62414289	53.6	5.12	466	5	18.24

C

MSTRSVSSSS YRRMFGGPGT ASRPSSSRSY VTTSTRTYSL GSALRPSTSR **SLYASSPGGV**
YATRSSAVRL RSSVPGVR**LL QDSVDFSLAD AINTEFK**NTR TNEKVELQEL NDRFANYIDK
VRFLEQQNK**I LLAELEQLK**G QGKSRLGDLY EEEMRELRRQ VDQLTNDKAR VEVERDNLAE
DIMRLREK**LQ EEMLQR**EEAE NTLQSFRQDV DNASLARLDL ERK**VESLQEE IAFLK**KLHEE
EIQELQAQIQ EQHVQIDVDV SKPDLTAALR DVRQQYESVA AKNLQEAEEW YKSKFADLSE
AANRNNDALR QAKQESTEYR **RQVQSLTCEV DALK**GTNESL ER**QMREMEEN FAVEAANYQD**
TIGRLQDEIQ NMKEEMARHL REYQDLLNVK **MALDIEIATY R**KLLEGEESR **ISLPLPNFSS**
LNLRETNLDS LPLVDTHSKR TLLIKTVETR DGQVINETSQ HHDDLE

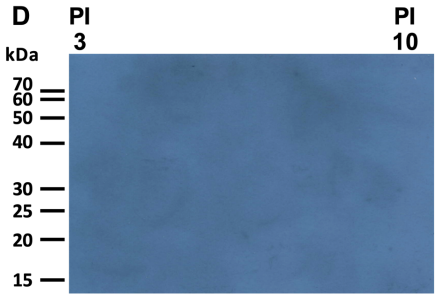

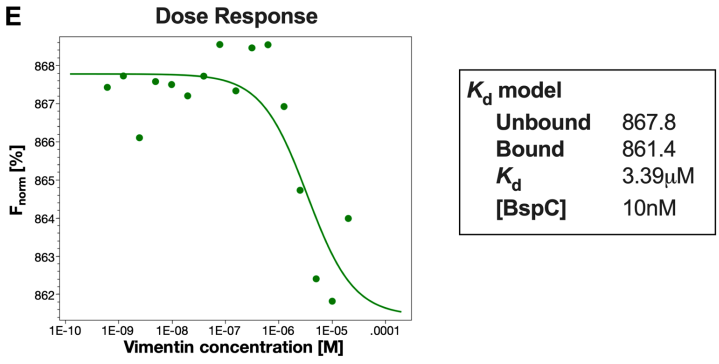

Supplemental Figure 2.4. (A) Far Western blot analysis of hBMEC membrane proteins using biotinylated BspC protein. Two spots (I and II) were identified on the x-ray film and aligned to the Coomassie stained gel. (B) Electrospray ionization-tandem mass spectrometry identifies spots I and II as vimentin. (C) The amino acid sequence of human vimentin, with the peptide sequences identified in the MS analysis underscored and bolded. (D) Control Far Western blot with the streptavidin antibody conjugated to HRP only. (E) Representative MST dose response curve quantifying the dissociation constant for the interaction between BspC and vimentin.

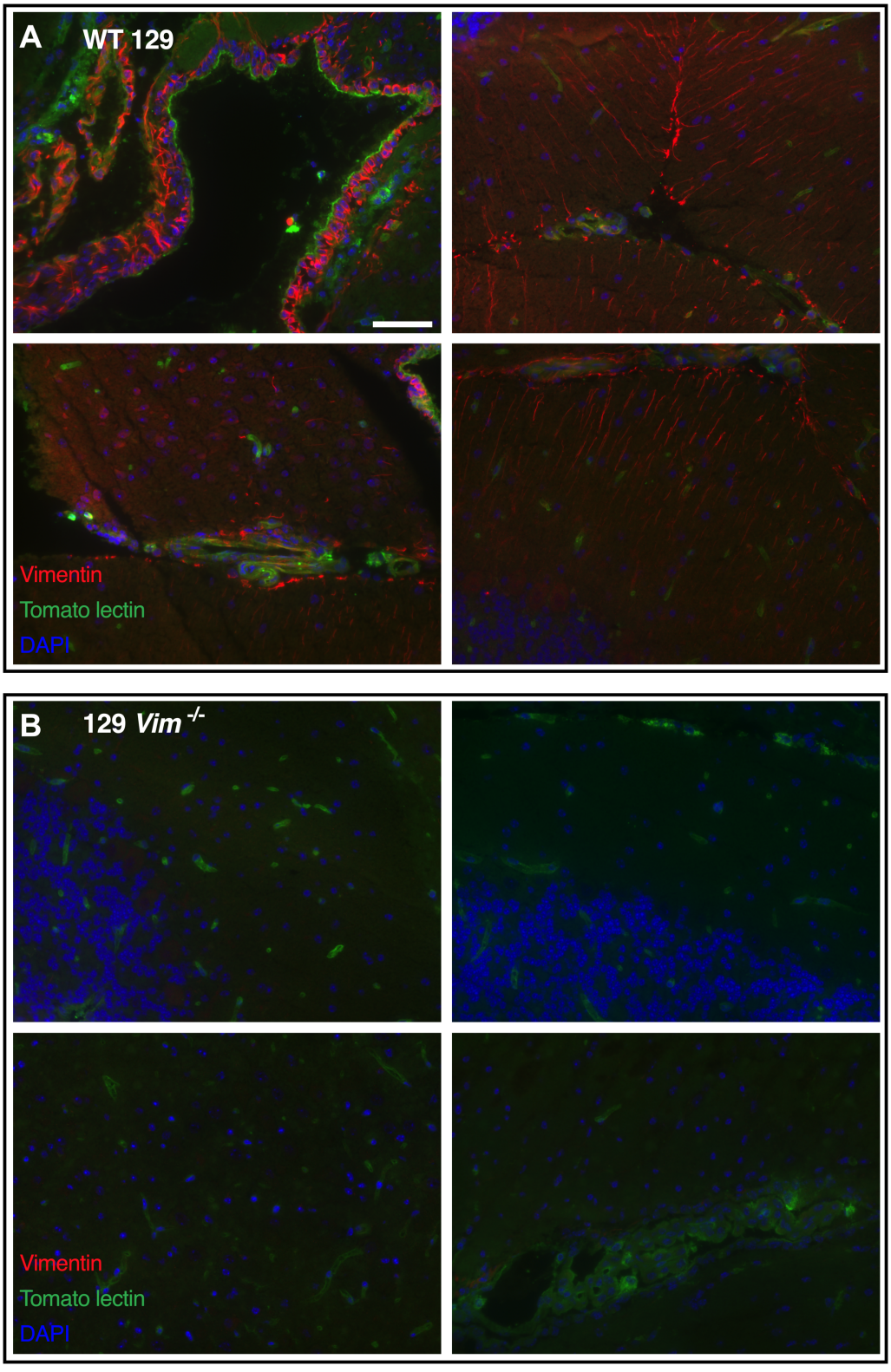

Supplemental Figure 2.5. Immunofluorescent staining of WT 129 (A) and 129 *Vim*$^{-/-}$ (B) brain tissue sections with an antibody to vimentin and with tomato lectin to label blood vessels. Nuclei were labelled with DAPI. Scale bar is 50 μm.

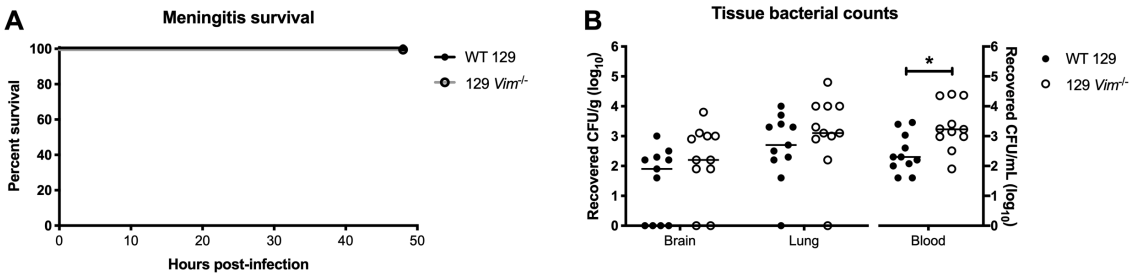

Supplemental Figure 2.6. (A) Kaplan-Meier plot showing survival of WT 129 mice or 129 *Vim*$^{-/-}$ mice challenged with GBS Δ*bspC* mutant. (B) 48h post-infection, mice were sacrificed and bacterial loads in brain, lung, and blood were quantified.

REFERENCES

1. **Thigpen MC, Whitney CG, Messonnier NE, Zell ER, Lynfield R, Hadler JL, Harrison LH, Farley MM, Reingold A, Bennett NM, Craig AS, Schaffner W, Thomas A, Lewis MM, Scallan E, Schuchat A, Emerging Infections Programs N.** 2011. Bacterial meningitis in the United States, 1998-2007. N Engl J Med **364:**2016-2025.

2. **Doran KS, Nizet V.** 2004. Molecular pathogenesis of neonatal group B streptococcal infection: no longer in its infancy. Mol Microbiol **54:**23-31.

3. **Abbott NJ, Patabendige AA, Dolman DE, Yusof SR, Begley DJ.** 2010. Structure and function of the blood-brain barrier. Neurobiol Dis **37:**13-25.

4. **Engelhardt B, Sorokin L.** 2009. The blood-brain and the blood-cerebrospinal fluid barriers: function and dysfunction. Semin Immunopathol **31:**497-511.

5. **Redzic Z.** 2011. Molecular biology of the blood-brain and the blood-cerebrospinal fluid barriers: similarities and differences. Fluids Barriers CNS **8:**3.

6. **Kim YS, Sheldon RA, Elliott BR, Liu Q, Ferriero DM, Tauber MG.** 1995. Brain injury in experimental neonatal meningitis due to group B streptococci. J Neuropathol Exp Neurol **54:**531-539.

7. **van Sorge NM, Doran KS.** 2012. Defense at the border: the blood-brain barrier versus bacterial foreigners. Future Microbiol **7:**383-394.

8. **Kim KS.** 2006. Microbial translocation of the blood-brain barrier. Int J Parasitol **36:**607-614.

9. **Kim KS.** 2003. Pathogenesis of bacterial meningitis: from bacteraemia to neuronal injury. Nat Rev Neurosci **4:**376-385.

10. **Doran KS, Engelson EJ, Khosravi A, Maisey HC, Fedtke I, Equils O, Michelsen KS, Arditi M, Peschel A, Nizet V.** 2005. Blood-brain barrier invasion by group B Streptococcus depends upon proper cell-surface anchoring of lipoteichoic acid. J Clin Invest **115:**2499-2507.

11. **Maisey HC, Quach D, Hensler ME, Liu GY, Gallo RL, Nizet V, Doran KS.** 2008. A group B streptococcal pilus protein promotes phagocyte resistance and systemic virulence. FASEB J **22:**1715-1724.

12. **Seo HS, Mu R, Kim BJ, Doran KS, Sullam PM.** 2012. Binding of glycoprotein Srr1 of Streptococcus agalactiae to fibrinogen promotes attachment to brain endothelium and the development of meningitis. PLoS Pathog **8:**e1002947.

13. **Cutting AS, Del Rosario Y, Mu R, Rodriguez A, Till A, Subramani S, Gottlieb RA, Doran KS.** 2014. The role of autophagy during group B Streptococcus infection of blood-brain barrier endothelium. J Biol Chem **289:**35711-35723.

14. **Brady LJ, Maddocks SE, Larson MR, Forsgren N, Persson K, Deivanayagam CC, Jenkinson HF.** 2010. The changing faces of Streptococcus antigen I/II polypeptide family adhesins. Mol Microbiol **77:**276-286.

15. **Rego S, Heal TJ, Pidwill GR, Till M, Robson A, Lamont RJ, Sessions RB, Jenkinson HF, Race PR, Nobbs AH.** 2016. Structural and Functional Analysis of Cell Wall-anchored Polypeptide Adhesin BspA in Streptococcus agalactiae. J Biol Chem **291:**15985-16000.

16. **Sitkiewicz I, Green NM, Guo N, Mereghetti L, Musser JM.** 2011. Lateral gene transfer of streptococcal ICE element RD2 (region of difference 2) encoding secreted proteins. BMC Microbiol **11:**65.

17. **Zhang S, Green NM, Sitkiewicz I, Lefebvre RB, Musser JM.** 2006. Identification and characterization of an antigen I/II family protein produced by group A Streptococcus. Infect Immun **74:**4200-4213.

18. **Franklin L, Nobbs AH, Bricio-Moreno L, Wright CJ, Maddocks SE, Sahota JS, Ralph J, O'Connor M, Jenkinson HF, Kadioglu A.** 2013. The AgI/II family adhesin AspA is required for respiratory infection by Streptococcus pyogenes. PLoS One **8:**e62433.

19. **Chuzeville S, Dramsi S, Madec JY, Haenni M, Payot S.** 2015. Antigen I/II encoded by integrative and conjugative elements of Streptococcus agalactiae and role in biofilm formation. Microb Pathog **88:**1-9.

20. **Pidwill GR, Rego S, Jenkinson HF, Lamont RJ, Nobbs AH.** 2018. Coassociation between Group B Streptococcus and Candida albicans Promotes Interactions with Vaginal Epithelium. Infect Immun **86**.

21. **Kelley LA, Mezulis S, Yates CM, Wass MN, Sternberg MJ.** 2015. The Phyre2 web portal for protein modeling, prediction and analysis. Nat Protoc **10:**845-858.

22. **Kollman JM, Pandi L, Sawaya MR, Riley M, Doolittle RF.** 2009. Crystal structure of human fibrinogen. Biochemistry **48:**3877-3886.

23. **Davies HD, Jones N, Whittam TS, Elsayed S, Bisharat N, Baker CJ.** 2004. Multilocus sequence typing of serotype III group B streptococcus and correlation with pathogenic potential. J Infect Dis **189:**1097-1102.

24. **Takahashi S, Adderson EE, Nagano Y, Nagano N, Briesacher MR, Bohnsack JF.** 1998. Identification of a highly encapsulated, genetically related group of invasive type III group B streptococci. J Infect Dis **177:**1116-1119.

25. **Chi F, Wang L, Zheng X, Wu CH, Jong A, Sheard MA, Shi W, Huang SH.** 2011. Meningitic Escherichia coli K1 penetration and neutrophil transmigration across the blood-brain barrier are modulated by alpha7 nicotinic receptor. PLoS One **6:**e25016.

26. **Doran KS, Chang JC, Benoit VM, Eckmann L, Nizet V.** 2002. Group B streptococcal beta-hemolysin/cytolysin promotes invasion of human lung epithelial cells and the release of interleukin-8. J Infect Dis **185:**196-203.

27. **Banerjee A, Kim BJ, Carmona EM, Cutting AS, Gurney MA, Carlos C, Feuer R, Prasadarao NV, Doran KS.** 2011. Bacterial Pili exploit integrin machinery to promote immune activation and efficient blood-brain barrier penetration. Nat Commun **2:**462.

28. **Doran KS, Fulde M, Gratz N, Kim BJ, Nau R, Prasadarao N, Schubert-Unkmeir A, Tuomanen EI, Valentin-Weigand P.** 2016. Host-pathogen interactions in bacterial meningitis. Acta Neuropathol **131:**185-209.

29. **Oeckinghaus A, Ghosh S.** 2009. The NF-kappaB family of transcription factors and its regulation. Cold Spring Harb Perspect Biol **1:**a000034.

30. **Keestra AM, van Putten JP.** 2008. Unique properties of the chicken TLR4/MD-2 complex: selective lipopolysaccharide activation of the MyD88-dependent pathway. J Immunol **181:**4354-4362.

31. **Nizet V, Kim KS, Stins M, Jonas M, Chi EY, Nguyen D, Rubens CE.** 1997. Invasion of brain microvascular endothelial cells by group B streptococci. Infect Immun **65:**5074-5081.

32. **Karimova G, Gauliard E, Davi M, Ouellette SP, Ladant D.** 2017. Protein-Protein Interaction: Bacterial Two-Hybrid. Methods Mol Biol **1615:**159-176.

33. **Dove SL.** 2003. Studying protein-protein interactions using a bacterial two-hybrid system. Methods Mol Biol **205:**251-265.

34. **Holmes JA, Follett SE, Wang H, Meadows CP, Varga K, Bowman GR.** 2016. Caulobacter PopZ forms an intrinsically disordered hub in organizing bacterial cell poles. Proc Natl Acad Sci U S A **113:**12490-12495.

35. **Jerabek-Willemsen M, Wienken CJ, Braun D, Baaske P, Duhr S.** 2011. Molecular interaction studies using microscale thermophoresis. Assay Drug Dev Technol **9:**342-353.

36. **Tomiyama L, Kamino H, Fukamachi H, Urano T.** 2017. Precise epitope determination of the anti-vimentin monoclonal antibody V9. Mol Med Rep **16:**3917-3921.

37. **Jorgensen ML, Moller CK, Rasmussen L, Boisen L, Pedersen H, Kristensen P.** 2017. An anti vimentin antibody promotes tube formation. Sci Rep **7:**3576.

38. **Mak TN, Bruggemann H.** 2016. Vimentin in Bacterial Infections. Cells **5**.

39. **Tettelin H, Masignani V, Cieslewicz MJ, Donati C, Medini D, Ward NL, Angiuoli SV, Crabtree J, Jones AL, Durkin AS, Deboy RT, Davidsen TM, Mora M, Scarselli M, Margarit y Ros I, Peterson JD, Hauser CR, Sundaram JP, Nelson WC, Madupu R, Brinkac LM, Dodson RJ, Rosovitz MJ, Sullivan SA, Daugherty SC, Haft DH, Selengut J, Gwinn ML, Zhou L, Zafar N, Khouri H, Radune D, Dimitrov G, Watkins K, O'Connor KJ, Smith S, Utterback TR, White O, Rubens CE, Grandi G, Madoff LC, Kasper DL, Telford JL, Wessels MR, Rappuoli R, Fraser CM.** 2005. Genome analysis of multiple pathogenic isolates of Streptococcus agalactiae: implications for the microbial "pan-genome". Proc Natl Acad Sci U S A **102:**13950-13955.

40. **Leito JT, Ligtenberg AJ, Nazmi K, de Blieck-Hogervorst JM, Veerman EC, Nieuw Amerongen AV.** 2008. A common binding motif for various bacteria of the bacteria-binding peptide SRCRP2 of DMBT1/gp-340/salivary agglutinin. Biol Chem **389:**1193-1200.

41. **Mollenhauer J, Wiemann S, Scheurlen W, Korn B, Hayashi Y, Wilgenbus KK, von Deimling A, Poustka A.** 1997. DMBT1, a new member of the SRCR superfamily, on chromosome 10q25.3-26.1 is deleted in malignant brain tumours. Nat Genet **17:**32-39.

42. **Holmskov U, Mollenhauer J, Madsen J, Vitved L, Gronlund J, Tornoe I, Kliem A, Reid KB, Poustka A, Skjodt K.** 1999. Cloning of gp-340, a putative opsonin receptor for lung surfactant protein D. Proc Natl Acad Sci U S A **96:**10794-10799.

43. **Madsen J, Mollenhauer J, Holmskov U.** 2010. Review: Gp-340/DMBT1 in mucosal innate immunity. Innate Immun **16:**160-167.

44. **Stoddard E, Cannon G, Ni H, Kariko K, Capodici J, Malamud D, Weissman D.** 2007. gp340 expressed on human genital epithelia binds HIV-1 envelope protein and facilitates viral transmission. J Immunol **179:**3126-3132.

45. **Larson MR, Rajashankar KR, Patel MH, Robinette RA, Crowley PJ, Michalek S, Brady LJ, Deivanayagam C.** 2010. Elongated fibrillar structure of a streptococcal adhesin assembled by the high-affinity association of alpha- and PPII-helices. Proc Natl Acad Sci U S A **107:**5983-5988.

46. **Maddocks SE, Wright CJ, Nobbs AH, Brittan JL, Franklin L, Stromberg N, Kadioglu A, Jepson MA, Jenkinson HF.** 2011. Streptococcus pyogenes antigen I/II-family polypeptide AspA shows differential ligand-binding properties and mediates biofilm formation. Mol Microbiol **81:**1034-1049.

47. **Purushotham S, Deivanayagam C.** 2014. The calcium-induced conformation and glycosylation of scavenger-rich cysteine repeat (SRCR) domains of glycoprotein 340 influence the high affinity interaction with antigen I/II homologs. J Biol Chem **289:**21877-21887.

48. **Petersen FC, Assev S, van der Mei HC, Busscher HJ, Scheie AA.** 2002. Functional variation of the antigen I/II surface protein in Streptococcus mutans and Streptococcus intermedius. Infect Immun **70:**249-256.

49. **Heddle C, Nobbs AH, Jakubovics NS, Gal M, Mansell JP, Dymock D, Jenkinson HF.** 2003. Host collagen signal induces antigen I/II adhesin and invasin gene expression in oral Streptococcus gordonii. Mol Microbiol **50:**597-607.

50. **Nobbs AH, Shearer BH, Drobni M, Jepson MA, Jenkinson HF.** 2007. Adherence and internalization of Streptococcus gordonii by epithelial cells involves beta1 integrin recognition by SspA and SspB (antigen I/II family) polypeptides. Cell Microbiol **9:**65-83.

51. **Burke FM, McCormack N, Rindi S, Speziale P, Foster TJ.** 2010. Fibronectin-binding protein B variation in Staphylococcus aureus. BMC Microbiol **10:**160.

52. **Ivaska J, Pallari HM, Nevo J, Eriksson JE.** 2007. Novel functions of vimentin in cell adhesion, migration, and signaling. Exp Cell Res **313:**2050-2062.

53. **Moisan E, Girard D.** 2006. Cell surface expression of intermediate filament proteins vimentin and lamin B1 in human neutrophil spontaneous apoptosis. J Leukoc Biol **79:**489-498.

54. **Boilard E, Bourgoin SG, Bernatchez C, Surette ME.** 2003. Identification of an autoantigen on the surface of apoptotic human T cells as a new protein interacting with inflammatory group IIA phospholipase A2. Blood **102:**2901-2909.

55. **Mor-Vaknin N, Punturieri A, Sitwala K, Markovitz DM.** 2003. Vimentin is secreted by activated macrophages. Nat Cell Biol **5:**59-63.

56. **Podor TJ, Singh D, Chindemi P, Foulon DM, McKelvie R, Weitz JI, Austin R, Boudreau G, Davies R.** 2002. Vimentin exposed on activated platelets and platelet microparticles localizes vitronectin and plasminogen activator inhibitor complexes on their surface. J Biol Chem **277:**7529-7539.

57. **Bryant AE, Bayer CR, Huntington JD, Stevens DL.** 2006. Group A streptococcal myonecrosis: increased vimentin expression after skeletal-muscle injury mediates the binding of Streptococcus pyogenes. J Infect Dis **193:**1685-1692.

58. **Koudelka KJ, Destito G, Plummer EM, Trauger SA, Siuzdak G, Manchester M.** 2009. Endothelial targeting of cowpea mosaic virus (CPMV) via surface vimentin. PLoS Pathog **5:**e1000417.

59. **Xu B, deWaal RM, Mor-Vaknin N, Hibbard C, Markovitz DM, Kahn ML.** 2004. The endothelial cell-specific antibody PAL-E identifies a secreted form of vimentin in the blood vasculature. Mol Cell Biol **24:**9198-9206.

60. **Zou Y, He L, Huang SH.** 2006. Identification of a surface protein on human brain microvascular endothelial cells as vimentin interacting with Escherichia coli invasion protein IbeA. Biochem Biophys Res Commun **351:**625-630.

61. **Mendez MG, Kojima S, Goldman RD.** 2010. Vimentin induces changes in cell shape, motility, and adhesion during the epithelial to mesenchymal transition. Faseb j **24:**1838-1851.

62. **Wang RC, Wei Y, An Z, Zou Z, Xiao G, Bhagat G, White M, Reichelt J, Levine B.** 2012. Akt-mediated regulation of autophagy and tumorigenesis through Beclin 1 phosphorylation. Science **338:**956-959.

63. **Yang J, Zou L, Yang Y, Yuan J, Hu Z, Liu H, Peng H, Shang W, Zhang X, Zhu J, Rao X.** 2016. Superficial vimentin mediates DENV-2 infection of vascular endothelial cells. Sci Rep **6:**38372.

64. **Yu YT, Chien SC, Chen IY, Lai CT, Tsay YG, Chang SC, Chang MF.** 2016. Surface vimentin is critical for the cell entry of SARS-CoV. J Biomed Sci **23:**14.

65. **Du N, Cong H, Tian H, Zhang H, Zhang W, Song L, Tien P.** 2014. Cell surface vimentin is an attachment receptor for enterovirus 71. J Virol **88:**5816-5833.

66. **Murli S, Watson RO, Galan JE.** 2001. Role of tyrosine kinases and the tyrosine phosphatase SptP in the interaction of *Salmonella* with host cells. Cell Microbiol **3:**795-810.

67. **Ghosh P, Halvorsen EM, Ammendolia DA, Mor-Vaknin N, O'Riordan MXD, Brumell JH, Markovitz DM, Higgins DE.** 2018. Invasion of the Brain by Listeria monocytogenes Is Mediated by InlF and Host Cell Vimentin. MBio **9**.

68. **Chi F, Jong TD, Wang L, Ouyang Y, Wu C, Li W, Huang SH.** 2010. Vimentin-mediated signalling is required for IbeA+ *E. coli* K1 invasion of human brain microvascular endothelial cells. Biochem J **427:**79-90.

69. **Russell MW, Bergmeier LA, Zanders ED, Lehner T.** 1980. Protein antigens of Streptococcus mutans: purification and properties of a double antigen and its protease-resistant component. Infect Immun **28:**486-493.

70. **Lehner T, Russell MW, Caldwell J, Smith R.** 1981. Immunization with purified protein antigens from Streptococcus mutans against dental caries in rhesus monkeys. Infect Immun **34:**407-415.

71. **Doran KS, Liu GY, Nizet V.** 2003. Group B streptococcal beta-hemolysin/cytolysin activates neutrophil signaling pathways in brain endothelium and contributes to development of meningitis. J Clin Invest **112:**736-744.

72. **Stevens C, Henderson P, Nimmo ER, Soares DC, Dogan B, Simpson KW, Barrett JC, Wilson DC, Satsangi J.** 2013. The intermediate filament protein, vimentin, is a regulator of NOD2 activity. Gut **62:**695-707.

73. **dos Santos G, Rogel MR, Baker MA, Troken JR, Urich D, Morales-Nebreda L, Sennello JA, Kutuzov MA, Sitikov A, Davis JM, Lam AP, Cheresh P, Kamp D, Shumaker DK, Budinger GR, Ridge KM.** 2015. Vimentin regulates activation of the NLRP3 inflammasome. Nat Commun **6:**6574.

74. **Wilson CB, Weaver WM.** 1985. Comparative susceptibility of group B streptococci and Staphylococcus aureus to killing by oxygen metabolites. J Infect Dis **152:**323-329.

75. **Da Costa AF, Pereira CS, Santos Gda S, Carvalho TM, Hirata R, Jr., De Mattos-Guaraldi AL, Rosa AC, Nagao PE.** 2011. Group B Streptococcus serotypes III and V induce apoptosis and necrosis of human epithelial A549 cells. Int J Mol Med **27:**739-744.

76. **Back CR, Sztukowska MN, Till M, Lamont RJ, Jenkinson HF, Nobbs AH, Race PR.** 2017. The Streptococcus gordonii Adhesin CshA Protein Binds Host Fibronectin via a Catch-Clamp Mechanism. J Biol Chem **292:**1538-1549.

77. **Xayarath B, Yother J.** 2007. Mutations blocking side chain assembly, polymerization, or transport of a Wzy-dependent Streptococcus pneumoniae capsule are lethal in the absence of suppressor mutations and can affect polymer transfer to the cell wall. J Bacteriol **189:**3369-3381.

78. **Pritzlaff CA, Chang JC, Kuo SP, Tamura GS, Rubens CE, Nizet V.** 2001. Genetic basis for the beta-haemolytic/cytolytic activity of group B Streptococcus. Mol Microbiol **39:**236-247.

79. **Woodcock DM, Crowther PJ, Doherty J, Jefferson S, DeCruz E, Noyer-Weidner M, Smith SS, Michael MZ, Graham MW.** 1989. Quantitative evaluation of Escherichia coli

host strains for tolerance to cytosine methylation in plasmid and phage recombinants. Nucleic Acids Res **17:**3469-3478.

80. **Park IH, Geno KA, Yu J, Oliver MB, Kim KH, Nahm MH.** 2015. Genetic, biochemical, and serological characterization of a new pneumococcal serotype, 6H, and generation of a pneumococcal strain producing three different capsular repeat units. Clin Vaccine Immunol **22:**313-318.

81. **Weksler BB, Subileau EA, Perriere N, Charneau P, Holloway K, Leveque M, Tricoire-Leignel H, Nicotra A, Bourdoulous S, Turowski P, Male DK, Roux F, Greenwood J, Romero IA, Couraud PO.** 2005. Blood-brain barrier-specific properties of a human adult brain endothelial cell line. FASEB J **19:**1872-1874.

82. **Weksler B, Romero IA, Couraud PO.** 2013. The hCMEC/D3 cell line as a model of the human blood brain barrier. Fluids Barriers CNS **10:**16.

83. **Llombart V, Garcia-Berrocoso T, Bech-Serra JJ, Simats A, Bustamante A, Giralt D, Reverter-Branchat G, Canals F, Hernandez-Guillamon M, Montaner J.** 2016. Characterization of secretomes from a human blood brain barrier endothelial cells in-vitro model after ischemia by stable isotope labeling with aminoacids in cell culture (SILAC). J Proteomics **133:**100-112.

84. **Ohtsuki S, Ikeda C, Uchida Y, Sakamoto Y, Miller F, Glacial F, Decleves X, Scherrmann JM, Couraud PO, Kubo Y, Tachikawa M, Terasaki T.** 2013. Quantitative targeted absolute proteomic analysis of transporters, receptors and junction proteins for validation of human cerebral microvascular endothelial cell line hCMEC/D3 as a human blood-brain barrier model. Mol Pharm **10:**289-296.

85. **van Sorge NM, Ebrahimi CM, McGillivray SM, Quach D, Sabet M, Guiney DG, Doran KS.** 2008. Anthrax toxins inhibit neutrophil signaling pathways in brain endothelium and contribute to the pathogenesis of meningitis. PLoS One **3:**e2964.

86. **Wu Y, Li Q, Chen XZ.** 2007. Detecting protein-protein interactions by Far western blotting. Nat Protoc **2:**3278-3284.

87. **Griffith KL, Wolf RE, Jr.** 2002. Measuring beta-galactosidase activity in bacteria: cell growth, permeabilization, and enzyme assays in 96-well arrays. Biochem Biophys Res Commun **290:**397-402.

Chapter 3

Characterization of a two-component system transcriptional regulator LtdR that impacts Group B Streptococcal colonization and disease

Liwen Deng[1,2], Rong Mu[1], Thomas A. Weston[1], Brady L. Spencer[2], Roxanne Liles[3], and Kelly S. Doran[1,2]

[1]Department of Immunology and Microbiology, University of Colorado School of Medicine, Aurora, CO, USA.
[2]Department of Cell and Molecular Biology, San Diego State University, San Diego, CA, USA.
[3]Department of Biology, Bakersfield College, Bakersfield, CA, USA.

Published in *Infection and Immunity*

June 2018

Volume 86. Issue 7. e00822-17

Short Title: LtdR regulation promotes GBS virulence

Key words: RNA sequencing, blood-brain barrier, cytokines, group B *Streptococcus*, meningitis, two-component regulatory systems, vaginal colonization

ABSTRACT

Streptococcus agalactiae (Group B *Streptococcus*, GBS) is often a commensal bacterium that colonizes healthy adults asymptomatically and is a frequent inhabitant of the vaginal tract in women. However, in immune-compromised individuals, particularly the newborn, GBS may transition to an invasive pathogen and cause serious disease. Despite currently recommended intrapartum antibiotic prophylaxis for GBS-positive mothers, GBS remains a leading cause of neonatal septicemia and meningitis. To adapt to the various host environments encountered during its disease cycle, GBS possesses multiple two-component regulatory systems (TCS). Here we investigate the contribution of a transcriptional regulator containing a LytTR domain, LtdR, to GBS pathogenesis. Disruption of the *ltdR* gene in the GBS chromosome resulted in a significant increase in bacterial invasion into human cerebral microvascular endothelial cells (hCMEC) *in vitro* as well as greater penetration of the Blood-Brain Barrier (BBB) and the development of meningitis *in vivo*. Correspondingly, infection of hCMEC with the Δ*ltdR* mutant resulted in increased secretion of pro-inflammatory cytokines IL-8, CXCL-1, and IL-6. Further, using a mouse model of GBS vaginal colonization, we observed that the Δ*ltdR* mutant was cleared more readily from the vaginal tract and also resulted in increased cytokine production from human vaginal epithelial cells. RNA-sequencing revealed global transcriptional differences between the Δ*ltdR* mutant and the parental WT GBS strain. These results suggest that LtdR regulates many bacterial processes that can influence GBS-host interactions to promote both bacterial persistence and disease progression.

INTRODUCTION

Streptococcus agalactiae (Group B *Streptococcus*, GBS) is a Gram-positive, β-hemolytic bacterium normally found in the human gastrointestinal and urogenital tracts of asymptomatic individuals. However, GBS possesses an array of virulence factors that renders it capable of causing invasive disease in susceptible hosts, including the newborn. Despite widespread intrapartum antibiotic administration to colonized mothers to prevent vertical transmission, GBS remains a leading cause of pneumonia, sepsis, and meningitis in neonates. (1, 2) Over the course of its disease cycle, GBS encounters very different host microenvironments and must adapt to successfully colonize and survive in different host niches. In bacteria, the ability to efficiently adjust to different environments is commonly mediated by signaling through two-component regulatory systems (TCS). (3, 4)

TCSs consist of a membrane bound histidine kinase sensor that, upon activation by an external signal, phosphorylates a cytoplasmic transcriptional regulator that affects expression of downstream gene targets. Of the 21 TCSs that have been described in GBS, only a few have been well characterized. (5-7) The TCS response regulator CiaR is known to play a role in promoting GBS survival within brain endothelial cells as well as host phagocytic cells such as neutrophils and macrophages. (8) The LiaR response regulator promotes GBS virulence by regulating cell wall synthesis in response to environmental stresses such as elevated temperature and the presence of antimicrobial peptides. (9) The best studied TCS in GBS is CovS/R (Control of virulence sensor/regulator), which regulates the expression of a variety of virulence factors that are important for GBS pathogenesis such as pili, which promote GBS attachment to host surfaces, and *cylE*, which is involved in the expression of beta-hemolysin/cytolysin (β-H/C). (10-12) We have shown previously that GBS strains lacking the *covR* gene are hyper-inflammatory and result in increased

sepsis and meningitis in murine infection models due to increased expression of β-H/C. (11) Interestingly, infection with GBS WT, Δ*covR* or Δ*cylE* strains revealed the β-H/C toxin as a key mediator in provoking an acute inflammatory response in vaginal epithelium, and that functional CovR regulation dampens cytokine production and promotes bacterial persistence in the mouse vaginal tract (13). These observations demonstrate the importance of TCS transcriptional regulators in regulating virulence factors in order to promote niche establishment.

While the majority of TCS transcriptional regulators possess a helix-turn-helix (HTH) DNA-binding domain, a small percentage of transcriptional regulators contain a LytTR non-HTH domain. (14-16) LytTR-containing proteins account for just ~2.7% of prokaryotic response regulators and predominantly regulate the production of virulence factors in pathogenic bacteria. (17) GBS possesses three TCS transcriptional regulators that include the LytTR DNA-binding domain (see Fig. 1A). Of these, the RgfA regulator (GBSCOH1_RS09095) has been previously characterized and may contribute to virulence by mediating GBS binding to host fibrinogen. (18) Another of these LytTR-containing response regulators, encoded by GBSCOH1_RS01195, has also been studied and is referred to as Rr2. (5) Rr2 is upregulated in GBS during stationary growth phase and is likely activated in response to stress conditions such as lack of nutrients, low pH, and the accumulation of toxic metabolites. (5) The GBS *rr2* gene is contained within a locus that is homologous to loci found in pathogens *Staphylococcus aureus* and *Streptococcus mutans* where it has been shown to regulate the expression of murein hydrolases encoded by the adjacent *lrgAB* operon. (19-22) In those pathogens, the rr2 regulator is known as "LytR" and has been shown to be important for cell wall turnover, cell autolysis, and biofilm formation. (23-25)

Here we investigate the third **L**yt**T**R-**d**omain containing TCS **r**egulator (GBSCOH1_RS05040), that we designate LtdR, and its role in GBS colonization and virulence.

Using targeted mutagenesis, we show that LtdR mediated regulation affects both the development of meningitis and vaginal persistence using mouse models of GBS colonization and invasive disease. Additionally, we observed that the loss of LtdR results in increased GBS invasion into host cells and increased inflammatory signaling by infected cells *in vitro*. Finally, we performed RNA-sequencing to identify LtdR regulated genes and observed global transcriptional changes in the Δ*ltdR* mutant strain.

MATERIALS AND METHODS

Bacterial strains and growth conditions.

GBS clinical isolate COH1 (serotype III) (26) and its isogenic Δ*ltdR* mutant were used for the experiments. GBS strains were grown in THB (Hardy Diagnostics) at 37°C, and growth was monitored by measuring the optical density at 600 nm (OD_{600}). *E. coli* strains Top 10 electrocompetent cells and MC1061 electrocompetent cells (Invitrogen), used for plasmid propagation, were grown in LB media. For antibiotic selection, 2 μg/mL chloramphenicol (Sigma) and 5 μg/mL erythromycin (Sigma) were incorporated into the growth medium for GBS, 300 μg/mL erythromycin for *E. coli*. Chemically defined medium (CDM) (27) and THB were used for growth comparison of GBS WT and the Δ*ltdR* mutant. To evaluate growth in CDM or THB, GBS was initially grown to log phase (optical density at 600nm [OD_{600}], 0.3) in THB. The cells were harvested by centrifugation, washed three times in an equivalent volume of phosphate-buffered saline (PBS) (GIBCO) and diluted 1 to 50 into media. Growth was monitored spectrophotometrically at a wavelength of 600nm.

Construction of the Δ*ltdR* deletion and complementary strains.

Deletion of the *ltdR* gene (GBSCOH1_RS05040) was performed in the genome of COH1. The following upstream and downstream primers were used to generate the forward fusion fragment: (5' gggactgacaacagaatcttg) and (5'cacaatgtaagagcg/tctgctataacgagg). The reverse fusion fragment was generated with the following: upstream (5' cctcgttatagcaga/cgctcttacattgtg) and downstream (5' cccaagtgctttatcaatagg) primers. The forward and reverse amplicons included GBSCOH1_RS05035 (forward fragment) and GBSCOH1_RS05045 (reverse fragment) sequences to be used as recombination homologous arms for allelic exchange. A 1999 bp fusion deletion product was generated with previously generated forward and reverse PCR products mixed in equal amounts in a PCR with the following primers: (5' gggactgacaacagaatcttg) and (5' cccaagtgctttatcaatagg). High fidelity enzyme (Roche) was used for all PCRs. The PCR product was digested and gel purified prior to cloning into the TOPO Blunt vector (Invitrogen). The resulting plasmid, TOPO/GBSCOH1_RS05040AD, was used to transform TOP 10 *E. coli* (Invitrogen). Selection of clones was performed according to the manufacturer's directions. Positive clones were screened by SphI restriction endonuclease digestion and plasmid sequencing (ASU). The TOPO/GBSCOH1_RS05040AD plasmid was digested with BamHI and EcoRI and ligated into a similarly digested pHY304, yielding pHY304/ GBSCOH1_RS05040AD, which was transformed directly into *E. coli* MC1061. Plasmid was propagated and isolated from *E. coli* for transformation of electrocompetent GBS strain COH1. The WT GBSCOH1_RS05040 chromosomal allele was replaced with the allele encoding the deletion fragment. The resulting strain was cultured at 30°C in the presence of erythromycin. Cells were shifted to 37°C in the presence of erythromycin to select for the chromosomal integration of pHY304/ GBSCOH1_RS05040AD. Integration was confirmed by the isolation of chromosomal DNA and subsequent PCR with the following primers: (5'- gggcatttaacgacgaaactg) and (5'

cgtcgttttacaacgtcgtga). Isolates with the integrated plasmid were chosen and passaged five times in the absence of erythromycin at 30°C. The resulting strain was then cured of the plasmid by passage at 37°C and screened for sensitivity to erythromycin. The chromosome of the GBS Δ*ltdR* was verified by PCR with primers that flanked the cloned region and were specific for the deleted sequence. For complementation studies, the full-length *ltdR* gene was amplified using the following primers: (5' ggtctagaaaaggtattgtatgaag), incorporating a XdaI restriction site, and (5' ggcatatggaataacttttcattagtta), incorporating a NdeI restriction site, and cloned into pDCerm plasmid. The Δ*ltdR* deletion strain was transformed with the recombinant plasmid to generate the complemented strain. The Δ*ltdR*p*ltdR* complemented strain was grown in the presence of erythromycin.

Hemolysis assay.

GBS strains were grown to OD_{600} of 0.4, then harvested by centrifugation and resuspended in PBS. 1×10^9 CFU were added to fresh sheep blood (VWR) in V-bottom 96-well plates (Corning). Plates were sealed and incubated at 37°C with agitation for 1 h. Plates were centrifuged at 200g for 10 min and 100μL of the supernatant were transferred to a flat-bottom 96-well plate. Absorbance at 541 nm (A541) was read and % hemolysis was calculated by comparing the A541 values for GBS treated wells to A541 values of blood incubated with water.

Flow cytometry.

Flow cytometry to determine capsule expression was performed as described in (28). Briefly, bacterial stocks were washed in sterile PBS + 0.5% bovine serum albumin (BSA), then incubated with ten-fold serial dilutions (ranging from 1:2000 to 1:200,000,000 final) of a

monoclonal anti-serotype III antibody or the monoclonal anti-serotype Ia isotype control, washed via centrifugation, and labeled with a donkey anti-mouse IgM conjugated to AlexaFluor 647 (Invitrogen) at 1:2000 dilution. All incubations were performed at 4°C with shaking. Samples were washed again then resuspended and read on a FACSCalibur flow cytometer (BD Biosciences) and analyzed using FlowJo v10. The monoclonal antibodies were purified and provided by Dr. John Kearney at the University of Alabama-Birmingham. For the histograms shown in Fig. 2C-D, the anti-serotype III and anti-serotype Ia isotype control antibodies were both used at a final dilution of 1:20,000.

Aggregation and clumping assays.

GBS strains were grown to OD_{600} of 0.4, then harvested by centrifugation and resuspended in PBS (for aggregation assay) or PBS with 0.1% fibrinogen (for clumping assay) in 1.75 mL Eppendorf tubes (E & K Scientific). 0.1 mL was pipetted from the top of the cells suspension after 150 min. and turbidity was measured at 600 nm.

Mouse models of hematogenous GBS meningitis and vaginal colonization.

Animal experiments were approved by the committee on the use and care of animals at San Diego State University (SDSU) protocol #16-10-021D and performed using accepted veterinary standards. We utilized a mouse GBS infection model as described previously. (29-31) Briefly, 8-week old male CD-1 mice (Charles River) were injected intravenously with 1×10^8 CFU of wild-type GBS or the isogenic Δ*ltdR* mutant. After 72 h, mice were euthanized and blood and brain tissue were collected. One half of each brain was fixed in 4% paraformaldehyde (Ricca Chemical Company) for histopathological analyses. Formalin fixed, paraffin embedded brains were

sectioned onto glass slides. The slides were stained using hematoxylin and eosin (Sigma) and images were taken using a Zeiss upright microscope with an attached Axiocam Icc3 camera. Adobe Photoshop and Illustrator was used to process images. The remaining tissue was homogenized, and the brain homogenates as well as blood and lung were plated on THB agar for enumeration of bacterial CFU.

The mouse model of GBS vaginal colonization was performed as described previously. (32) 10-week old female CD-1 mice (Charles River) were injected intraperitoneally with 0.5mg 17β-estradiol (Sigma) suspended in 100 μL sesame oil one day prior to inoculation with GBS. Mice were vaginally inoculated with 1×10^7 CFU of wild-type GBS or the isogenic Δ*ltdR* mutant, and on subsequent days, the vaginal lumen was swabbed with a sterile ultrafine swab. Recovered GBS were enumerated on CHROMagar StrepB agar (DRG International).

Cell lines and infection assays.

The well-characterized human cerebral microvascular endothelial cell line (hCMEC/D3)(33-36), referred to as hCMEC, was obtained from Millipore and was maintained in EndoGRO-MV Complete Media Kit supplemented with 1ng/mL FGF-2 (Millipore) at 37°C with 5% CO_2. The human brain microvascular endothelial cell line (hBMEC), was cultured as described previously (37) in RPMI 1640 (Corning Cellgro) containing 10% fetal bovine serum (Atlanta Biologicals), 10% Nu-serum (BD Biosciences), and 1% nonessential amino acids (Gibco) at 37°C with 5% CO_2. The immortalized human vaginal epithelial cell line (hVEC) was obtained from American Type Culture Collection (VK2/E6E7, ATCC CRL-2616) and was maintained in keratinocyte serum-free medium (KSFM) (Gibco) with 0.1 ng/ml human recombinant epidermal

growth factor (EGF) (Gibco) and 0.05 mg/ml bovine pituitary extract (Gibco) at 37°C with 5% CO_2 as described previously. (38)

Assays to determine the total number of cell surface-adherent or intracellular bacteria were performed as described previously. (30) Briefly, bacteria were grown to mid-log phase to infect cell monolayers (1×10^5 CFU at a multiplicity of infection [MOI] of 1). Total cell-associated GBS were recovered following a 30 min incubation, while intracellular GBS were recovered after 2 h infection and 2 h incubation with 100 μg gentamicin (Sigma) and 5 μg penicillin (Sigma) to kill all extracellular bacteria. To assess intracellular survival, cells were treated with antibiotics for up to 8 h after a 2 h infection with GBS. Cells were detached with 0.1 ml of 0.25% trypsin-EDTA solution and lysed with addition of 0.4 ml of 0.025% Triton X-100 by vigorous pipetting. The lysates were then serially diluted and plated on THB agar to enumerate bacterial CFU.

Electron Microscopy.

For scanning electron microscopy, bacteria were grown to log phase and in THB containing human fibrinogen (100 μg/mL). They were then fixed for 10 min using a one-step method with 2.5% glutaraldehyde, 1% osmium tetraoxide, 0.1M sodium cacodylate. Bacteria were collected on 0.4 μM polycarbonate filters by passing the solution through a swinnex device outfitted on a 10 mL syringe. The filters were dehydrated through a series of increasing ethanol concentrations and then dried in a Tousimis SAMRI-790 critical point drying machine. The dried filters were mounted on SEM sample stubs with double-sided carbon tape, coated with 6nm platinum using a Quorom Q150ts high-resolution coater and imaged on with an FEI FEG450 scanning electron microscope. For transmission electron microscopy, hBMEC were grown in 24-well plates to confluence and GBS was subsequently added to monolayers as described above. Following a 2 h incubation,

monolayers were washed with PBS and collected by centrifugation. Pellets were fixed in 2% glutaraldehyde, 4% formaldehyde in 0.1M cacodylate buffer at pH 7.4 for 2 h at room temperature. Pellets were then fixed again in 1% osmium tetroxide in 0.1M cacodylate buffer for 1 h. After rinsing with water, samples were dehydrated with increasing series of concentrations of ethanol and left on a rotator overnight in a 50% solution of Spurr resin and acetone. Samples were placed in 100% Spurr the next day and placed on a rotator for several hours before transferring to fresh 100% Spurr and polymerized in an oven for 24 h at 60°C. The sample blocks were sectioned at 50 nm on a Leica ultramicrotome and picked up on formvar-coated copper grids. Grids with sections were stained with uranyl acetate and lead citrate, viewed using a Tecnai-12 (FEI) transmission electron microscope and photographed using a Zeiss 215 side mount digital camera. Images were generated using AMT image capture software. Adobe Photoshop and Illustrator was used to process images.

RT-qPCR and ELISA.

GBS were grown to mid-log phase and 1×10^6 CFU (MOI, 10) were added to hCMEC/D3 or hVEC monolayers and incubated at 37°C with 5% CO_2 for 6 h. Cells were then lysed, total RNA was extracted (Macherey-Nagel), and cDNA was synthesized (Quanta Biosciences) according to the manufacturer's instructions. Primers and primer efficiencies for IL-8, CXCL-1, IL-6, and GAPDH were utilized as previously described. (39) IL-8, CXCL-1, and IL-6 protein from hCMEC/D3 and hVEC supernatants were detected by enzyme-linked immunosorbent assay according to the manufacturer's instructions (R&D systems). For Bacterial RT-qPCR, triplicate cultures of WT GBS, the Δ*ltdR* mutant, and the complemented strain were grown at 37°C in THB. Growth of GBS strains was monitored by measuring optical density and samples were collected at

OD_{600} of 0.2, 0.5, and 1. Bacteria were collected and RNA isolated as above and cDNA was synthesized (Quanta Biosciences). qPCR primers are listed in supplemental table 3.

Generation of RNA-Seq data.

Triplicate cultures of WT GBS and the Δ*ltdR* mutant were grown at 37°C in THB. Growth of GBS strains was monitored by measuring optical density and samples were collected at OD_{600} of 0.2, 0.5, and 1.0 to correspond with late lag, exponential, and stationary growth phases. Bacteria were isolated from media by centrifugation and resuspended in Trizol reagent (Thermo Fisher). 0.1mm diameter zirconia/silica beads (BioSpec Products) were added to the bacterial suspensions and the bacteria were lysed by beating for 2 minutes at max speed on a bead beater (BioSpec Products). RNA was isolated following the manufacturer's protocol using the Direct-Zol RNA MiniPrep Plus kit (Zymo Research). Illumina cDNA libraries were generated using a modified version of the RNAtag-seq protocol (40). Briefly, 500ng-1µg of total RNA was fragmented, depleted of genomic DNA, dephosphorylated, and ligated to DNA adapters carrying 5'-AN8-3' barcodes of known sequence with a 5' phosphate and a 3' blocking group. Barcoded RNAs were pooled and depleted of rRNA using the RiboZero rRNA depletion kit (Epicentre). Pools of barcoded RNAs were converted to Illumina cDNA libraries in 2 main steps: (i) reverse transcription of the RNA using a primer designed to the constant region of the barcoded adaptor with addition of an adapter to the 3' end of the cDNA by template switching using SMARTScribe (Clontech) as described (41); (ii) PCR amplification using primers whose 5' ends target the constant regions of the 3' or 5' adaptors and whose 3' ends contain the full Illumina P5 or P7 sequences. cDNA libraries were sequenced on the Illumina Nextseq 500 platform to generate paired end reads.

Analysis of RNA-Seq data.

Sequencing reads from each sample in a pool were demultiplexed based on their associated barcode sequence using custom scripts. Up to 1 mismatch in the barcode was allowed provided it did not make assignment of the read to a different barcode possible. Barcode sequences were removed from the first read as were terminal G's from the second read that may have been added by SMARTScribe during template switching. Reads were aligned to NCBI reference sequence NZ_HG939456.1 using BWA (42) and reads counts were assigned to genes and other genomic features using custom scripts. Differential expression analysis was conducted with DESeq2 (43). Visualization of raw sequencing data and coverage plots in the context of genome sequences and gene annotations was conducted using GenomeView (44).

Data analysis.

GraphPad Prism version 7.0 was used for statistical analysis and statistical significance was accepted at *P* values of <0.05. Statistical analysis for the hematogenous meningitis experiments, bacterial adherence and invasion assays, cytokine RT-qPCR, and ELISA was performed using the *t* test. Statistical analysis for the vaginal colonization experiments comparing CFU values for WT GBS and Δ*ltdR* recovered from the mouse vaginal lumen each day was performed using the Mann-Whitney test. For RNA-sequencing, genes were considered significantly differentially expressed if there was a 1.5-fold difference and if the *P* value was below 0.05. Venn diagrams were calculated using the Area-Proportional Venn Diagram tool (BioInfoRx).

RESULTS

Construction and characterization of the *ltdR* deletion strain.

The LtdR transcriptional regulator possesses the REC signal receiver domain and the LytTR DNA-binding domain. (Fig. 1A) The *ltdR* gene locus is distinct from the loci of the other two LytTR-containing two-component system transcriptional regulators. The *ltdR* gene is directly downstream of the *ltdS* histidine kinase sensor gene, and this operon is upstream of a gene encoding a putative carbon starvation gene. The *rr2* gene is also downstream of the gene encoding its histidine kinase and upstream of the *lrg* murein hydrolase genes. The gene encoding the RgfA regulator appears upstream of the gene for its cognate kinase RgfC. (Fig. 1B) We performed precise insertional mutagenesis to generate the Δ*ltdR* mutant GBS strain in the highly encapsulated, hyper-virulent COH1 background (sequence type [ST]-17, serotype III). (45, 46) Additionally, the *ltdR* gene was cloned into the pDCerm vector to complement the Δ*ltdR* mutant strain. Using NCBI BLAST, we determined that the *ltdR* gene in COH1 is 99% homologous to *ltdR* genes in the GBS strains 2603V/R (ST-110, serotype V), CJB111 (ST-1, serotype V), NEM316 (ST-23, serotype III), A909 (ST-7, serotype Ia), and H36B (ST-6, serotypte Ib). Analysis of growth demonstrated that the Δ*ltdR* mutant COH1 strain grew similarly to the parental WT strain in rich (THB) and chemically defined media (CDM). (Fig. 2A-B) Bacterial numbers were also assessed by plating and CFU at various growth phases and CFU counts were similar between the WT and Δ*ltdR* mutant strain. (data not shown) Additionally, there was no difference in capsule abundance and hemolytic ability between the WT and the Δ*ltdR* mutant strain (Fig. 2C-F). However, scanning electron microscopy revealed that the Δ*ltdR* mutant appears to aggregate or cluster more readily than the WT strain, which could suggest a difference in cell division or surface architecture. (Fig. 2G-H) Quantitative assays further demonstrated that the Δ*ltdR* mutant exhibited

increased aggregation and clumping phenotypes compared to the WT and complemented strains. (Fig. 2I-J)

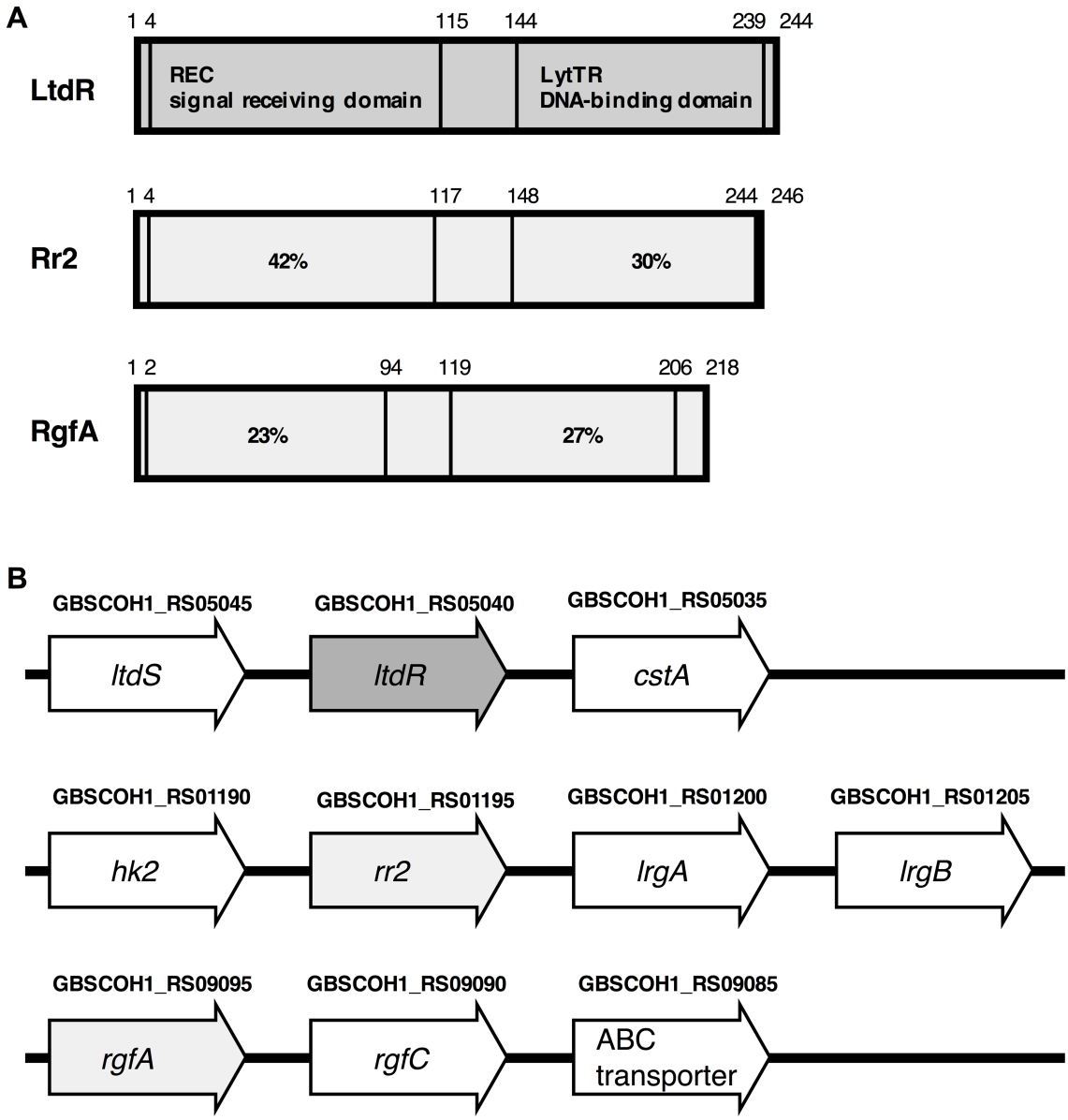

Figure 3.1. (A) Schematic diagram of LytTR-containing two-component system transcriptional regulator proteins. Percent identity of the primary amino acid sequences Rr2 and RgfA REC and LytTR domains to LtdR is indicated. (B) Schematic of the *ltdR*, *rr2*, and *rgfA* containing gene loci. Gene locus tags published in NCBI reference sequence NZ_HG939456.1 are indicated above the gene annotations.

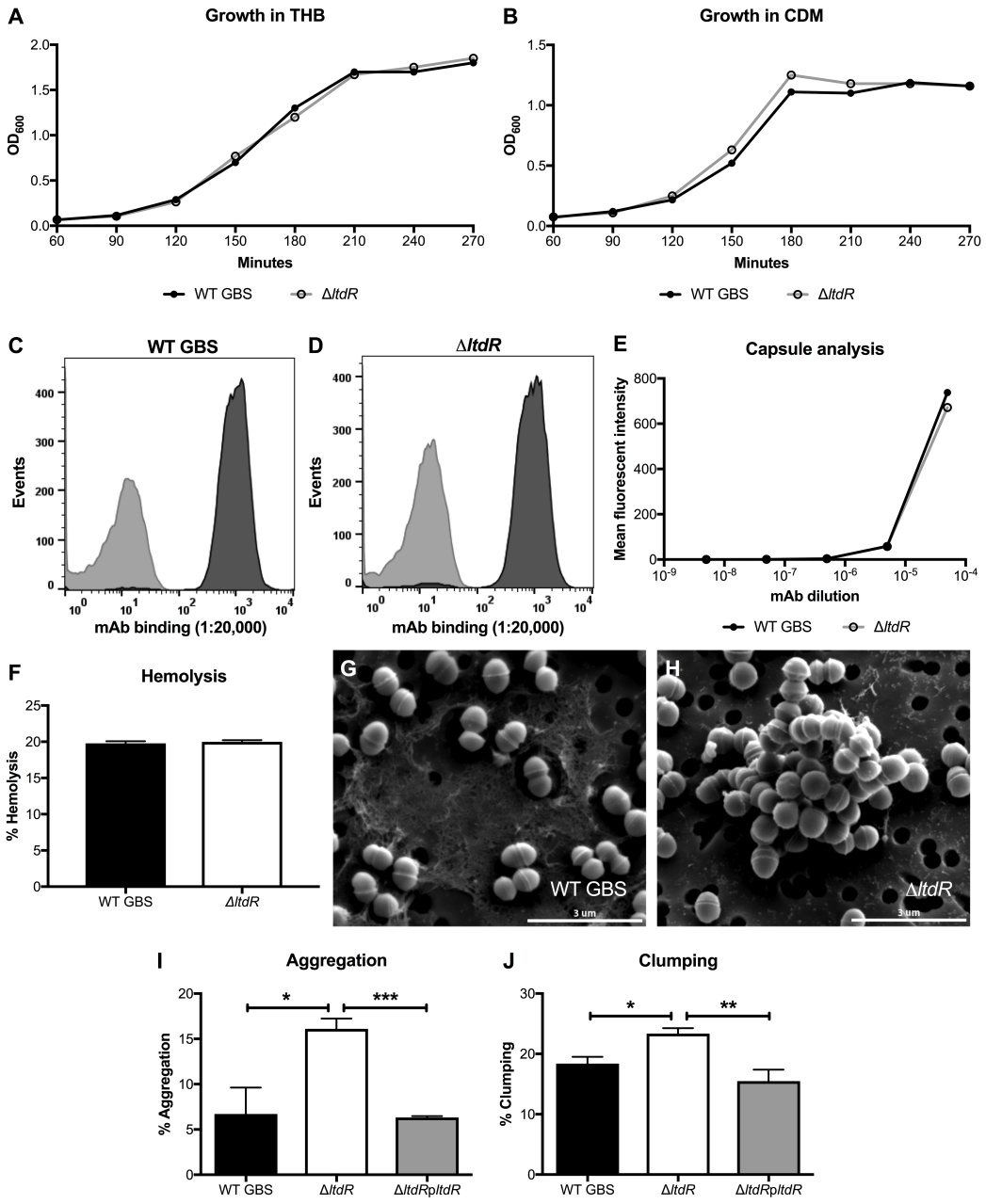

Figure 3.2. (A and B) Growth curve for WT GBS and the Δ*ltdR* mutant in THB (A) and CDM (B) at 37°C. (C-E) Flow cytometry using serial dilutions of a monoclonal antibody to the serotype III capsule to determine the presence of capsule in WT GBS (C) and the Δ*ltdR* mutant (D). A monoclonal antibody to the serotype Ia capsule was used as the isotype control. (F) Hemolysis assay comparing hemolysis of sheep blood by WT GBS and the Δ*ltdR* mutant. Representative data of 1 of at least 2 independent experiments are shown. (G and H) Scanning electron microscopy images of WT GBS (G) and Δ*ltdR* (H) mutant strains. (I) Aggregation assay comparing aggregation of WT GBS, the Δ*ltdR* mutant, and the complemented strain in THB. (J) Clumping assay comparing clumping of the WT GBS, the Δ*ltdR* mutant, and the complemented strain in THB containing 0.1% fibrinogen

Loss of *ltdR* results in increased pathogenesis of meningitis *in vivo*.

To determine whether LtdR contributes to GBS virulence *in vivo*, we utilized a murine model of GBS hematogenous meningitis. (29-31) Mice were challenged with either WT GBS or the isogenic Δ*ltdR* mutant as described in the Methods. At the experimental endpoint mice were euthanized and brain, blood, and lung tissue were collected to determine bacterial loads. We recovered similar numbers of Δ*ltdR* mutant GBS from mouse blood and lung compared to WT, however we observed a significant increase in the amounts of Δ*ltdR* mutant GBS recovered from the brain tissue. (Fig. 3A-C) Histopathological examination of fixed tissue revealed meningeal thickening as well as the presence of inflammatory infiltrates in the brains of mice infected with the Δ*ltdR* mutant. (Fig. 3D-F)

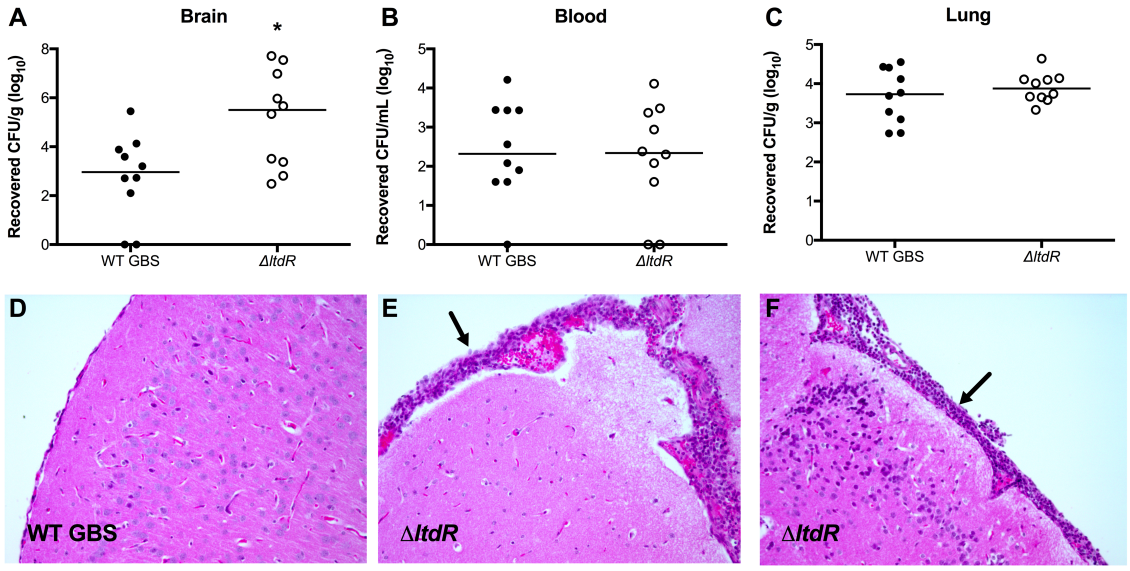

Figure 3.3. Mouse model of GBS meningitis. (A-C) 72-hours after infection, mice were euthanized and bacterial loads in the brain (A), blood (B), and lung (C) were assessed. (D-F) Representative images of hematoxylin and eosin stained brain sections from mice inoculated with WT (D) or Δ*ltdR* mutant (E and F) GBS strains. Arrows indicate areas of neutrophil infiltration and meningeal thickening. Representative data of 1 of 3 independent experiments is shown.∗, $P < 0.05$.

Loss of *ltdR* promotes bacterial invasion into endothelial cells and stimulates cytokine secretion *in vitro*.

Because we observed increased bacterial load in the brains of mice challenged with the Δ*ltdR* mutant, we next characterized the ability of the Δ*ltdR* mutant to invade human cerebral microvascular endothelial cells (hCMEC), the cells that constitute the blood-brain barrier (BBB). Using transmission electron microscopy, we first visualized more intracellular bacteria in brain endothelial cells following infection with the Δ*ltdR* mutant compared to the WT strain. (Fig. 4A-B) We then performed a quantitative cell invasion assay as described previously (29, 47) and in the Methods. Monolayers of hCMEC were infected with WT, the Δ*ltdR* mutant, or the complemented strain with an inoculum of 10^5 CFU/well (MOI of 1); data are expressed as percent recovered intracellular GBS after 2 h of incubation plus 2 h of treatment with antibiotics to kill extracellular bacteria. As shown in Figure 4C the Δ*ltdR* mutant strain exhibited a significant increase in hCMEC invasion ($P < 0.0005$) compared to the WT strain. Furthermore, complementation of the Δ*ltdR* mutant lowered invasion ability to close to that of WT (Fig. 4C). To determine whether the increased invasion observed with the Δ*ltdR* mutant could be explained by increased attachment to host cells, we examined the amount of total cell-associated (surface adherent plus intracellular) GBS to hCMEC, however we observed no significant difference between the WT and the Δ*ltdR* mutant strains. (Fig. 4D) Further, to assess whether the observed increase in recovered intracellular bacteria by the Δ*ltdR* mutant was due to enhanced survival or bacterial replication of the Δ*ltdR* mutant within hCMEC, we performed additional experiments to measure intracellular survival over time. We recovered intracellular bacteria up to 8-hours post-infection and determined that the Δ*ltdR* mutant was able to survive inside hCMEC at levels

comparable to those of WT COH1. (Fig. 4E) These data suggest that LtdR contributes primarily to bacterial invasion into brain endothelial cells.

Since we observed increased inflammatory infiltrate, predominately neutrophils, in tissues surrounding the brains of mice challenged with Δ*ltdR* mutant compared to the WT strain, we hypothesized that LtdR mediated regulation may impact the host inflammatory response. We have shown previously that GBS infection elicits cytokine and chemokine signaling that promotes neutrophil influx into the central nervous system (CNS) (37) To examine if cytokine/chemokine expression was altered during infection with the Δ*ltdR* mutant, we infected hCMEC with WT, the Δ*ltdR* mutant, or the complemented mutant strain and measured transcript abundance and protein production of major neutrophil chemoattractants, IL-8 and CXCL-1, as well as the proinflammatory cytokine IL-6. Cells infected with the Δ*ltdR* mutant GBS had significantly higher levels of transcript and secreted protein than uninfected cells or cells infected with WT GBS. Complementation of the *ltdR* mutation lowered cytokine expression of infected hCMEC cells to levels similar to WT infected cells. (Fig. 5A-F) Taken together, these data suggest that the loss of LtdR enhances GBS invasion into the brain endothelium and this may result in the stimulation of cytokine release from host cells.

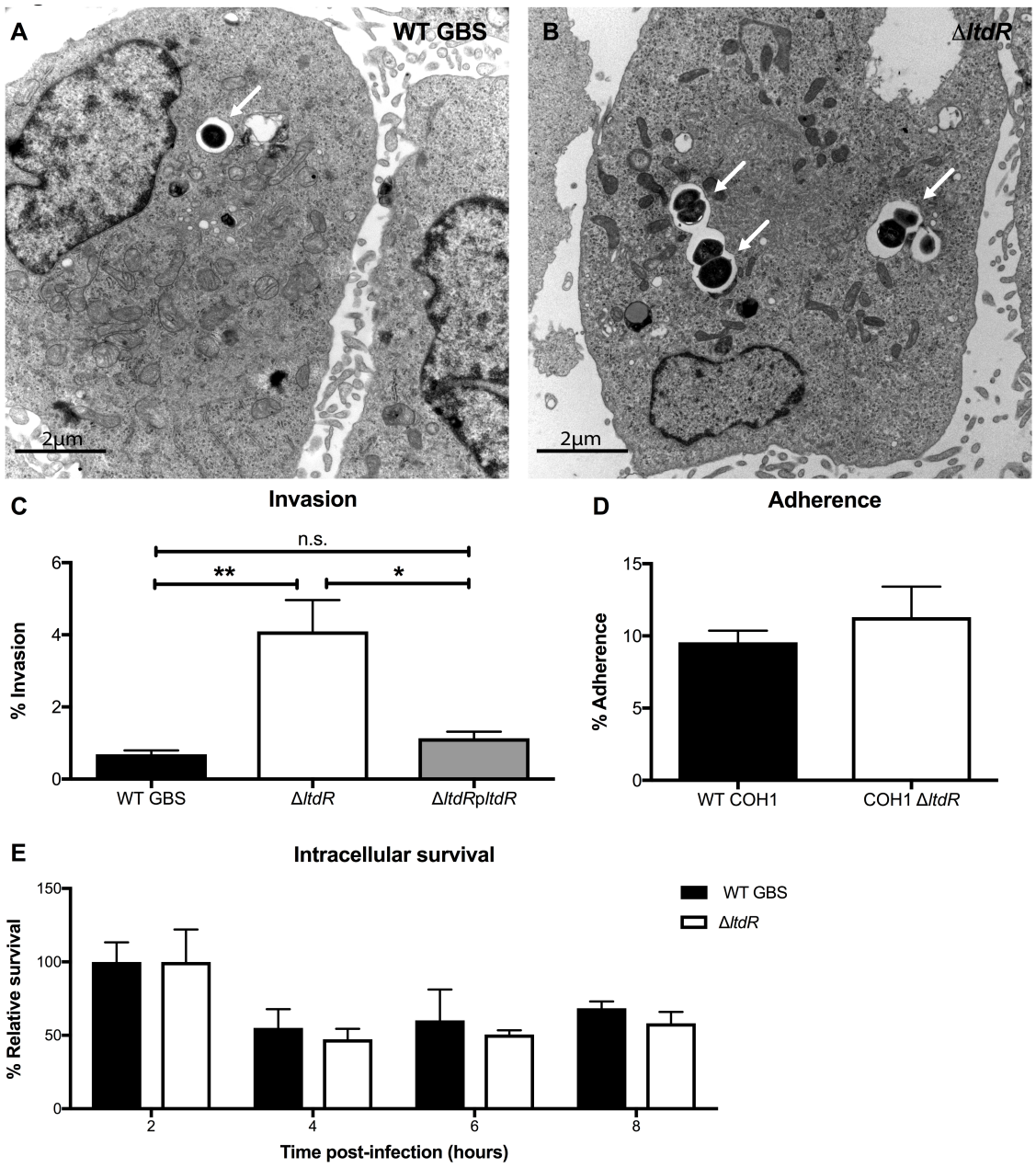

Figure 3.4. LtdR regulation influences GBS invasion into the brain endothelium. (A and B) Transmission electron micrographs of hBMEC infected with WT (A) or Δ*ltdR* mutant (B) GBS. (C) Invasion of WT GBS, the Δ*ltdR* mutant, and the complemented strain into hCMEC was quantified after a 2 h infection. (D) Adherence of WT GBS and the Δ*ltdR* mutant strain to hCMEC was assessed after a 30 min incubation. (E) Intracellular survival of WT GBS and the Δ*ltdR* mutant strain were compared up to 8 h post-infection relative to WT and the Δ*ltdR* mutant at 2 h post-infection. Experiments were performed at least 3 times in triplicate and error bars represent SD; a representative experiment is shown. *, $P < 0.05$; **, $P < 0.005$; ***, $P < 0.0005$.

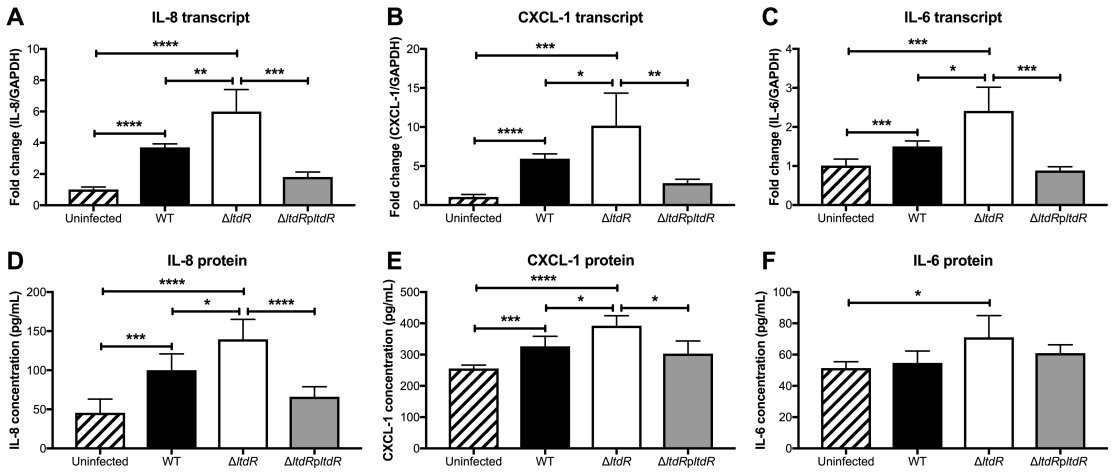

Figure 3.5. LtdR impacts cytokine expression by infected hCMEC. (A-C) hCMEC were infected with GBS for 5 h, then the cells were collected and transcript levels of IL-8 (A), CXCL-1 (B), and IL-6 (C) was quantified by RT-qPCR. (D-F) hCMEC cell supernatant was collected for detection of IL-8 (D), CXCL-1 (E), and IL-6 (F) protein secretion during GBS infection. Experiments were performed at least 3 times in triplicate and error bars represent SD; a representative experiment is shown. *, $P < 0.05$; **, $P < 0.005$; ***, $P < 0.0005$; ****, $P < 0.00005$.

LtdR contributes to vaginal colonization.

To examine the function of LtdR in a different host niche, we utilized a murine model of GBS vaginal colonization (32) to characterize the role of LtdR regulation in colonization. Mice (8 weeks old) were treated with 17β-estradiol 1 day prior to bacterial inoculation. GBS WT or the Δ*ltdR* mutant (1×10^7) was inoculated directly into the vagina, and on successive days, the vaginal lumen was swabbed and recovered bacteria quantified on agar plates to determine bacterial persistence and changes in bacterial load over time. Similar numbers of both strains were recovered from the mouse vagina on day one post-inoculation. However, the animals challenged with Δ*ltdR* mutant strain cleared the GBS more rapidly than mice that were inoculated with the WT strain. (Fig. 6A) This result could mean that the Δ*ltdR* mutant was less able to attach to vaginal epithelium, however, we observed that, similar to our observations with brain endothelium, the Δ*ltdR* mutant was more invasive than WT GBS into human vaginal epithelial cells (hVEC), but not significantly

more adherent (Fig. 6B-C). We have previously shown that GBS infection of hVEC results in activation of numerous immune pathways including cytokines and chemokines involved in leukocyte recruitment and activation (13). To determine whether LtdR plays a role in inflammatory signaling, we infected hVEC with WT, Δ*ltdR* mutant, or the complemented strain and detected the highest levels of IL-8, CXCL-1, IL-6 transcripts and secreted protein from the cells infected with the Δ*ltdR* mutant strain. (Fig. 6D-I) Thus, as we observed in brain endothelium, LtdR regulation also impacts the host inflammatory response in vaginal epithelial cells.

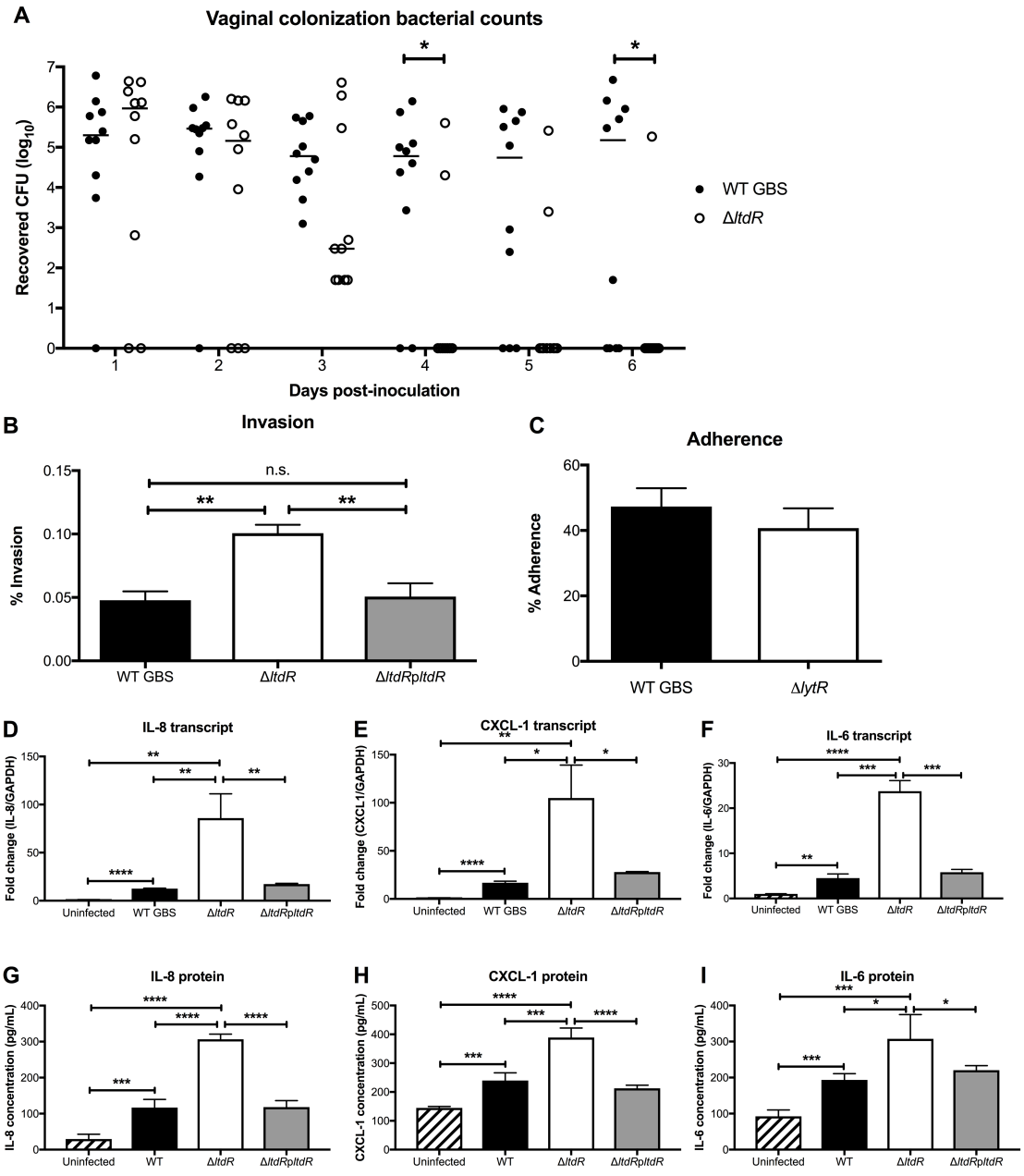

Figure 3.6. LtdR plays a role in GBS persistence and inflammation in the vaginal tract. (A) Murine vaginal colonization model. Mice were inoculated with either WT or the Δ*ltdR* mutant GBS strains and bacterial load was monitored daily. (B) Invasion of WT GBS, the Δ*ltdR* mutant, and the complemented strain into hVEC was quantified after a 2 h infection. (C) Adherence of WT GBS and the Δ*ltdR* mutant was assessed after a 30 min incubation. (D-F) hVEC were infected with GBS for 5 h, then transcript levels of IL-8 (D), CXCL-1 (E), and IL-6 (F) were assessed by RT-qPCR. (G-I) ELISA to quantify secreted IL-8 (G), CXCL-1 (H), and IL-6 (I) by hVEC was performed following a 5 h infection with GBS strains. Experiments were performed at least 3 times in triplicate and error bars represent SD; a representative experiment is shown. *, $P < 0.05$; **, $P < 0.005$; ***, $P < 0.0005$; ****, $P < 0.00005$.

LtdR regulation impacts many bacterial cell processes.

Thus far we have observed that LtdR contributes to both colonization and invasive disease. Because GBS colonization and meningitis occur in different host niches, we hypothesized that LtdR may regulate multiple bacterial pathways to affect GBS interactions within different host cell environments. To characterize the impact of LtdR regulation on global gene transcription, we performed RNA-sequencing analysis of the Δ*ltdR* mutant as well as the parental WT strain grown to OD = 0.2, 0.5, and 1.0. We observed significant global changes at all growth phases, with the highest number of significantly differentially expressed genes at early stationary phase (OD = 1.0); in total 135 genes were downregulated and 109 genes upregulated in the Δ*ltdR* mutant compared to the WT strain (Fig. 7A-E, and Supplemental Table 1) We classified these genes based on Clusters of Orthologous Genes (COG) categories. (48, 49) The majority of differentially expressed genes at all three growth phases are involved in metabolic pathways. There were also increases in the expression of genes involved in RNA processing in the WT strain. Interestingly, the expression of a number of transcriptional regulators (all classified under the signal transduction COG) is higher in the Δ*ltdR* mutant strain at early stationary phase (Fig. 7F). In our examination of the differentially expressed transcripts, we saw little overlap of genes affected between the three growth phases. (Fig. 7A-E). These results suggest that the effects of LtdR regulation are variable depending on growth phase. GBSCOH1_RS09570, which encodes a bifunctional homocysteine S-methyltransferase/methylentetrahydrofolate reductase, was the transcript that was more abundant in WT GBS at every time point compared to the Δ*ltdR* mutant. This enzyme functions in methionine metabolism pathways. The gene that was more abundant in the Δ*ltdR* mutant compared to WT at all time points was GBSCOH1_RS05780, which encodes the LysR family transcriptional regulator MtaR. MtaR has previously been shown to regulate the expression of the methionine

transport genes *metQ1* (GBSCOH1_RS07790), *pdsM* (GBSCOH1_RS07785), *metN* (GBSCOH1_RS07780), and *metP* (GBSCOH1_RS07775). (27, 50) In our RNA-seq analysis, *metQ1, pdsM, and metN* transcripts were significantly higher in the Δ*ltdR* mutant at the earliest time point while just *metQ1* was increased in the Δ*ltdR* mutant in mid-log phase and none of genes in the methionine metabolism operon were significantly differentially expressed at the latest time point. RT-qPCR was used to validate some of these and other select transcripts that were significantly higher or lower in the Δ*ltdR* mutant as determined by RNA-sequencing. We observed that differences in transcript abundance between WT GBS and Δ*ltdR* mutant cultures by RT-qPCR were similar to those seen by RNA-sequencing (Supplemental Table 2). We further observed that the complemented strain had significantly lower expression of select transcripts that are highly upregulated in the Δ*ltdR* mutant compared to the WT strain (Supplemental Fig. 1). The results of our RNA-seq and RT-qPCR analysis of the WT, Δ*ltdR* mutant and complemented strains indicate that LtdR may regulate many cellular pathways including methionine uptake and metabolism as well as expression of potential virulence factors.

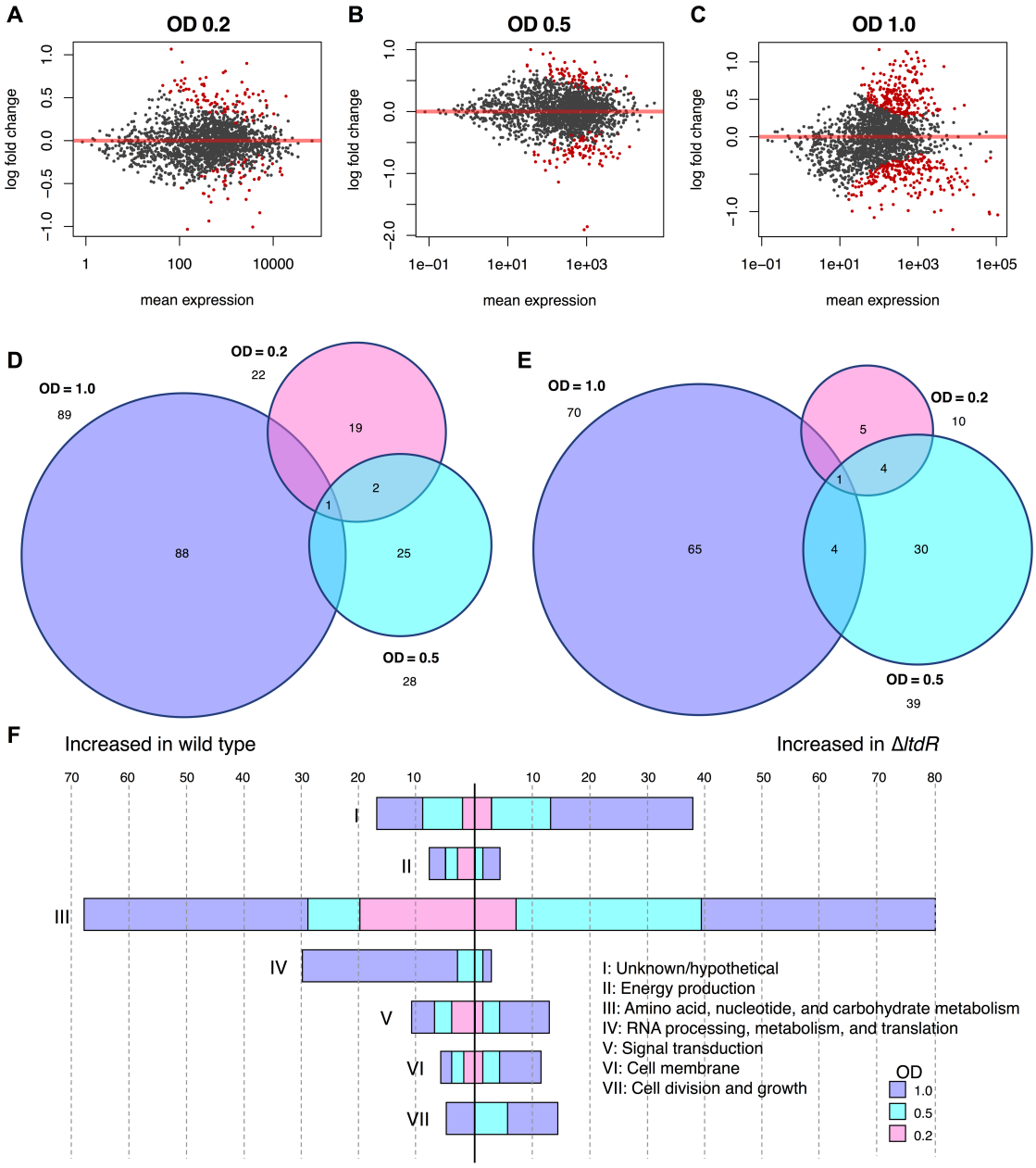

Figure 3.7. RNA-sequencing to identify LtdR regulated processes. (A-C) MA-plots highlighting differentially expressed genes ($P_{adj} < 0.1$) between WT GBS and the Δ*ltdR* mutant in red at different growth phases. OD_{600} of 0.2 (A), OD_{600} of 0.5 (B), and OD_{600} of 1.0 (C) correspond to late lag phase, exponential phase, and early stationary phase, respectively. (D and E) Venn diagrams of genes expressed significantly ($P_{adj} < 0.05$) higher in WT GBS compared to the Δ*ltdR* mutant (D) and transcripts that were significantly higher in the Δ*ltdR* mutant strain compared to WT (E). (F) Significantly differentially expressed genes ($P_{adj} < 0.05$) were classified according to Cluster of Orthologous Genes (COG) categories.

DISCUSSION

Bacteria use TCSs to monitor and respond to environmental signals. GBS possesses 21 TCSs (6), about twice as many as other closely related pathogens such as *Streptococcus pyogenes, Streptococcus pneumoniae*, and *Streptococcus mutans*, all of which encode just thirteen TCSs in their genomes. (51-53) Three of the GBS TCS transcriptional regulators contain the rare LytTR DNA-binding domain. (5) Because LytTR-containing response regulators predominantly influence virulence in Gram-positive pathogens (15, 17), we have explored the role of the previously uncharacterized LtdR regulator in GBS meningitis and vaginal persistence. In this study, we show that LtdR regulation can impact GBS infection and colonization by influencing host inflammatory responses.

It is likely that GBS invasion into BBB endothelial cells is the critical first step for the development of meningitis. (2) Our data suggest that LtdR plays a role in promoting GBS invasion into host cells. We found that the Δ*ltdR* mutant is significantly more invasive than the parental WT GBS strain without any difference in attachment to host cells or survival within cells for up to 8 hours. Additionally, we were able to recover more Δ*ltdR* mutant GBS than WT GBS from the brain tissue of infected mice while we observed similar bacterial loads in other tissues. These observations suggest that LtdR regulates factors that specifically promote uptake of GBS into brain endothelial cells without affecting GBS attachment to host cells. Subsequent to bacterial BBB invasion, the stimulation of host immune pathways is essential to the progression of meningitis. The release of inflammatory factors by brain endothelial cells, microglia, astrocytes, and infiltrating immune cells can exacerbate neuronal injury. (54) An analysis of the global transcription profile in BBB endothelium showed that the expression of many chemokines and cytokines is increased in response to GBS infection, with IL-8, CXCL-1, and IL-6 among the most

highly induced. (37) In this current study we found that disrupting LtdR regulation results in increased expression of those three cytokines. IL-8 and CXCL-1 are major neutrophil chemoattractants known to orchestrate neutrophil activation and recruitment during GBS infection (31, 55), while IL-6, another pro-inflammatory cytokine that is elevated in the cerebrospinal fluid of meningitis patients, has also been shown to be secreted by brain endothelial cells during GBS infection. (37) Although an inflammatory response may be beneficial as a host defense against bacterial infections, excess inflammation can exacerbate the symptoms of bacterial meningitis and can be detrimental during an acute infection. (56, 57) We observed that mice infected with the Δ*ltdR* mutant GBS strain exhibited higher brain bacterial loads and increased meningeal inflammation compared to animals challenged with WT GBS. Thus, LtdR regulation impacts bacterial BBB penetration and disease progression during GBS meningitis.

While increased inflammation can be associated with worse prognosis in invasive bacterial infections such as meningitis, we have observed that stimulation of the host immune system is associated with bacterial clearance during vaginal colonization. (13, 58) We have previously investigated the ability of different GBS strains to successfully colonize the murine vaginal tract and found that the less inflammatory strains persisted the longest. (38) Here, we observed that the Δ*ltdR* mutant GBS strain promoted increased levels of proinflammatory cytokines/chemokines from vaginal epithelial cells and did not persist in the mouse vagina compared to WT GBS. These results are consistent with previous studies showing that the upregulation of proinflammatory signaling pathways are associated with GBS clearance from the vaginal tract. (13, 59) Further, our data suggest that the LtdR/S system is necessary for limiting the expression of GBS virulence factors during colonization, thereby reducing host innate immune responses to promote stable vaginal persistence.

We identify the GBS LtdR response regulator as a key player in inducing inflammation in both brain endothelial cells and vaginal epithelial cells; however, the exact mechanism(s) by which GBS LtdR controls gene expression to promote proinflammatory signaling remain unclear. To further understand how the LtdS/R system contributes to colonization and disease pathogenesis we performed RNA sequencing to compare the transcriptional profiles of the GBS WT and Δ*ltdR* mutant strains. Our analysis revealed dramatic transcriptional differences between WT GBS and the Δ*ltdR* mutant strain. We detected the highest number of significantly differentially expressed transcripts between the two strains at the later growth phase, suggesting that LtdR regulation may be most active during stationary phase. Overall there were 135 genes that were down regulated and 109 genes that were induced in the Δ*ltdR* mutant compared to the WT strain; thus, LtdR appears to act as both a positive and negative regulator. Genes that appear to be negatively regulated by LtdR include those involved in signal transduction, cell division and growth, cell membrane, as well as almost 40 genes that have a hypothetical or unknown function. Interestingly, in a previous study the *ltdR* gene was deleted in a different GBS background, specifically the serotype V CJB111 strain (mutant designated as *Δrr11*). (5) While the impact of Rr11 on pathogenesis was not characterized, it was reported using microarray analysis that Rr11 similarly regulates genes involved in metabolism. (5)

Many TCS sensor kinases are stimulated by stress conditions that are present during stationary phase such as lack of nutrients, low pH, and the accumulation of toxic metabolites, and our observations suggest that the LtdS/R TCS may also play a role in adaptation to different growth environments. Future studies to determine the signal(s) being sensed by the LtdS sensor kinase will be of interest. We saw a number of genes associated methionine metabolism expressed higher in the Δ*ltdR* mutant compared to WT GBS. GBS requires methionine for growth but cannot

synthesize the amino acid, so it must scavenge methionine from its environment. Previous work has shown that a GBS strain lacking the MtaR methionine transport regulator exhibits growth defects in media with physiological methionine concentrations and is attenuated in an *in vivo* rat sepsis model. (27, 50) While we observed no differences in growth between WT and the Δ*ltdR* mutant GBS strains in THB and CDM, further characterizing the role of LtdR regulation in GBS growth and survival in blood, serum, and other methionine-low conditions is warranted.

We also observed that the gene encoding the pore-forming toxin hemolysin III as well as the directly upstream gene encoding a MerR domain containing transcriptional regulator, which likely regulates hemolysin III expression, were upregulated in the Δ*ltdR* mutant compared to WT. Hemolysin III from *Bacillus cereus* has been shown to lyse erythrocytes and in *Virbrio vulnificus* the toxin is known to impact virulence in a mouse model of infection. (60, 61) However, nothing is known about the role of hemolysin III in GBS colonization and invasive disease. Our results suggest the LtdR regulation might affect hemolysin III expression. As the GBS β h/c toxin is known to promote neutrophilic chemokine signaling in BBB endothelium (29) further studies on hemolysin III and its contribution to proinflammatory responses during GBS colonization and disease progression will be of interest.

This study demonstrates the importance of LtdR regulation to the progression of GBS meningitis as well as GBS persistence within the vaginal tract during colonization. Our results are consistent with previous reports that suggest GBS must tightly regulate expression of virulence and inflammatory factors in order to promote a colonizing state, and that changes in expression levels of these factors contribute to disease progression. Future studies are aimed at determining the specific LtdR regulated genes that contribute to bacterial invasion and host proinflammatory

signaling, which may provide important targets for preventing GBS colonization and subsequent invasive disease.

ACKNOWLEDGEMENTS

We thank Kwang Sik Kim and Monique Stins (Johns Hopkins) for providing hBMEC, John Kearney (University of Alabama at Birmingham) for providing anti-serotype III and anti-serotype Ia GBS IgM antibodies, and Jonathan Livny (Broad Institute of MIT and Harvard) for helpful discussions. RNA-Seq libraries were constructed and sequenced at the Broad Institute of MIT and Harvard by Jessica Alexander at the Microbial 'Omics Core and by the Genomics Platform, respectively. The Microbial 'Omics Core at the Broad Institute of MIT and Harvard also provided guidance on experimental design and conducted preliminary analysis for all RNA-Seq data. This study was supported by the Rees Stealy Research Foundation/SDSU Heart Institute and San Diego Chapter ARCS scholarships to L.D., and the NIH/NINDS R01-NS051247 to K.S.D.

Chapter 3, in full, is a reprint of the material as it appears in: Deng L, Mu R, Weston TA, Spencer BL, Liles RP, Doran KS. Characterization of a two-component system transcriptional regulator, LtdR, that impacts Group B streptococcal colonization and disease. *Infect Immun*. 86(7). 2018. The dissertation author was the primary investigator and author of this paper.

SUPPLEMENTAL MATERIALS

Supplemental Table 3.2. Results of RT-qPCR to confirm select RNA-sequencing hits. Fold changes comparing WT expression to the Δ*ltdR* mutant strain expression of GBSCOH1_RSO5780 (MtaR), GBS COH1_RS06260 (hemolysin III), GBSCOH1_RS06255 (hemolysin III regulator), GBSCOH1_RS07960 (3-hydroxybutyryl-CoA dehydrogenase), GBSCOH1_RS07790 (MetQ), GBSCOH1_RS08590 (hypothetical protein), GBSCOH1_RS09575 (5-methyltetrahydropteroyltriglutamate homocysteine S-methyltransferase), GBSCOH1_RS09570 (bifunctional homocysteine S-methyltransferase/methylenetetrahydrofolate reductase), and GBSCOH1_RS00325 (N-acetylmannosamine-6-phosphate 2-epimerase) are shown. Statistically significant fold change values ($P < 0.05$) are indicated in bold.

	RNA-seq			RT-qPCR		
Gene	**0.2**	**0.5**	**1**	**0.2**	**0.5**	**1**
GBSCOH1_RS05780	**0.488996**	**0.518046**	**0.473386**	**0.645774**	**0.412867**	**0.170214**
GBSCOH1_RS06260	**0.497740**	**0.275491**	*1.243439*	**0.337296**	**0.239892**	**0.266474**
GBSCOH1_RS06255	**0.622054**	**0.266453**	*1.218117*	**0.432325**	**0.235464**	**0.346495**
GBSCOH1_RS07960	*0.877456*	*0.766039*	**0.423566**	*0.962943*	*0.773328*	**0.087253**
GBSCOH1_RS07790	**0.522476**	**0.658644**	*0.832567*	**0.447618**	**0.419600**	**0.530920**
GBSCOH1_RS08590	**2.092841**	*1.390108*	*1.223710*	**1.901458**	*1.169179*	**0.198603**
GBSCOH1_RS09575	**2.000487**	**1.884210**	*1.086967*	**1.464651**	*3.040556*	*1.180139*
GBSCOH1_RS09570	**1.587386**	**1.905671**	**1.614243**	**1.732657**	**2.568016**	**0.319847**
GBSCOH1_RS00325	*0.843503*	*1.245606*	**2.241504**	**1.580136**	*1.251066*	**1.634435**

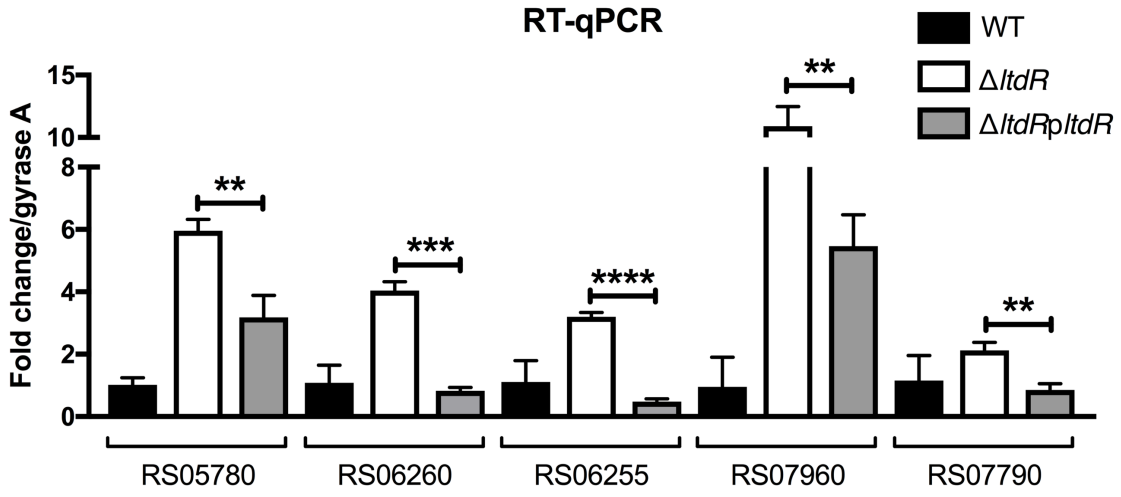

Supplemental Figure 3.1. RT-qPCR to compare gene expression between WT, the Δ*ltdR* mutant, and the complemented strains.

REFERENCES

1. **Thigpen MC, Whitney CG, Messonnier NE, Zell ER, Lynfield R, Hadler JL, Harrison LH, Farley MM, Reingold A, Bennett NM, Craig AS, Schaffner W, Thomas A, Lewis MM, Scallan E, Schuchat A, Emerging Infections Programs N.** 2011. Bacterial meningitis in the United States, 1998-2007. N Engl J Med **364:**2016-2025.

2. **Doran KS, Nizet V.** 2004. Molecular pathogenesis of neonatal group B streptococcal infection: no longer in its infancy. Mol Microbiol **54:**23-31.

3. **Beier D, Gross R.** 2006. Regulation of bacterial virulence by two-component systems. Curr Opin Microbiol **9:**143-152.

4. **Bassler BL, Losick R.** 2006. Bacterially speaking. Cell **125:**237-246.

5. **Faralla C, Metruccio MM, De Chiara M, Mu R, Patras KA, Muzzi A, Grandi G, Margarit I, Doran KS, Janulczyk R.** 2014. Analysis of two-component systems in group B Streptococcus shows that RgfAC and the novel FspSR modulate virulence and bacterial fitness. MBio **5:**e00870-00814.

6. **Glaser P, Rusniok C, Buchrieser C, Chevalier F, Frangeul L, Msadek T, Zouine M, Couve E, Lalioui L, Poyart C, Trieu-Cuot P, Kunst F.** 2002. Genome sequence of Streptococcus agalactiae, a pathogen causing invasive neonatal disease. Mol Microbiol **45:**1499-1513.

7. **Tettelin H, Masignani V, Cieslewicz MJ, Eisen JA, Peterson S, Wessels MR, Paulsen IT, Nelson KE, Margarit I, Read TD, Madoff LC, Wolf AM, Beanan MJ, Brinkac LM, Daugherty SC, DeBoy RT, Durkin AS, Kolonay JF, Madupu R, Lewis MR, Radune D, Fedorova NB, Scanlan D, Khouri H, Mulligan S, Carty HA, Cline RT, Van Aken SE, Gill J, Scarselli M, Mora M, Iacobini ET, Brettoni C, Galli G, Mariani M, Vegni F, Maione D, Rinaudo D, Rappuoli R, Telford JL, Kasper DL, Grandi G, Fraser CM.** 2002. Complete genome sequence and comparative genomic analysis of an emerging human pathogen, serotype V Streptococcus agalactiae. Proc Natl Acad Sci U S A **99:**12391-12396.

8. **Quach D, van Sorge NM, Kristian SA, Bryan JD, Shelver DW, Doran KS.** 2009. The CiaR response regulator in group B Streptococcus promotes intracellular survival and resistance to innate immune defenses. J Bacteriol **191:**2023-2032.

9. **Klinzing DC, Ishmael N, Dunning Hotopp JC, Tettelin H, Shields KR, Madoff LC, Puopolo KM.** 2013. The two-component response regulator LiaR regulates cell wall stress responses, pili expression and virulence in group B Streptococcus. Microbiology **159:**1521-1534.

10. **Landwehr-Kenzel S, Henneke P.** 2014. Interaction of Streptococcus agalactiae and Cellular Innate Immunity in Colonization and Disease. Front Immunol **5:**519.

11. **Lembo A, Gurney MA, Burnside K, Banerjee A, de los Reyes M, Connelly JE, Lin WJ, Jewell KA, Vo A, Renken CW, Doran KS, Rajagopal L.** 2010. Regulation of CovR expression in Group B Streptococcus impacts blood-brain barrier penetration. Mol Microbiol **77:**431-443.

12. **Jiang SM, Cieslewicz MJ, Kasper DL, Wessels MR.** 2005. Regulation of virulence by a two-component system in group B streptococcus. J Bacteriol **187:**1105-1113.

13. **Patras KA, Wang NY, Fletcher EM, Cavaco CK, Jimenez A, Garg M, Fierer J, Sheen TR, Rajagopal L, Doran KS.** 2013. Group B Streptococcus CovR regulation modulates host immune signalling pathways to promote vaginal colonization. Cell Microbiol **15:**1154-1167.

14. **Aravind L, Anantharaman V, Balaji S, Babu MM, Iyer LM.** 2005. The many faces of the helix-turn-helix domain: transcription regulation and beyond. FEMS Microbiol Rev **29:**231-262.

15. **Galperin MY.** 2008. Telling bacteria: do not LytTR. Structure **16:**657-659.

16. **Behr S, Heermann R, Jung K.** 2016. Insights into the DNA-binding mechanism of a LytTR-type transcription regulator. Biosci Rep **36**.

17. **Nikolskaya AN, Galperin MY.** 2002. A novel type of conserved DNA-binding domain in the transcriptional regulators of the AlgR/AgrA/LytR family. Nucleic Acids Res **30:**2453-2459.

18. **Al Safadi R, Mereghetti L, Salloum M, Lartigue MF, Virlogeux-Payant I, Quentin R, Rosenau A.** 2011. Two-component system RgfA/C activates the fbsB gene encoding major fibrinogen-binding protein in highly virulent CC17 clone group B Streptococcus. PLoS One **6:**e14658.

19. **Ahn SJ, Rice KC, Oleas J, Bayles KW, Burne RA.** 2010. The Streptococcus mutans Cid and Lrg systems modulate virulence traits in response to multiple environmental signals. Microbiology **156:**3136-3147.

20. **Ahn SJ, Qu MD, Roberts E, Burne RA, Rice KC.** 2012. Identification of the Streptococcus mutans LytST two-component regulon reveals its contribution to oxidative stress tolerance. BMC Microbiol **12:**187.

21. **Brunskill EW, Bayles KW.** 1996. Identification of LytSR-regulated genes from Staphylococcus aureus. J Bacteriol **178:**5810-5812.

22. **Brunskill EW, Bayles KW.** 1996. Identification and molecular characterization of a putative regulatory locus that affects autolysis in Staphylococcus aureus. J Bacteriol **178:**611-618.

23. **Brunskill EW, de Jonge BL, Bayles KW.** 1997. The Staphylococcus aureus scdA gene: a novel locus that affects cell division and morphogenesis. Microbiology **143 (Pt 9):**2877-2882.

24. **Sharma-Kuinkel BK, Mann EE, Ahn JS, Kuechenmeister LJ, Dunman PM, Bayles KW.** 2009. The Staphylococcus aureus LytSR two-component regulatory system affects biofilm formation. J Bacteriol **191:**4767-4775.

25. **Yang SJ, Xiong YQ, Yeaman MR, Bayles KW, Abdelhady W, Bayer AS.** 2013. Role of the LytSR two-component regulatory system in adaptation to cationic antimicrobial peptides in Staphylococcus aureus. Antimicrob Agents Chemother **57:**3875-3882.

26. **Chaffin DO, Beres SB, Yim HH, Rubens CE.** 2000. The serotype of type Ia and III group B streptococci is determined by the polymerase gene within the polycistronic capsule operon. J Bacteriol **182:**4466-4477.

27. **Shelver D, Rajagopal L, Harris TO, Rubens CE.** 2003. MtaR, a regulator of methionine transport, is critical for survival of group B streptococcus in vivo. J Bacteriol **185:**6592-6599.

28. **Park IH, Geno KA, Yu J, Oliver MB, Kim KH, Nahm MH.** 2015. Genetic, biochemical, and serological characterization of a new pneumococcal serotype, 6H, and generation of a pneumococcal strain producing three different capsular repeat units. Clin Vaccine Immunol **22:**313-318.

29. **Doran KS, Chang JC, Benoit VM, Eckmann L, Nizet V.** 2002. Group B streptococcal beta-hemolysin/cytolysin promotes invasion of human lung epithelial cells and the release of interleukin-8. J Infect Dis **185:**196-203.

30. **Doran KS, Engelson EJ, Khosravi A, Maisey HC, Fedtke I, Equils O, Michelsen KS, Arditi M, Peschel A, Nizet V.** 2005. Blood-brain barrier invasion by group B Streptococcus depends upon proper cell-surface anchoring of lipoteichoic acid. J Clin Invest **115:**2499-2507.

31. **Banerjee A, Kim BJ, Carmona EM, Cutting AS, Gurney MA, Carlos C, Feuer R, Prasadarao NV, Doran KS.** 2011. Bacterial Pili exploit integrin machinery to promote immune activation and efficient blood-brain barrier penetration. Nat Commun **2:**462.

32. **Patras KA, Doran KS.** 2016. A Murine Model of Group B Streptococcus Vaginal Colonization. J Vis Exp doi:10.3791/54708.

33. **Weksler B, Romero IA, Couraud PO.** 2013. The hCMEC/D3 cell line as a model of the human blood brain barrier. Fluids Barriers CNS **10:**16.

34. **Weksler BB, Subileau EA, Perriere N, Charneau P, Holloway K, Leveque M, Tricoire-Leignel H, Nicotra A, Bourdoulous S, Turowski P, Male DK, Roux F, Greenwood J, Romero IA, Couraud PO.** 2005. Blood-brain barrier-specific properties of a human adult brain endothelial cell line. FASEB J **19:**1872-1874.

35. **Llombart V, Garcia-Berrocoso T, Bech-Serra JJ, Simats A, Bustamante A, Giralt D, Reverter-Branchat G, Canals F, Hernandez-Guillamon M, Montaner J.** 2016. Characterization of secretomes from a human blood brain barrier endothelial cells in-vitro model after ischemia by stable isotope labeling with aminoacids in cell culture (SILAC). J Proteomics **133:**100-112.

36. **Ohtsuki S, Ikeda C, Uchida Y, Sakamoto Y, Miller F, Glacial F, Decleves X, Scherrmann JM, Couraud PO, Kubo Y, Tachikawa M, Terasaki T.** 2013. Quantitative targeted absolute proteomic analysis of transporters, receptors and junction proteins for validation of human cerebral microvascular endothelial cell line hCMEC/D3 as a human blood-brain barrier model. Mol Pharm **10:**289-296.

37. **Doran KS, Liu GY, Nizet V.** 2003. Group B streptococcal beta-hemolysin/cytolysin activates neutrophil signaling pathways in brain endothelium and contributes to development of meningitis. J Clin Invest **112:**736-744.

38. **Patras KA, Rosler B, Thoman ML, Doran KS.** 2015. Characterization of host immunity during persistent vaginal colonization by Group B Streptococcus. Mucosal Immunol **8:**1339-1348.

39. **van Sorge NM, Ebrahimi CM, McGillivray SM, Quach D, Sabet M, Guiney DG, Doran KS.** 2008. Anthrax toxins inhibit neutrophil signaling pathways in brain endothelium and contribute to the pathogenesis of meningitis. PLoS One **3:**e2964.

40. **Shishkin AA, Giannoukos G, Kucukural A, Ciulla D, Busby M, Surka C, Chen J, Bhattacharyya RP, Rudy RF, Patel MM, Novod N, Hung DT, Gnirke A, Garber M, Guttman M, Livny J.** 2015. Simultaneous generation of many RNA-seq libraries in a single reaction. Nat Methods **12:**323-325.

41. **Zhu YY, Machleder EM, Chenchik A, Li R, Siebert PD.** 2001. Reverse transcriptase template switching: a SMART approach for full-length cDNA library construction. Biotechniques **30:**892-897.

42. **Li H, Durbin R.** 2009. Fast and accurate short read alignment with Burrows-Wheeler transform. Bioinformatics **25:**1754-1760.

43. **Love MI, Huber W, Anders S.** 2014. Moderated estimation of fold change and dispersion for RNA-seq data with DESeq2. Genome Biol **15:**550.

44. **Abeel T, Van Parys T, Saeys Y, Galagan J, Van de Peer Y.** 2012. GenomeView: a next-generation genome browser. Nucleic Acids Res **40:**e12.

45. **Davies HD, Jones N, Whittam TS, Elsayed S, Bisharat N, Baker CJ.** 2004. Multilocus sequence typing of serotype III group B streptococcus and correlation with pathogenic potential. J Infect Dis **189:**1097-1102.

46. **Takahashi S, Adderson EE, Nagano Y, Nagano N, Briesacher MR, Bohnsack JF.** 1998. Identification of a highly encapsulated, genetically related group of invasive type III group B streptococci. J Infect Dis **177:**1116-1119.

47. **Chi F, Wang L, Zheng X, Wu CH, Jong A, Sheard MA, Shi W, Huang SH.** 2011. Meningitic Escherichia coli K1 penetration and neutrophil transmigration across the blood-brain barrier are modulated by alpha7 nicotinic receptor. PLoS One **6:**e25016.

48. **Natale DA, Galperin MY, Tatusov RL, Koonin EV.** 2000. Using the COG database to improve gene recognition in complete genomes. Genetica **108:**9-17.

49. **Tatusov RL, Galperin MY, Natale DA, Koonin EV.** 2000. The COG database: a tool for genome-scale analysis of protein functions and evolution. Nucleic Acids Res **28:**33-36.

50. **Bryan JD, Liles R, Cvek U, Trutschl M, Shelver D.** 2008. Global transcriptional profiling reveals Streptococcus agalactiae genes controlled by the MtaR transcription factor. BMC Genomics **9:**607.

51. **Graham MR, Smoot LM, Migliaccio CA, Virtaneva K, Sturdevant DE, Porcella SF, Federle MJ, Adams GJ, Scott JR, Musser JM.** 2002. Virulence control in group A Streptococcus by a two-component gene regulatory system: global expression profiling and in vivo infection modeling. Proc Natl Acad Sci U S A **99:**13855-13860.

52. **Throup JP, Koretke KK, Bryant AP, Ingraham KA, Chalker AF, Ge Y, Marra A, Wallis NG, Brown JR, Holmes DJ, Rosenberg M, Burnham MK.** 2000. A genomic analysis of two-component signal transduction in Streptococcus pneumoniae. Mol Microbiol **35:**566-576.

53. **Ajdic D, McShan WM, McLaughlin RE, Savic G, Chang J, Carson MB, Primeaux C, Tian R, Kenton S, Jia H, Lin S, Qian Y, Li S, Zhu H, Najar F, Lai H, White J, Roe BA, Ferretti JJ.** 2002. Genome sequence of Streptococcus mutans UA159, a cariogenic dental pathogen. Proc Natl Acad Sci U S A **99:**14434-14439.

54. **Kim KS.** 2003. Pathogenesis of bacterial meningitis: from bacteraemia to neuronal injury. Nat Rev Neurosci **4:**376-385.

55. **Banerjee A, Van Sorge NM, Sheen TR, Uchiyama S, Mitchell TJ, Doran KS.** 2010. Activation of brain endothelium by pneumococcal neuraminidase NanA promotes bacterial internalization. Cell Microbiol **12:**1576-1588.

56. **Brouwer MC, McIntyre P, Prasad K, van de Beek D.** 2015. Corticosteroids for acute bacterial meningitis. Cochrane Database Syst Rev doi:10.1002/14651858.CD004405.pub5**:**CD004405.

57. **Chang YC, Olson J, Beasley FC, Tung C, Zhang J, Crocker PR, Varki A, Nizet V.** 2014. Group B Streptococcus engages an inhibitory Siglec through sialic acid mimicry to blunt innate immune and inflammatory responses in vivo. PLoS Pathog **10:**e1003846.

58. **Sheen TR, Jimenez A, Wang NY, Banerjee A, van Sorge NM, Doran KS.** 2011. Serine-rich repeat proteins and pili promote Streptococcus agalactiae colonization of the vaginal tract. J Bacteriol **193:**6834-6842.

59. **Carey AJ, Tan CK, Mirza S, Irving-Rodgers H, Webb RI, Lam A, Ulett GC.** 2014. Infection and cellular defense dynamics in a novel 17beta-estradiol murine model of chronic human group B streptococcus genital tract colonization reveal a role for hemolysin in persistence and neutrophil accumulation. J Immunol **192:**1718-1731.

60. **Baida GE, Kuzmin NP.** 1996. Mechanism of action of hemolysin III from Bacillus cereus. Biochim Biophys Acta **1284:**122-124.

61. **Chen YC, Chang MC, Chuang YC, Jeang CL.** 2004. Characterization and virulence of hemolysin III from Vibrio vulnificus. Curr Microbiol **49:**175-179.

Chapter 4

Identification of key determinants of Staphylococcus aureus vaginal colonization

Liwen Deng[1,2], Katrin Schilcher[1], Lindsey R. Burcham[1], Jakub M. Kwiecinski[1], Paige M. Johnson[1], Steven R. Head[3], David E. Heinrichs[4], Alexander R. Horswill1[5], Kelly S. Doran[1,2]

[1]Department of Immunology and Microbiology, University of Colorado School of Medicine, Aurora, CO, USA.
[2]Department of Cell and Molecular Biology, San Diego State University, San Diego, CA, USA.
[3]Next Generation Sequencing Core, The Scripps Research Institute, La Jolla, CA, USA.
[4]Department of Microbiology and Immunology, University of Western Ontario, London, Ontario, Canada.
[5]Department of Veterans Affairs Eastern Colorado Healthcare System, Aurora, Colorado, USA.

Submitted to *mBio* September 2019

Running title: Characterization of *S. aureus* vaginal colonization

Key words: vaginal colonization, *Staphylococcus aureus*, MRSA, fibrinogen, iron, RNA sequencing

ABSTRACT

Staphylococcus aureus is an important pathogen responsible for nosocomial and community acquired infections in humans, and methicillin-resistant *S. aureus* (MRSA) infections have continued to increase despite wide-spread preventative measures. *S. aureus* can colonize the female vaginal tract and reports have suggested an increase in MRSA infections in pregnant and postpartum women as well as outbreaks in newborn nurseries. Currently, little is known about specific factors that promote MRSA vaginal colonization and subsequent infection. To study *S. aureus* colonization of the female reproductive tract in a mammalian system, we developed a mouse model of *S. aureus* vaginal carriage and demonstrated that both hospital-associated and community-associated MRSA isolates can colonize the murine vaginal tract. Immunohistochemical analysis revealed an increase in neutrophils in the vaginal lumen during MRSA colonization. Additionally, we observed that a mutant lacking fibrinogen binding adhesins exhibited decreased persistence within the mouse vagina. To further identify novel factors that promote vaginal colonization, we performed RNA-sequencing to determine the transcriptome of MRSA growing in vivo during vaginal carriage at 5 hours, 1-day, and 3-days post-inoculation. Over 25% of bacterial genes were differentially regulated at all time points during colonization compared to laboratory cultures. The most highly induced genes were those involved in iron acquisition, including the Isd system and siderophore transport systems. Mutants deficient in these pathways did not persist as well during in vivo colonization. These results reveal that fibrinogen binding as well as the capacity to overcome host nutritional limitation are important determinants of MRSA vaginal colonization.

IMPORTANCE

Staphylococcus aureus is an opportunistic pathogen able to cause a wide variety of infections in humans. Recent reports have suggested an increasing prevalence of MRSA in pregnant and postpartum women, coinciding with the increased incidence of MRSA infections in the NICU and newborn nurseries. Vertical transmission from mothers to infants at delivery is a likely route of MRSA acquisition by the newborn, however, essentially nothing is known about host and bacterial factors that influence MRSA carriage in the vagina. Here, we established a mouse model of vaginal colonization and observed that multiple MRSA strains can persist in the vaginal tract. Additionally, we determined that MRSA interactions with fibrinogen as well as iron uptake can promote vaginal persistence. This study is the first to identify molecular mechanisms which govern vaginal colonization by MRSA, the critical initial step preceding infection and neonatal transmission.

INTRODUCTION

Staphylococcus aureus is a commensal of approximately 20% of the healthy adult population (1) and also an opportunistic bacterial pathogen able to cause a wide variety of infections ranging in severity from superficial skin lesions to more serious invasive and life-threatening infections such as endocarditis and septicemia. Prevalence of *S. aureus* infections has increased due to higher rates of colonization, immunosuppressive conditions, greater use of surgical implants, and dramatic increases in antibiotic resistance (2, 3). Compared to antibiotic-susceptible strains, methicillin-resistant *S. aureus* (MRSA) infections exhibit elevated mortality rates, require longer hospital stays, and exert a higher financial burden on patients and healthcare institutions (4). Over the past 20 years, MRSA strains have expanded from healthcare settings and

began infecting otherwise healthy individuals in the community ("community-associated" MRSA (CA-MRSA))(5). USA300 isolates are the most problematic lineage of CA-MRSA that have emerged and clonally expanded across the US, reaching epidemic levels in many hospital settings (6, 7).

Methicillin-susceptible *S. aureus* and MRSA possesses many virulence factors that promote bacterial persistence and invasive infections in different host sites. These virulence factors include cell wall-anchored surface proteins that facilitate *S. aureus* adherence to and invasion of host cells (8), proteases that modulate the host immune response to the bacterium (9), as well as pore-forming toxins such as α-toxin and the bicomponent leukocidins that lyse host cells (10). The expression of these various virulence determinants is dependent on factors such as growth rate, the availability of certain nutrients, host interactions, and the presence of antimicrobial compounds (8, 11-13).

Nasal carriage is known to be a risk factor for *S. aureus* infections both in the hospital and in the community with individuals often being infected with the strain that they carry (14). *S. aureus* can colonize the moist squamous epithelium in the anterior nares (15, 16), a process which depends upon specific interactions between bacterial cell adhesins and epithelial cell ligands. Two *S. aureus* surface proteins, clumping factor B (ClfB) and iron regulated surface determinant A (IsdA), have been strongly implicated in nasal colonization. Both ClfB and IsdA were shown to promote adhesion to nasal epithelium *in vitro* (17) and colonization of the nares of rodents (18, 19) and, in the case of ClfB, humans (20). ClfB is a member of a family of proteins that are structurally related to clumping factor A (ClfA), the archetypal fibrinogen (Fg) binding protein of *S. aureus*. ClfB has been shown to bind Fg, as well as cytokeratin 10, by the "dock, lock, and latch" mechanism first defined for the Fg binding proteins SdrG and ClfA (21, 22). Additional

surface proteins shown to contribute to bacterial attachment to nasal epithelial cells *in vitro* include *S. aureus* surface protein G (SasG) and the serine-aspartate repeat proteins SdrC and SdrD (23).

While a ubiquitous colonizer of the skin and mucous membranes, *S. aureus,* including antibiotic sensitive and resistant strains, has also been reported to colonize the vagina in up to 22% of pregnant women (24-29). A study that examined MRSA colonization showed that out of 5,732 mothers, 3.5% were colonized by MRSA in the genital tract during pregnancy (24). Another recent study of 1834 mothers showed that 4.7% were colonized vaginally by multidrug-resistant *S. aureus* (30). Reports have suggested an increasing prevalence in the USA300 lineage of MRSA in pregnant and postpartum women, coinciding with the increased incidence in the NICU and in newborn nurseries (31-36). MRSA outbreaks in NICUs can be difficult to control and have been associated with significant morbidity and mortality (33). Vertical transmission from mothers to infants at delivery has been proposed as a possible mechanism of neonatal CA-MRSA acquisition (30, 37), and while it is clear that *S. aureus* and MRSA can colonize the vaginal tract during pregnancy, essentially nothing is known about specific bacterial factors that promote vaginal persistence.

In this study, we have adapted a murine model of vaginal colonization by Group B *Streptococcus* (GBS) (38), to investigate MRSA vaginal colonization. We determined that divergent MRSA strains, CA-MRSA USA300 and HA-MRSA252, can persist within the mouse vaginal tract and that three mouse strains, CD-1, C57BL/6, and BALB/c, can be colonized with MRSA. We detected fluorescent MRSA in the vaginal lumen as well as cervical and uterine tissues of colonized mice and immunohistochemical staining showed an increase of neutrophils in colonized mice compared to naïve mice. We found that a MRSA strain lacking fibrinogen-binding surface adhesins was attenuated in both *in vitro* and *in vivo* models of vaginal colonization. Lastly,

RNA-sequencing analysis of bacteria growing *in vivo* revealed the importance of iron homeostasis in promoting MRSA persistence within the mouse vagina. Mutant USA300 strains lacking the siderophore transporter FhuCBG or the cell-surface heme receptor IsdB were significantly attenuated in their ability to colonize the vaginal tract *in vivo*.

RESULTS

MRSA colonization of the reproductive tract.

To characterize the ability of MRSA to attach to epithelial cells of the lower female reproductive tract, we performed quantitative adherence assays with community-associated USA300 strain LAC (39) and hospital-acquired strain MRSA252 (40) as described in (41) and in the Methods. An inoculum of 10^5 CFU/well (MOI = 1) was added to confluent monolayers of immortalized human vaginal (VK2), ectocervical (Ect1), and endocervical (End1) epithelial cells. Following a 30-minute incubation, the cells were washed to remove all nonadherent bacteria. Data are expressed as percent recovered cell-associated MRSA relative to the initial inoculum. Both strains exhibited substantial adherence to all three cell lines, ranging from 30-57% of the original inoculum (Fig. 1A and B). Next, we assessed the ability of both MRSA strains to initiate colonization of the murine vaginal tract. 8-week old female CD-1 mice were treated with 17β-estradiol 1-day before inoculation with 10^7 CFU of either USA300 or MRSA252. The next day the vaginal lumen was swabbed and then we euthanized the animals and collected the vagina, cervix, and uterus from each mouse to quantify bacterial load. The total CFU from the swab or tissue homogenates was determined by plating on *S. aureus* CHROMagar supplemented with cefoxitin. Both strains of MRSA were recovered from the majority of mice 1-day post-inoculation in all tissues, and the CFU recovered from the swab were similar to the total CFU counts from the

vaginal tissue homogenates (Fig. 1C and D). This level and range in recovered CFU is similar to what we have observed using this mouse model for GBS colonization (38). In a subsequent experiment, mice were inoculated with USA300 expressing a fluorescent DsRed protein and we harvested the female reproductive tract 1-day post-colonization for histological analysis. We made serial sections of these tissues and performed H&E staining to examine overall tissue morphology (Fig 1E, G, and I) and fluorescent microscopy to visualize USA300 (Fig 1F, H, J, K, and L). We observed numerous red fluorescent bacteria contained within the lumen of the vagina (red arrows) (Fig. 1F). We could also see MRSA in the cervical and uterine lumen, as well as within the lamina propria of those organs (green arrows) (Fig. 1H, J, K, and L).

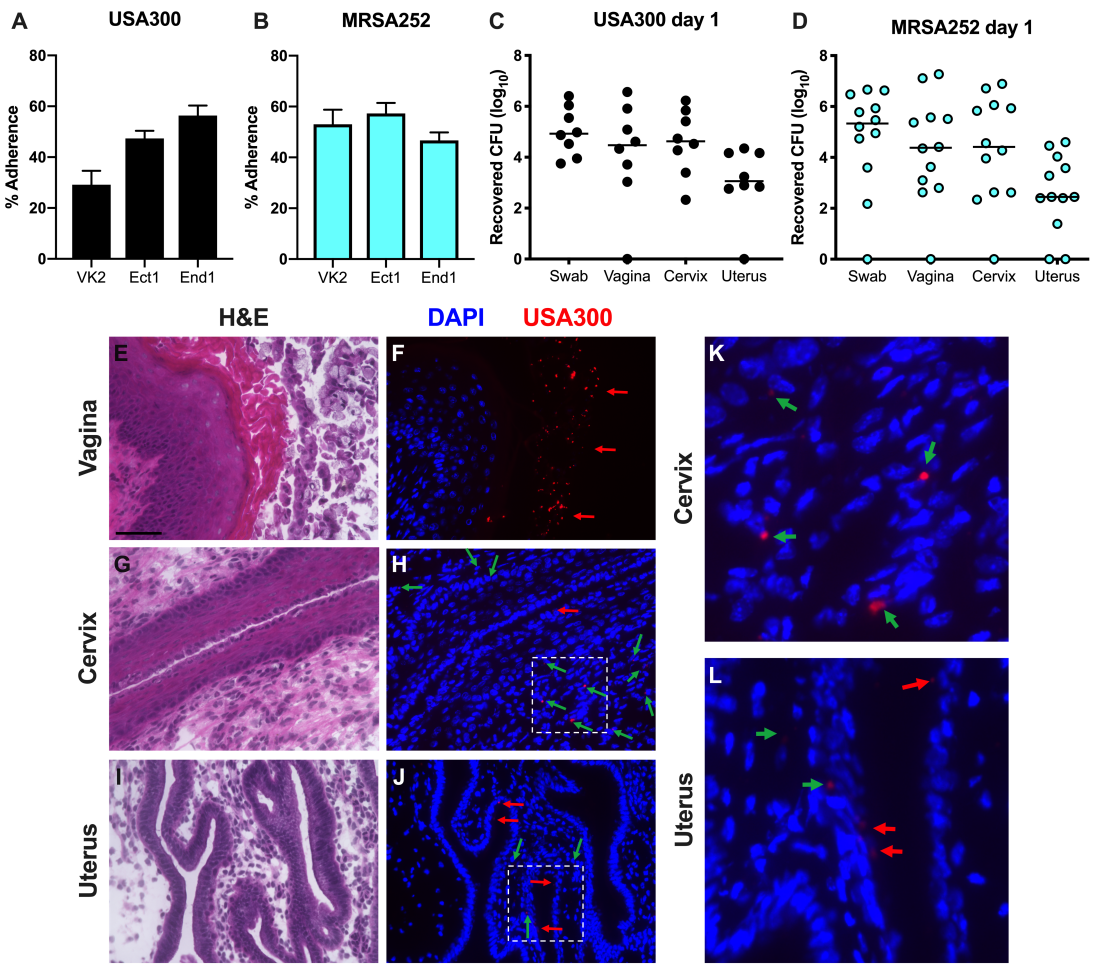

Figure 4.1. Modeling MRSA vaginal colonization. (A and B) Adherence of USA300 (A) and MRSA252 (B) to human vaginal (VK2), ectocervical (Ect1), and endocervical (End1) endothelial cells. (C and D) CFU counts from vaginal swabs, vagina, cervix, and uterus recovered 1-day post-inoculation with USA300 (C) or MRSA252 (D). Lines represent median CFU. (E-L) Mice were colonized with DsRed expressing USA300. 1-day post-inoculation, the female reproductive tract was harvested and 6μm sections of the vagina (E and F), cervix (G, H, and K), and uterus (I, J, and L) were either stained with H&E (E, G, I) or labelled with DAPI and imaged with an epifluorescent microscope to visualize nuclei and USA300 (F, H, J, K, and L). The areas highlighted in (H) and (J) are expanded in (K) and (L). USA300 in the lumen of tissues are indicated with red arrows, and USA300 within the lamina propia are indicated with green arrows. Scale bar in (E) is 100μm.

MRSA vaginal persistence and host response.

To assess vaginal persistence, mice were colonized with USA300 or MRSA252 and swabbed to determine bacterial load over time. We recovered similar CFU from mice colonized with either MRSA strain and we observed that both strains exhibited similar persistence within the

mouse vagina. While all mice were initially highly colonized by both MRSA strains, some remained highly colonized while MRSA was cleared from other mice. (Fig. 2A and B). We also assessed USA300 vaginal colonization for multiple mouse strains and observed the highest mean CFUs from BALB/c mice while C57BL/6 and CD-1 mice were colonized to a lower level (Fig. S1). Furthermore, MRSA was cleared more rapidly from the vaginal tract of CD-1 mice and persisted the longest in BALB/c mice (Fig. S1).

As we observed eventual clearance of MRSA from the vaginal tract, we examined the presence of neutrophils in vaginal tissue of mice colonized with MRSA compared to naïve mice. Previous studies have shown that neutrophils respond to vaginal colonization by pathogenic *Streptococcus* species, namely GBS and *Streptococcus pyogenes* (Group A *Streptococcus*, GAS), and that neutrophils contribute to host defense and ultimate bacterial clearance (42-44). To visualize neutrophils during colonization by MRSA, we collected vaginal tissues from mice 1-day and 3-days post-inoculation with USA300 and made serial sections for H&E staining and labelling with an antibody against the neutrophil marker Gr-1. H&E analysis showed that there were no obvious differences in morphology of the vaginal lumen between naïve and colonized mice (Fig. 2C, E, G, I, K, and M). We observed very few Gr-1 positive cells in the tissue sections form naïve mice (Fig. 2D and F). In contrast to those from naïve mice, the tissue sections from mice colonized with USA300 for 1-day contained numerous neutrophils within the vaginal lamina propria (Fig. 2H and J). At 3-days post-inoculation we detected neutrophils within the vaginal lumen (Fig. 2L and N).

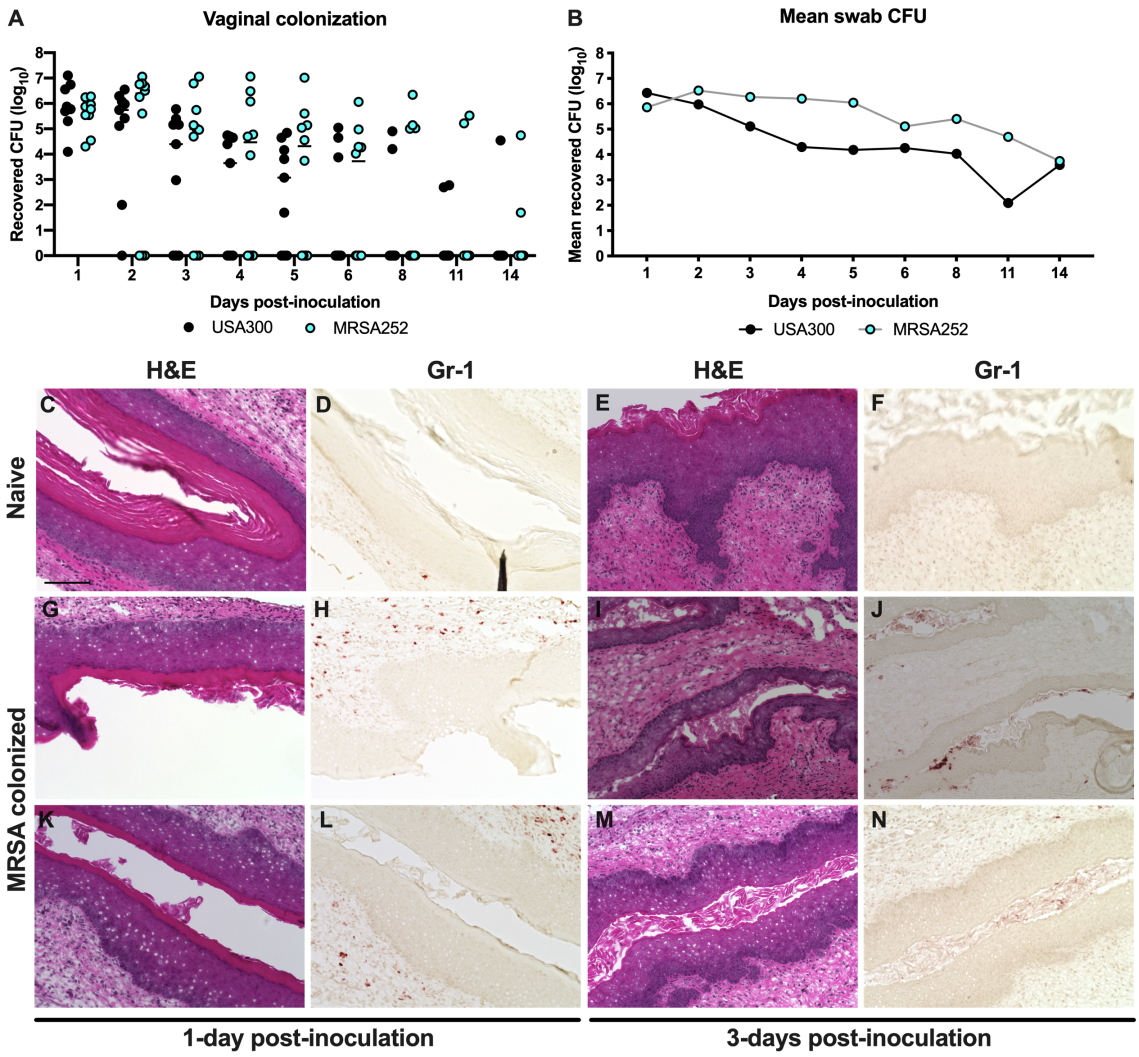

Figure 4.2. MRSA vaginal persistence and host response. (A and B) USA300 and MRSA252 persistence within the CD-1 mouse vaginal tract. CFU counts for individual mice (A) and mean recovered CFU from vaginal swabs (B) were monitored for 14 days. Lines in (A) represent median CFU. (C-N) Histology of the mouse vagina during MRSA colonization. Mice were pre-treated with 17β-estradiol and either remained naïve (C-F) or were inoculated with 10^7 CFU of USA300 (G-N). 6μm serial sections were stained with H&E (C, E, G, I, K, M) or labelled with an antibody against Gr-1 (D, F, H, J, L, N). Scale bar in (C) is 100μm.

Adherence to fibrinogen impacts MRSA vaginal colonization.

In a previous study, we demonstrated that GBS Fg binding contributed to vaginal persistence (45). Also, several studies have shown the importance of *S. aureus* interactions with extracellular matrix components, including Fg, in colonization and disease progression (46-49). USA300 binding to Fg is primarily mediated by the four sortase-anchored surface adhesins ClfA, ClfB, FnbA, and FnbB. (8, 46, 50). The serine-aspartate adhesins SdrC, SdrD, and SdrE are in the same protein family as ClfA/B (51) and have been reported to bind nasal epithelia (23). To eliminate these adherence functions, a USA300 strain was engineered where all of these adhesins were deleted or disrupted by incorporating four separate mutations (Δ*clfA clfB*::Tn Δ*fnbAB sdrCDE*::Tet; hereafter called "Fg adhesin mutant"). Compared to WT USA300, the Fg adhesin mutant was significantly less adherent to Fg (Fig. 3A). Quantitative adherence assays showed that the fibrinogen adhesin mutant exhibited decreased attachment to VK2 vaginal epithelial cells (Fig. 3B), and we could visualize this difference via Gram staining (Fig. 3C and D). Further, the Fg adhesin mutant was also less adherent to Ect1 and End1 cervical epithelial cells (Fig. 3E and F). To assess the impact of these important surface adhesins during *in vivo* colonization, we co-challenged mice with both WT USA300 and the Fg adhesin mutant. Initially we recovered similar CFUs of both strains from the mice. However, by 3-days post-inoculation, mice were significantly less colonized by the Fg adhesin mutant compared to WT USA300 (Fig. 3G). At 5-days post-inoculation, we could recover WT USA300 CFU from 60% of the mice while only 30% were still colonized by the Fg adhesin mutant (Fig. 3G).

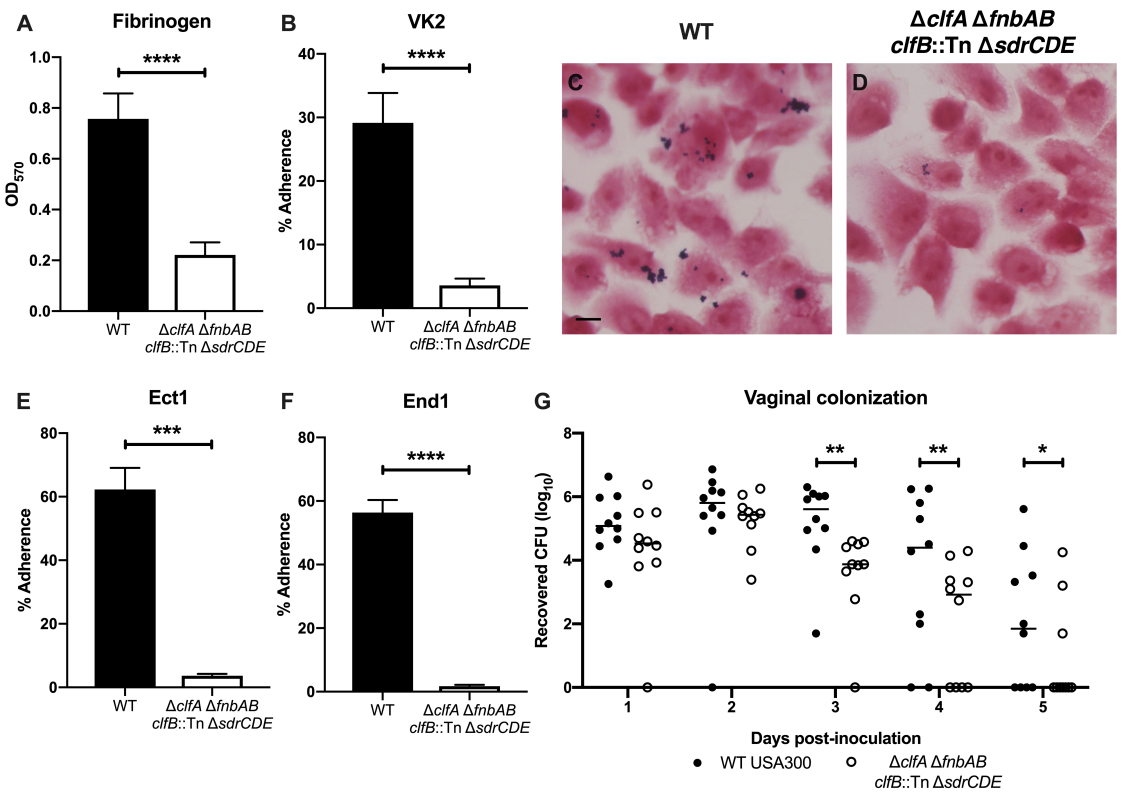

Figure 4.3. Adherence to fibrinogen impacts MRSA vaginal colonization. (A) Adherence of WT USA300 and the Fg adhesin mutant to Fg. (B-D) Adherence to VK2 cells. Monolayers of VK2 cells were inoculated with WT USA300 or the Fg adhesin mutant for a quantitative adherence assay (B) or Gram stains (C and D). Scale bar in (C) is 10 µm. (E and F) Adherence to Ect1 (E) and End1 (F) epithelial cells. (G) WT USA300 and the Fg adhesin co-colonization. Statistical analysis (A, B, E, and F) Unpaired t test. (G) Two-way ANOVA with Sidak's multiple comparisons test. * $P < 0.05$; *** $P < 0.0005$; **** $P < 0.00005$.

Transcriptome analysis during MRSA vaginal colonization

Although the Fg adhesin mutant was impaired in vaginal persistence compared to WT USA300, we did not observe a significant difference in recovered CFUs between the two strains during the first two days of colonization, and a few mice remained colonized with the Fg adhesin mutant at later time points (Fig. 1G). Thus, we hypothesized that other bacterial factors are involved in promoting MRSA vaginal carriage. To determine the impact of vaginal colonization on MRSA gene expression, we performed transcriptome analysis by RNA-sequencing of USA300

recovered from the mouse vagina compared to USA300 cultured under laboratory conditions. For these experiments, we utilized the CD-1 mouse strain as likely in this background the bacteria encounter more host pressure to maintain colonization. Mice were pre-treated with 17β-Estradiol, inoculated with 10^7 CFU of USA300, and swabbed at 5hrs, 1-day, and 3-days post-inoculation for RNA isolation. The same mice were swabbed 2-, 4-, 6-, and 8-days post-inoculation for CFU enumeration (Fig. 4A and B). Based on swab CFU counts, we selected samples from 18 mice (purple circles) for RNA-sequencing analysis (Fig. 4B). RNA samples from 6 mouse swabs were pooled to generate 3 replicates for each time-point to compare to triplicate culture samples. Principle component analysis (PCA) for all of the samples showed that culture samples clustered separately from mouse samples (Fig. 4C). Next, we compared mouse samples from each time point to the culture samples and observed 709 genes were significantly down-regulated (Fig. 4D) and 741 genes were significantly upregulated (Fig. 4E) in the mouse (Table. S1.) Volcano plots of the $\log_2$(fold change) vs. $-\log_{10}$(P value) show that many of the differentially upregulated and downregulated changes were highly significant at all three time points compared to culture (Fig. 4F-H). We observed significant overlap in differentially expressed transcripts at the various time points; over half of the differentially upregulated and downregulated genes were the same at all three time points (Fig. 4E).

We identified genes encoding transcriptional regulators, toxins, extracellular enzymes, and extracellular matrix-binding surface proteins that were significantly upregulated at all three time points (Table 1). Interestingly, while only one immune evasion factor, chemotaxis inhibitor (*chs*), was upregulated at all three time points, additional immune evasion genes were significantly upregulated at 3-days post-inoculation. We observed a similar trend with genes encoding components of the type VII secretion system (T7SS), which has been shown to contribute to *S.*

aureus virulence and competition with other microbes in polymicrobial settings (52, 53). At 5 hrs post-inoculation, only 5 T7SS genes were significantly upregulated while 14 genes were upregulated at 1-day and 3-days post-inoculation (Table 1).

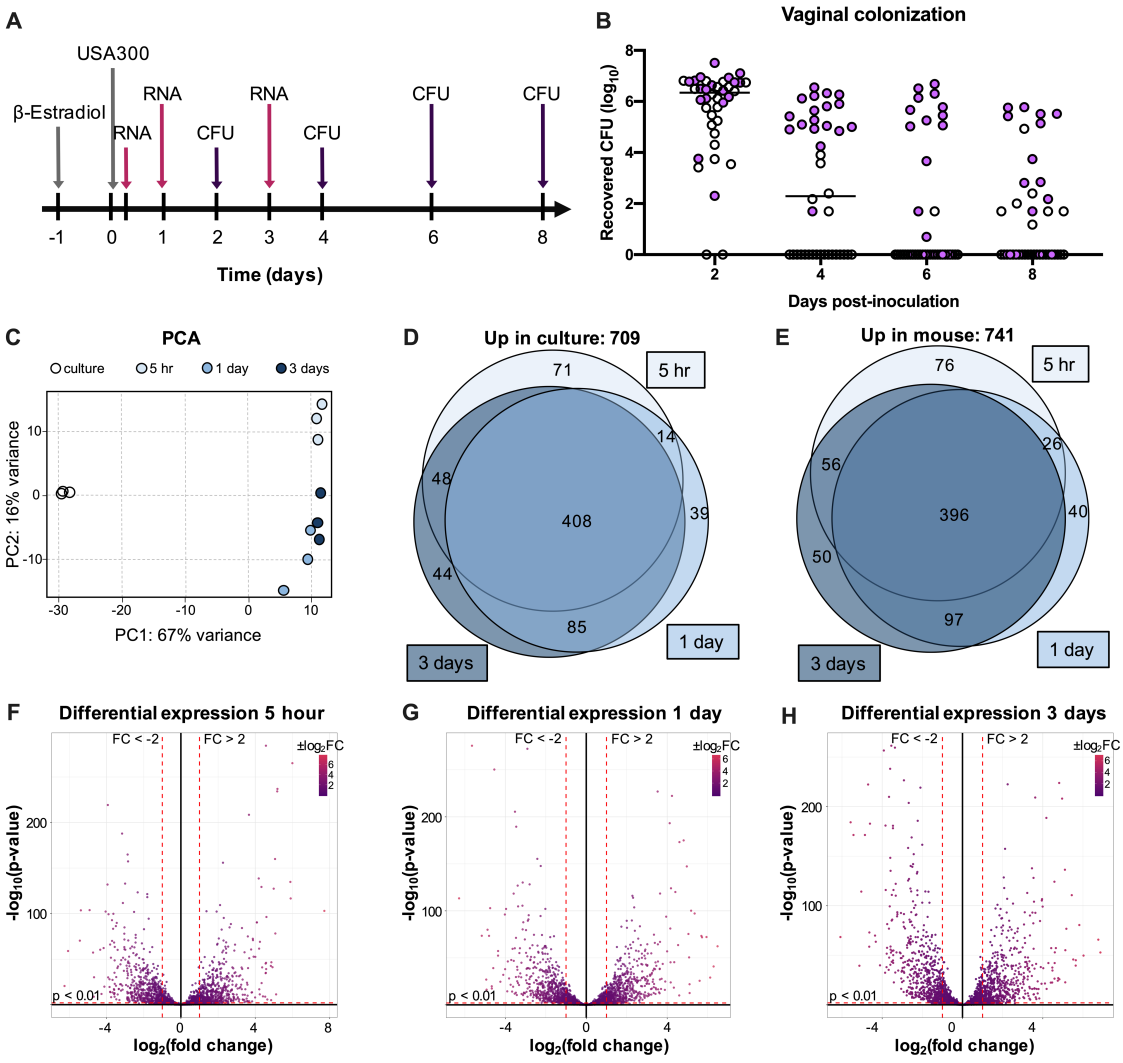

Figure 4.4. Transcriptome analysis during MRSA vaginal colonization. (A) Experimental design for RNA-sequencing analysis of mouse vaginal swabs. (B) CFU counts from mouse vaginal swabs. Samples chosen for RNA-sequencing are highlighted in purple. (C) PCA plot for triplicate samples of culture, 5hr, 1-day, and 3-days swabs. (D and E) Venn diagrams showing genes expressed at significantly higher levels (fold change > 2, P value < 0.01) in culture (D) or in mouse swab samples (E). (F-H) Volcano plots highlighting genes that are differentially expressed in swab samples from 5hrs (F), 1-day (G), and 3-days (H) post-inoculation compared to culture.

Table 4.1. Virulence factors which were significantly upregulated during vaginal colonization. Genes which encode transcriptional regulators, toxins, secreted enzymes, and ECM binding factors and were differentially expressed in mouse swab samples at all three time points are listed with their respective fold changes relative to growth in TSB. Immune modulation and T7SS genes which were not significantly differentially expressed at all time points are indicated with asterisks.

Category	Locus tag	Gene	Fold change		
			5 hours	1 day	3 days
transcriptional regulation	SAUSA300_0195	*rpiRb*	3	3	3
	SAUSA300_0218	*hptS*	3	3	4
	SAUSA300_0255	*lytR*	6	7	6
	SAUSA300_0878	LysR family transcriptional regulator	9	5	5
	SAUSA300_1220	LuxR family DNA-binding response regulator	2	2	2
	SAUSA300_1257	*msrR*	5	5	4
	SAUSA300_1514	*fur*	3	3	2
	SAUSA300_1717	*arsR*	7	4	5
	SAUSA300_1798	*airR*	4	4	4
	SAUSA300_1799	*airS*	3	4	4
	SAUSA300_2098	*czrA*	15	13	15
	SAUSA300_2300	TetR family transcriptional regulator	3	3	3
	SAUSA300_2322	TetR family transcriptional regulator	4	4	4
	SAUSA300_2336	MerR family transcriptional regulator	3	2	3
	SAUSA300_2347	*nirR*	12	8	7
	SAUSA300_2437	*sarT*	11	18	13
	SAUSA300_2566	*arcR*	4	4	6
	SAUSA300_2571	*argR*	3	4	6
	SAUSA300_2640	Xre family transcriptional regulator	5	9	11
toxins	SAUSA300_0800	*sek*	6	7	7
	SAUSA300_0801	*seq*	4	6	5
	SAUSA300_1058	*hla*	19	6	18
	SAUSA300_1918	truncated beta-hemolysin	14	2	9
extracellular enzymes	SAUSA300_0923	*htrA*	3	4	4
	SAUSA300_0951	*sspA*	2	12	13
	SAUSA300_1753	*splF*	12	3	24
	SAUSA300_1755	*splD*	13	5	28
	SAUSA300_1756	*splC*	11	3	22
	SAUSA300_1757	*splB*	12	4	21
	SAUSA300_2572	*aur*	4	15	12
ECM binding	SAUSA300_0546	*sdrC*	6	12	16
	SAUSA300_0547	*sdrD*	9	19	22
	SAUSA300_0774	*empbp*	35	4	8
immune modulation	SAUSA300_1059	superantigen-like protein	10	3	4
	SAUSA300_1060	superantigen-like protein	12	4	6
	SAUSA300_1061	superantigen-like protein	8	6	7
	SAUSA300_1920*	*chs*	29	3	8
	SAUSA300_0224*	*coa*			4
	SAUSA300_0836*	*dltB*			2
	SAUSA300_0837*	*dltC*			2
	SAUSA300_1053*	formyl peptide receptor-like 1 inhibitory protein			4
	SAUSA300_1055*	*efb*			2
	SAUSA300_2364*	*sbi*			2
type VII secretion system	SAUSA300_0279*	*esaA*			5
	SAUSA300_0280*	*essA*			2
	SAUSA300_0281*	*esaB*		4	4
	SAUSA300_0282	*essB*	2	6	6
	SAUSA300_0283*	*essC*		3	3
	SAUSA300_0284*	*esxC*		3	2
	SAUSA300_0286*	*essE*		3	3
	SAUSA300_0287*	*esxD*		3	3
	SAUSA300_0288*	*essD*		2	
	SAUSA300_0290	DUF5079 family protein	6	9	9
	SAUSA300_0291	DUF5080 family protein	5	7	6
	SAUSA300_0298	*essI5*	3	4	3
	SAUSA300_0299*	*essI6*		2	
	SAUSA300_0300*	*essI7*		2	2
	SAUSA300_0302	*essI9*	3	5	5
	SAUSA300_0303*	DUF4467 domain-containing protein		2	3

Iron homeostasis impacts vaginal persistence.

Though there were global transcriptional changes, the most highly-significant, differentially-expressed transcripts belonged to iron uptake and export systems. The most highly induced was the iron-surface determinant *isd* heme acquisition system (*isdBACDEFG* and *srtB)*. Other genes included those involved in the production of the siderophore staphyloferrin B (SB) (*sbnABCDEFGHI*) as well as its importer (*sirAB*), the staphyloferrin A (SA) importer (*htsABC*), the xeno-siderophore transporter (*fhuCB*), as well as the catechol/catecholamine iron transporter system (*sstABCD*). Lastly, the heme-regulated export *hrt* system, was highly down-regulated during colonization (*hrtAB*). (Fig. 5A) (54-57). As these results strongly suggest that the vaginal environment is iron limited, we performed inductively coupled plasma mass spectrometry (ICP-MS) to determine the iron concentration in vaginal lavage fluid from naïve mice and mice colonized with USA300. We observed a very low concentration of iron (0.52 μM), irrespective of MRSA colonization, compared to the level present in tryptic soy broth (TSB) (10 μM) (Fig. 5B).

To confirm the differential expression of iron-uptake systems by USA300, we incubated USA300 in mouse vaginal lavage fluid and performed RT-qPCR to compare transcripts of select iron-homeostasis genes between bacteria grown in lavage fluid and bacteria cultured under laboratory conditions in TSB. Similar to our RNA-seq results, the RT-qPCR analysis revealed an increase in *sirB*, *sbnA*, *isdB*, *isdD*, *srtB*, *htsC*, and *htsB* transcripts in MRSA cultured in vaginal lavage fluid (Fig. 5C to 5I). Additionally, *hrtA* and *hrtB* were significantly downregulated in MRSA from vaginal lavage compared to MRSA grown in TSB (Fig. 5J and 5K).

To assess the impact of iron uptake by MRSA on vaginal persistence, we co-colonized mice with WT USA300 and either Δ*fhuCBG* or *isdB*::Tn mutants. In addition to its role in the

uptake of xeno-siderophores, the FhuC ATP-ase also provides energy needed for uptake of the siderophores staphyloferrin A and staphyloferrin B. Therefore, the Δ*fhuCBG* mutant is defective in the transport of all siderophores (58). Also, our RNA-seq results show that at all three time points, the most highly upregulated gene was *isdB*, which encodes the hemoglobin-binding surface protein that transports heme to downstream components of the *isd* system (55). *isdB* transcripts from mouse samples were increased 210-fold at 5hrs, 90-fold at 1-day, and 117-fold at 3-days post-inoculation compared to culture (Table S1 and Fig. 5A). Compared to WT USA300, the Δ*fhuCBG* mutant and the *isdB*::Tn mutant were cleared significantly faster from the mouse vagina (Fig. 5L and M). Because a previous study reported that IsdB may impact bacterial attachment to host cells (59), we quantified adherence of the *isdB*::Tn mutant to VK2, Ect1, and End1 cells *in vitro* and observed no defect compared to WT USA300 (Fig. S2).

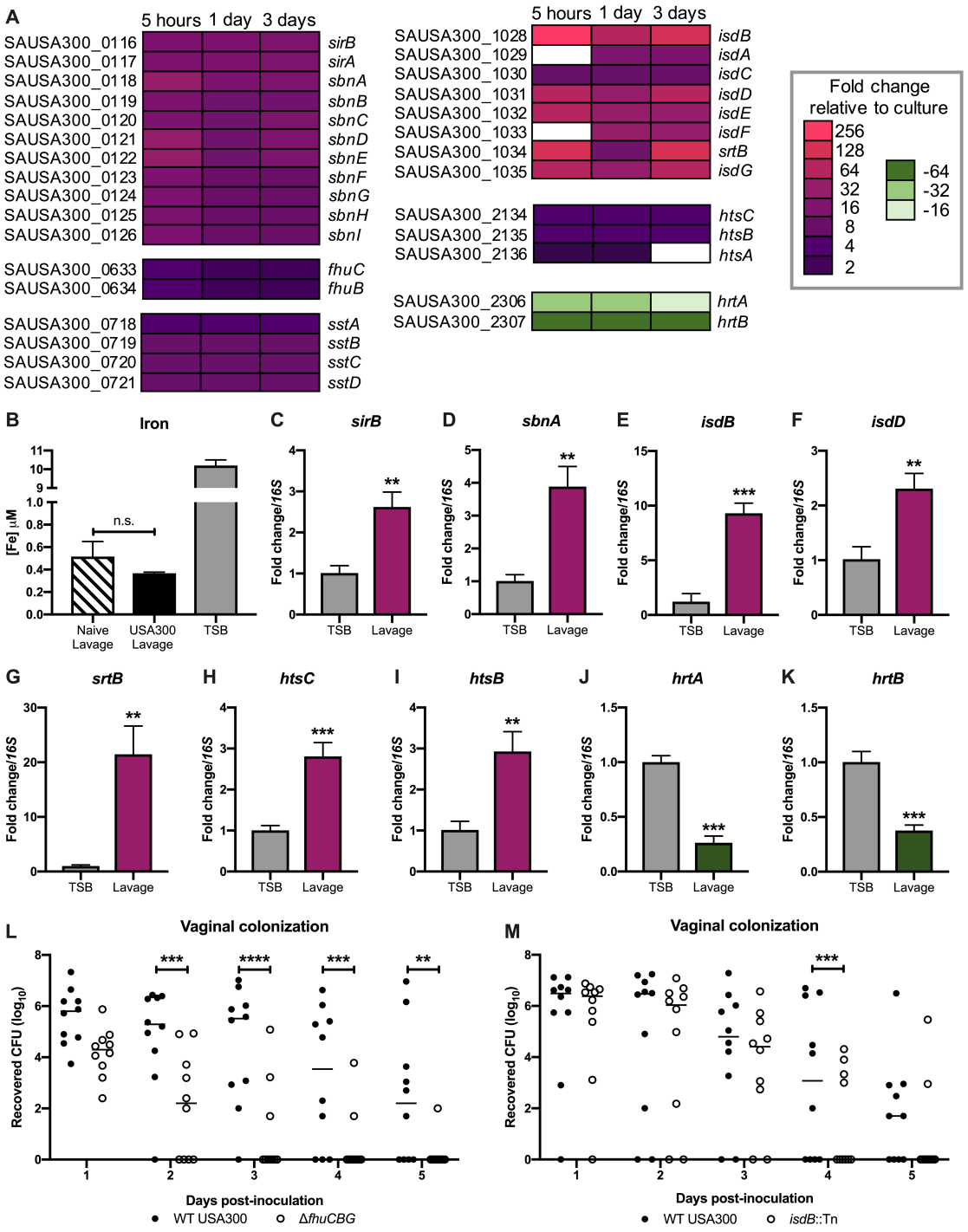

Figure 4.5. Iron homeostasis impacts vaginal persistence. (A) Differential expression of genes in iron-acquisition and iron-export pathways. (B) ICP-MS analysis of vaginal lavage from naïve and colonized mice, and TSB. (C-K) RT-qPCR confirmation of select RNA-sequencing iron-homeostasis hits. (L) Co-colonization with WT USA300 and Δ*fhuCBG* mutant. (M) Co-colonization with WT USA300 and *isdB*::Tn mutant. Statistical analysis: (B) One-way ANOVA. (C-K) Unpaired t test. (L and M) Two-way ANOVA with Sidak's multiple comparisons test.

DISCUSSION

S. aureus is capable of causing disease at nearly every site of the body (60), and MRSA colonization of the skin as well as mucosal sites, such as the nares and the vaginal tract, is a necessary initial step preceding the development of invasive disease (27, 37, 61-63). While many studies have investigated host and bacterial determinants of *S. aureus* colonization of the skin and nares as well as subsequent infection, little is known about factors which influence vaginal niche establishment and persistence. Because vaginal carriage during pregnancy represents a major risk factor for transmission of this pathogen to the newborn (24, 25, 64, 65), we utilized *in vitro* and *in vivo* models of MRSA vaginal colonization to identify determinants of persistence within the female reproductive tract. The results of our study reveal that MRSA can interact directly with the female reproductive tract epithelium *in vitro* and *in vivo*, and that the expression of cell-wall anchored Fg binding adhesins as well as iron-acquisition systems promote MRSA vaginal colonization.

The effect of *S. aureus* colonization on the host immune response has been well-characterized at many epithelial sites. *S. aureus* on the skin promotes a robust inflammatory response involving both the innate and adaptive immune system (66, 67). Neutrophils in particular are rapidly and highly recruited to the site of *S. aureus* skin infection and are key mediators of clearance of the pathogen (68-75). Our studies on GBS vaginal carriage have shown a clear role for neutrophils in combatting GBS colonization of this host site (43, 76). Additionally, neutrophils have been shown to respond to other common pathogens of the vaginal tract such as the fungus *Candida albicans* (77, 78) and the Gram-negative bacterium *Neisseria gonorrhoeae* (79). In this study, we observed an increased neutrophil presence in the vaginal tissues from mice colonized by MRSA compared to naïve controls. Interestingly, while there is obvious neutrophil infiltration of

the lamina propria of the vagina 1-day post-colonization with MRSA, we did not detect neutrophils in the vaginal lumen at this early time point. In contrast, at 3-days post-inoculation, we could visualize many neutrophils within the vaginal lumen. The timing of the infiltration of neutrophils into the vaginal lumen coincides with the increased expression of immune evasion factors by MRSA; in our RNA-sequencing analysis we observed significant upregulation of these factors at 3-days post-inoculation and not at earlier time points. Future studies aimed at further characterizing the dynamics of neutrophil response to MRSA in the female reproductive tract and their extravasation into the vaginal lumen may reveal new insights into host immune responses common to all vaginal pathogens as well as those specific to MRSA.

The impact of *S. aureus* interactions with Fg on colonization and disease at various tissue sites has been well-characterized. In the context of invasive infections, Fg and fibrin can promote clearance of *S. aureus* by containing the bacteria within aggregates (80, 81). Additionally, Fg can stimulate the production of inflammatory cytokines and activate neutrophils (82-84). However, *S. aureus* has also been shown to target Fg to promote persistence and disease in the host. The bacterium can interact with Fg in order to coagulate or to form clumps which help it evade immune detection, and this clumping is mediated by surface Fg binding adhesins including ClfA, ClfB (46, 85-88). There is also evidence that *S. aureus* can alter gene regulation in the presence of fibrinogen-containing clumps to enhance expression of virulence determinants (89). Moreover, *S. aureus* can use Fg as part of its biofilm structure to promote persistence within the host (90). Our data suggest that, in the context of vaginal colonization, MRSA interactions with Fg are necessary for persistence within the host. A mutant deficient in Fg binding was significantly impaired in its ability to adhere to human female reproductive tract cells *in vitro* and was also rapidly cleared

from the vaginal tract *in vivo* compared to the WT. These results hint that the benefits of MRSA binding to Fg outweigh the potential detriments for the pathogen during vaginal colonization.

While a majority of mice rapidly clear the Fg adhesin mutant during vaginal colonization, it is able to persist in some of the animals (Fig. 3G). This result suggests that there are likely other factors that contribute to *in vivo* vaginal colonization. To identify additional determinants of vaginal persistence, we performed RNA-sequencing to profile the transcriptome of MRSA during vaginal colonization. We observed that over one-quarter of the genes of USA300 were differentially expressed during *in vivo* colonization, and over half of those genes were differentially expressed at all three *in vivo* time points that were analyzed. Of note, many of the most highly and significantly differentially expressed genes belonged to iron-acquisition or iron-homeostasis pathways. Our observation that genes involved in iron uptake were upregulated was not surprising since their expression is controlled by iron levels and our ICP-MS data revealed the vaginal environment to be limited in iron (Fig. 5B). Using our *in vivo* murine vaginal colonization model, we confirmed that mutants in *fhuCBG* and *isdB* exhibited decreased persistence compared to the isogenic WT MRSA strain. Numerous reports have demonstrated the importance of nutrient iron for *S. aureus* growth and pathogenicity (55, 91, 92), and the results of our study highlight the necessity of this metal for MRSA persistence within the vaginal environment. That the Δ*fhuCBG* mutant was attenuated in this model was interesting because, while FhuCBG is known to transport hydroxamate-type siderophores which *S. aureus* does not synthesize (57, 93), FhuC is also the ATP-ase which provides energy for uptake of both SA and SB siderophores (55, 58). Both WT and the Δ*fhuCBG* mutant should, under the iron-restricted conditions during vaginal colonization, express SA and SB. Given that the Δ*fhuCBG* mutant cannot transport these siderophores, the

extracellular environment becomes more iron restricted to the mutant as it cannot access SA-Fe and SB-Fe chelates.

The limitation of iron is a major host mechanism for defending against pathogens because this metal is vital for bacterial growth and metabolic processes (55, 94, 95). Other transcriptomic studies examining *S. aureus* growing *in vivo* during invasive infections have shown that the bacteria respond to nutrient limitation within the host. One study which compared the transcriptomes of *S. aureus* in a murine osteomyelitis model to bacteria grown under laboratory conditions revealed the importance of iron homeostasis mechanisms, especially the Isd pathway, during chronic infection (96). Another analysis of USA300 gene expression during human and mouse infections also showed upregulation of iron transporters *in vivo* (97). Interestingly, many reports have shown that neutrophils can play an active role in limiting iron in numerous host sites, including the vagina, during exposure to a bacterial pathogen (98-101). The precise mechanisms by which the host restricts iron availability during colonization warrants further research as this would provide insight into the exact function of neutrophils in controlling MRSA vaginal persistence.

We have developed a murine model of *S. aureus* vaginal colonization and this study is the first to investigate the molecular mechanisms that promote vaginal carriage and persistence by MRSA. This mouse model will be useful for continued studies on MRSA-host interactions within a mucosal environment. Here we demonstrate the importance of Fg binding as well as iron-acquisition in promoting long-term colonization. Additionally, we observed that neutrophils respond to MRSA presence in the vagina and that the bacteria upregulate the expression of immune-modulating genes during the course of colonization. Further investigation into these

specific colonization determinants could yield therapeutic interventions to treat MRSA persistence within this host niche.

MATERIALS AND METHODS

Bacterial strains and culture conditions.

S. aureus strains USA300 (39) and MRSA252 (40) were used for the experiments. *S. aureus* was grown in tryptic soy broth (TSB) at 37℃ and growth was monitored by measuring the optical density at 600nm (OD_{600}). For selection of *S. aureus* mutants, TSA (tryptic soy agar) was supplemented with chloramphenicol (Cm) (10 μg/mL), erythromycin (Erm) (3 μg/mL), or tetracycline (Tet) (1 μg/mL).

To generate the Fg adhesin mutant, first the *fnbAB* operon was deleted using allelic replacement. Phages 80α or 11 were used for transduction between *S. aureus* strains (102). The *fnbAB* markerless deletion plasmid pHC94 was constructed using Gibson assembly with the plasmid backbone coming from amplification of pJB38 (103) using primers pJB R2 and pJB38 F2. The region upstream of *fnbA* was amplified with primers fnbAB delA and fnbAB delB, and the region downstream of *fnbB* was amplified using fnbAB delC and fnb delD (Table S2). The resulting plasmid was electroporated in *S. aureus* RN4220 (104), selecting on TSA Cm plates at 30°C. The plasmid was then transduced into *S. aureus* strain LAC Δ*clfA* (85). Individual colonies were streaked on TSA Cm plates incubated at 42°C to select for integration of the plasmid into the chromosome. Single colonies were grown in TSB at 30°C and re-inoculated into fresh media for several days before plating on TSA containing anhydrotetracycline (0.3 μg/mL) to select for loss of the plasmid, creating the LAC Δ*clfA* Δ*fnbAB* mutant. The *clfB*::Tn mutation was than transduced

into this background from the Nebraska Transposon Mutant Library (105) and selected on TSA Erm plates.

The *isdB mariner*-based transposon *bursa aurealis* mutation (JE2 *isdB*::ΦNΣ, NE1102) from the Nebraska Transposon Library (105) into USA300 LAC with phage 11 as described previously (106). *S. aureus* genomic DNA of LAC* *isdB*::ΦNΣ was isolated using Puregene DNA purification kit (Qiagen) and the transposon insertion was verified by PCR with primers KAS249 and KAS250 (Table S2) .

The *fhuCBG* mutant (58) and the DsRed expressing USA300 strain were generated previously (107).

***In vitro* MRSA adherence assays.**

Immortalized VK2 human vaginal epithelial cells, Ect1 human ectocevical endothelial cells, and End1 human endocervical epithelial cells were obtained from the American Type Culture Collection (VK2.E6E7, ATCC CRL-2616; Ect1/E6E7, ATCC CRL-2614; End1/E6E7, ATCC CRL-2615) and were maintained in keratinocyte serum-free medium (KSFM; Gibco) with 0.1 ng/mL human recombinant epidermal growth factor (EGF; Gibco) and 0.05 mg/ml bovine pituitary extract (Gibco) at 37°C with 5% CO_2.

Assays to determine cell surface-adherent MRSA were performed as described previously (41). Briefly, bacteria were grown to mid-log phase to infect cell monolayers (multiplicity of infection [MOI] = 1). After a 30-min. incubation, cells were detached with 0.1 mL of 0.25% trypsin-EDTA solution and lysed with addition of 0.4 mL of 0.025% TritonX-100 by vigorous pipetting. The lysates were then serially diluted and plated on TSA to enumerate the bacterial CFU.

Experiments were performed at least three times with each condition in triplicate, and results from a representative experiment are shown.

Crystal violet fibrinogen adhesion assays were performed as described in (85). Briefly, 96-well plates (Corning) were coated with 20 μg/mL of human fibrinogen and incubated with 100 μL of bacterial suspensions in PBS at OD_{600} = 1.0 for 1h at 37°C. Wells were then washed and dried, and the adherent bacteria were stained with 0.1% crystal violet. The bound crystal violet stain was solubilized with 33% acetic acid and measured at OD_{570}.

For Gram staining analysis, VK2 monolayers were grown in tissue culture treated chamber slides (ThermoFisher) and infected with either WT USA300 or the fibrinogen adhesin mutant at an MOI of 20. Following a 30 min incubation, the cell monolayers were washed to remove any non-adherent bacteria then fixed with 10% formalin (Fisher) and Gram stained (Sigma).

Murine vaginal colonization model.

Animal experiments were approved by the Institutional Animal Care and Use Committee at the University of Colorado-Anschutz Medical Campus protocol #00316 and performed using accepted veterinary standards. A mouse vaginal colonization model for GBS was adapted for our studies (38). 8-week old female CD-1 (Charles River), C57BL/6 (Jackson), and BALB/c (Jackson) mice were injected intraperitoneally with 0.5 mg 17β-estradiol (Sigma) 1 day prior to colonization with MRSA. Mice were vaginally inoculated with 10^7 CFU of MRSA in 10μL PBS and on subsequent days the vaginal lumen was swabbed with a sterile ultrafine swab (Puritan). To assess tissue CFU, mice were euthanized according to approved veterinary protocols and the female reproductive tract tissues were placed into 500μL PBS and bead beat for 2 min to homogenize the

tissues. The recovered MRSA was serially diluted and enumerated on CHROMagar (Hardy Diagnostics) supplemented with 5.2 μg/mL of cefoxitin.

Histology.

Mouse female reproductive tract was harvested and embedded into OCT compound (Sakura) and sectioned with a CM1950 freezing cryostat (Leica). For fluorescence microscopy, coverslips were mounted with VECTASHIELD mounting medium with DAPI (Vector Labs). H&E staining was performed using reagents from Sigma. Immunohistochemical analysis was performed using a biotinylated primary antibody against Gr-1 (Biolegend), Streptavidin conjugated to horse radish peroxidase (Jackson Immunoresearch), and AEC peroxidase substrate kit (Vector Labs). Images were taken with a BZ-X710 microscope (Keyence).

Generation of RNA-sequencing data.

10^7 CFU of USA300 were inoculated into the mouse vagina and mice were swabbed vaginally 5 hrs, 1-day, and 3-days post-inoculation for RNA recovery. Vaginal swabs were placed into TRIzol reagent (Thermo Fisher), vortexed to dissociated bacteria from swabs, and stored at -80°C. Swabs samples from 6 mice were pooled and bacteria were lysed by beating for 2 min at maximum speed on a bead beater (BioSpec Products). RNA was isolated by following the manufacturer's protocol using a Direct-Zol RNA MiniPrep Plus kit (Zymo Research). For each sample, 120 ng total RNA was ribodepleted using the Ribo-Zero Magenetic Gold Kit (Epidemiology) from Epicentre (Illumina) following the manufacurer's protocol. Ribodeplete RNA was then prepared into sequence libraries using the RNA Ultra II kit (New Enlgand Biolabs) following the manufacturer's protocol without fragmentation. Libraries underwent 9 cycles of

PCR efore 1X Ampure Bead purification (Beckman Coulter). Libraries were quantified, pooled, and sequenced on an Illumina NextSeq500 with 75-base single reads targeting 20M reads per samples.

Analysis of RNA-sequencing data.

Sequencing reads were aligned to the NCBI reference sequence with GenBank accession number NC_007793.1 and expression levels were calculated using Geneious 11.1.5. Transcripts with an adjusted P value < 0.05 and $\log_2$fold change ±1 were considered significantly differentially expressed. PCA and volcano plots were generated using the ggplot2 package in R. Venn diagrams were generated using the area-proportional Venn diagram tool (BioInfoRx).

ICP-MS analysis

Triplicate samples of mouse vaginal lavage and TSB samples were sent to the University of Nebraska Spectroscopy and Biophysics Core. Fe56 and Fe57 isotope measurements were combined to show total iron levels.

RT-qPCR confirmation of RNA-sequencing.

Vaginal lavage fluid was collected as described in (38) and filtered through 0.22μm Spin-X centrifuge tube filters (Costar) to remove contaminants. Triplicated log phase cultures of USA300 were pelleted and resuspended in filtered lavage fluid. Following a 2-hour incubation at 37°C, bacteria were collected by centrifugation and resuspended in Trizol, lysed by bead beating, and RNA was isolated using the Direct-Zol RNA MiniPrep Plus kit as described above. RNA was treated with Turbo DNase (Invitrogen) to remove contaminating DNA. cDNA was generated using

the Quanta cDNA synthesis kit (Quanta Biosciences) and qPCR was performed using PerfeCTa SYBR Green reagent (Quanta) and a CFX96 Real-Time PCR thermal cycler (Bio-rad). Fold changes were calculated using the Livak method (108).

Data analysis.

GraphPad Prism version 7.0 was used for statistical analysis and statistical significance was accepted at P values of < 0.05 ($* P < 0.05$; $** P < 0.00005$; $*** P < 0.0005$; $**** P < 0.00005$). Specific tests are indicated in figure legends.

ACKNOWLEDGEMENTS

We thank Dr. Heidi A. Crosby for help in strain construction and the Array and NGS Core Facility at The Scripps Research Institute, Director Steven Head, for performing RNAseq analysis. This study was supported by the Rees Stealy Research Foundation/ SDSU Heart Institute and San Diego Chapter ARCS Scholarships to L.D., an American Heart Association postdoctoral fellowship 17POST33670580 to J.M.K., the Canadian Institutes of Health Research to D.E.H., and the NIH/NIAID R21 AI130857 to A.R.H. and K.S.D.

Chapter 4, in full, is currently in submission to *mBio*, 2019. Deng L, Schilcher K, Burcham LR, Kwiecinski JM, Johnson PM, Head SR, Heinrichs DE, Horswill AR, Doran KS. Identification of key determinants of *Staphylococcus aureus* vaginal colonization. The dissertation author was the primary investigator and author of this paper.

SUPPLEMENTAL MATERIALS

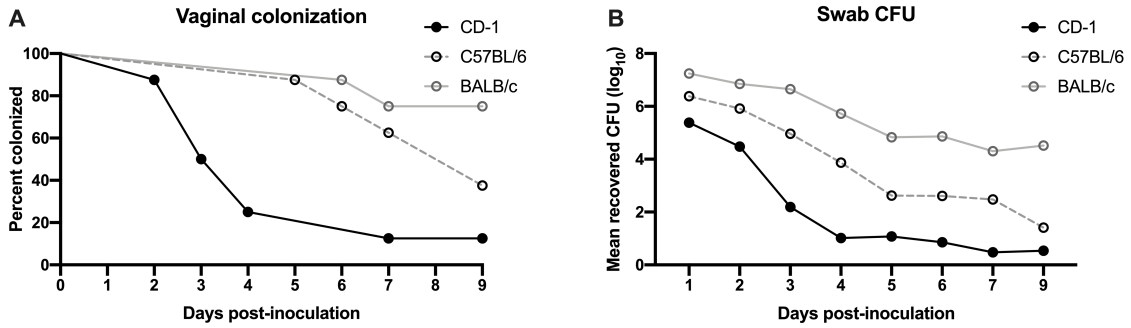

Supplemental Figure 4.1. USA300 vaginal colonization in different mouse strains. CD-1, C57BL/6, and BALB/c mice were inoculated with 10^7 CFU of USA300 and the percent of mice colonized (A) as well as mean vaginal swab CFU (B) were monitored for 9 days.

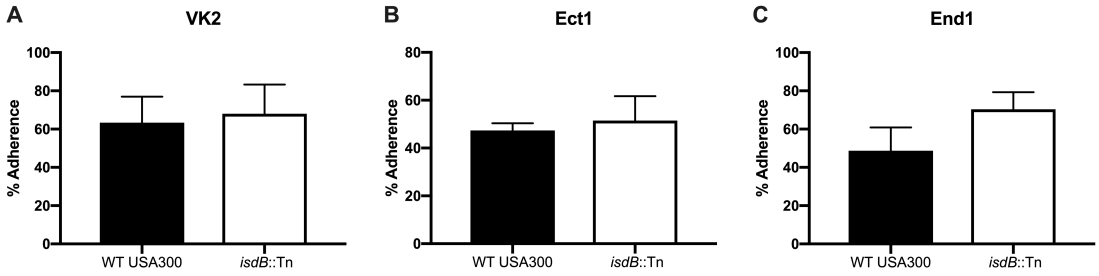

Supplemental Figure 4.2. WT USA300 and *isdB*::Tn adherence to (A) VK2, (B) End1, and (C) Ect1 cells.

Supplemental Table 4.2. List of primers used in this study.

	Primer name	Sequence
construction of Fg adhesin mutant	pJB38 rev2	GAGCTCGAATTCTTGAAGACGAAAGG
	pJB38 fwd 2	GTCGACCTGCAGGCATGC
	fnbAB delA	GAGGCCCTTTCGTCTTCAAGAATTCGAGCTCGTAGCTGCGATTTCAACTACAGG
	fnbAB delB	ATTTCTGCGTAACTCGAGGGTACCGCTAGCAATGCCGTACCTAAGATTGTTTTTC
	fnbAB delC	AGGTACGGCATTGCTAGCGGTACCCTCGAGCGCAGAAATAAAAAGAATCACAAAGC
	fnbAB delD	GTGAAATCAGAGCTTGCATGCCTGCAGGTCGACCGTCCGTTTTTAGTTAATGGGTC
construction of *isdB* ::Tn mutant	KAS249	TCTCCAAAATTGACCTGATTGT
	KAS250	AGCAGTTGCAAGTCCAACAA
RT-qPCR	16S F	ACTTCGGGAAACCGGAGCTAAT
	16S R	TGCAGCGCGGATCCATCTATAA
	sirB F	TGTCACCAGGTACGGTGATACAG
	sirB R	CAAGGGCAGCACCAGTCAATAA
	sbnA F	GGCATATTTGCCGGAGGTTCAA
	sbnA R	ACGATCGCCTCGATCTGGTAAA
	isdB F	GTCATCACTAGGCGTTGCATCTG
	isdB R	GCTTCTGTATTTGTACCACCTGTTTCT
	isdD F	AATCAGATACTAAGGAAAGACGTACTAGC
	isdD R	CCTGATGCTTTAGGTCGCTCA
	srtB F	CGAGAACATCGACGTAAAGGTAGTATTT
	srtB R	TCAAACATCGTATTATCACCGACATGG
	htsC F	TCTTAGGTGCCTTTGCAGTAAGTTTAT
	htsC R	CGCCGTACATATTGCGCCTATT
	htsB R	GCCAAGGATGATTGCAGGGTTAT
	htsB R	GATGCACCAGAACTGACACCAAA
	hrtA F	CGTAGGTCAAGAAGCGGGAATG
	hrtA R	CTGATGCGGATATACATTCAAGCGA
	hrtB F	CACAACAACAACGTGATGAGCTTAAT
	hrtB R	CGGTGCTTGCTCTGCTTGATAA

REFERENCES

1. **Kluytmans J, van Belkum A, Verbrugh H.** 1997. Nasal carriage of Staphylococcus aureus: epidemiology, underlying mechanisms, and associated risks. Clin Microbiol Rev **10:**505-520.

2. **Chambers HF, Deleo FR.** 2009. Waves of resistance: Staphylococcus aureus in the antibiotic era. Nat Rev Microbiol **7:**629-641.

3. **DeLeo FR, Chambers HF.** 2009. Reemergence of antibiotic-resistant Staphylococcus aureus in the genomics era. J Clin Invest **119:**2464-2474.

4. **Lee BY, Singh A, David MZ, Bartsch SM, Slayton RB, Huang SS, Zimmer SM, Potter MA, Macal CM, Lauderdale DS, Miller LG, Daum RS.** 2013. The economic burden of community-associated methicillin-resistant Staphylococcus aureus (CA-MRSA). Clin Microbiol Infect **19:**528-536.

5. **David MZ, Daum RS.** 2010. Community-associated methicillin-resistant Staphylococcus aureus: epidemiology and clinical consequences of an emerging epidemic. Clin Microbiol Rev **23:**616-687.

6. **Kennedy AD, Otto M, Braughton KR, Whitney AR, Chen L, Mathema B, Mediavilla JR, Byrne KA, Parkins LD, Tenover FC, Kreiswirth BN, Musser JM, DeLeo FR.** 2008. Epidemic community-associated methicillin-resistant Staphylococcus aureus: recent clonal expansion and diversification. Proc Natl Acad Sci U S A **105:**1327-1332.

7. **Li M, Diep BA, Villaruz AE, Braughton KR, Jiang X, DeLeo FR, Chambers HF, Lu Y, Otto M.** 2009. Evolution of virulence in epidemic community-associated methicillin-resistant Staphylococcus aureus. Proc Natl Acad Sci U S A **106:**5883-5888.

8. **Foster TJ, Geoghegan JA, Ganesh VK, Hook M.** 2014. Adhesion, invasion and evasion: the many functions of the surface proteins of Staphylococcus aureus. Nat Rev Microbiol **12:**49-62.

9. **Pietrocola G, Nobile G, Rindi S, Speziale P.** 2017. Staphylococcus aureus Manipulates Innate Immunity through Own and Host-Expressed Proteases. Front Cell Infect Microbiol **7:**166.

10. **Seilie ES, Bubeck Wardenburg J.** 2017. Staphylococcus aureus pore-forming toxins: The interface of pathogen and host complexity. Semin Cell Dev Biol **72:**101-116.

11. **Bretl DJ, Elfessi A, Watkins H, Schwan WR.** 2019. Regulation of the Staphylococcal Superantigen-Like Protein 1 Gene of Community-Associated Methicillin-Resistant Staphylococcus aureus in Murine Abscesses. Toxins (Basel) **11**.

12. **Taglialegna A, Varela MC, Rosato RR, Rosato AE.** 2019. VraSR and Virulence Trait Modulation during Daptomycin Resistance in Methicillin-Resistant Staphylococcus aureus Infection. mSphere **4**.

13. **Jenul C, Horswill AR.** 2018. Regulation of Staphylococcus aureus Virulence. Microbiol Spectr **6**.

14. **Wertheim HF, Vos MC, Ott A, van Belkum A, Voss A, Kluytmans JA, van Keulen PH, Vandenbroucke-Grauls CM, Meester MH, Verbrugh HA.** 2004. Risk and outcome of nosocomial Staphylococcus aureus bacteraemia in nasal carriers versus non-carriers. Lancet **364:**703-705.

15. **Cole AM, Tahk S, Oren A, Yoshioka D, Kim YH, Park A, Ganz T.** 2001. Determinants of Staphylococcus aureus nasal carriage. Clin Diagn Lab Immunol **8:**1064-1069.

16. **Peacock SJ, de Silva I, Lowy FD.** 2001. What determines nasal carriage of Staphylococcus aureus? Trends Microbiol **9:**605-610.

17. **O'Brien LM, Walsh EJ, Massey RC, Peacock SJ, Foster TJ.** 2002. Staphylococcus aureus clumping factor B (ClfB) promotes adherence to human type I cytokeratin 10: implications for nasal colonization. Cell Microbiol **4:**759-770.

18. **Clarke SR, Brummell KJ, Horsburgh MJ, McDowell PW, Mohamad SA, Stapleton MR, Acevedo J, Read RC, Day NP, Peacock SJ, Mond JJ, Kokai-Kun JF, Foster SJ.** 2006. Identification of in vivo-expressed antigens of Staphylococcus aureus and their use in vaccinations for protection against nasal carriage. J Infect Dis **193:**1098-1108.

19. **Schaffer AC, Solinga RM, Cocchiaro J, Portoles M, Kiser KB, Risley A, Randall SM, Valtulina V, Speziale P, Walsh E, Foster T, Lee JC.** 2006. Immunization with Staphylococcus aureus clumping factor B, a major determinant in nasal carriage, reduces nasal colonization in a murine model. Infect Immun **74:**2145-2153.

20. **Wertheim HF, Walsh E, Choudhurry R, Melles DC, Boelens HA, Miajlovic H, Verbrugh HA, Foster T, van Belkum A.** 2008. Key role for clumping factor B in Staphylococcus aureus nasal colonization of humans. PLoS Med **5:**e17.

21. **Ponnuraj K, Bowden MG, Davis S, Gurusiddappa S, Moore D, Choe D, Xu Y, Hook M, Narayana SV.** 2003. A "dock, lock, and latch" structural model for a staphylococcal adhesin binding to fibrinogen. Cell **115:**217-228.

22. **Bowden MG, Heuck AP, Ponnuraj K, Kolosova E, Choe D, Gurusiddappa S, Narayana SV, Johnson AE, Hook M.** 2008. Evidence for the "dock, lock, and latch" ligand binding mechanism of the staphylococcal microbial surface component recognizing adhesive matrix molecules (MSCRAMM) SdrG. J Biol Chem **283:**638-647.

23. **Corrigan RM, Miajlovic H, Foster TJ.** 2009. Surface proteins that promote adherence of Staphylococcus aureus to human desquamated nasal epithelial cells. BMC Microbiol **9:**22.

24. **Andrews WW, Schelonka R, Waites K, Stamm A, Cliver SP, Moser S.** 2008. Genital tract methicillin-resistant Staphylococcus aureus: risk of vertical transmission in pregnant women. Obstet Gynecol **111:**113-118.

25. **Beigi R, Hanrahan J.** 2007. Staphylococcus aureus and MRSA colonization rates among gravidas admitted to labor and delivery: a pilot study. Infect Dis Obstet Gynecol **2007:**70876.

26. **Chen KT, Huard RC, Della-Latta P, Saiman L.** 2006. Prevalence of methicillin-sensitive and methicillin-resistant Staphylococcus aureus in pregnant women. Obstet Gynecol **108:**482-487.

27. **Creech CB, Litzner B, Talbot TR, Schaffner W.** 2010. Frequency of detection of methicillin-resistant Staphylococcus aureus from rectovaginal swabs in pregnant women. Am J Infect Control **38:**72-74.

28. **Dancer SJ, Noble WC.** 1991. Nasal, axillary, and perineal carriage of Staphylococcus aureus among women: identification of strains producing epidermolytic toxin. J Clin Pathol **44:**681-684.

29. **Reiss-Mandel A, Rubin C, Maayan-Mezger A, Novikov I, Jaber H, Dolitzky M, Freedman L, Rahav G, Regev-Yochay G.** 2019. Patterns and Predictors of Staphylococcus aureus Carriage during the First Year of Life: a Longitudinal Study. J Clin Microbiol **57**.

30. **Lin J, Yao Z.** 2018. Maternal-Infant Correlation of Multidrug-Resistant Staphylococcus aureus Carriage: A Prospective Cohort Study. Front Pediatr **6:**384.

31. **Bratu S, Eramo A, Kopec R, Coughlin E, Ghitan M, Yost R, Chapnick EK, Landman D, Quale J.** 2005. Community-associated methicillin-resistant Staphylococcus aureus in hospital nursery and maternity units. Emerg Infect Dis **11:**808-813.

32. **Laibl VR, Sheffield JS, Roberts S, McIntire DD, Trevino S, Wendel GD, Jr.** 2005. Clinical presentation of community-acquired methicillin-resistant Staphylococcus aureus in pregnancy. Obstet Gynecol **106:**461-465.

33. **Nambiar S, Herwaldt LA, Singh N.** 2003. Outbreak of invasive disease caused by methicillin-resistant Staphylococcus aureus in neonates and prevalence in the neonatal intensive care unit. Pediatr Crit Care Med **4:**220-226.

34. **Saiman L, Cronquist A, Wu F, Zhou J, Rubenstein D, Eisner W, Kreiswirth BN, Della-Latta P.** 2003. An outbreak of methicillin-resistant Staphylococcus aureus in a neonatal intensive care unit. Infect Control Hosp Epidemiol **24:**317-321.

35. **Seybold U, Halvosa JS, White N, Voris V, Ray SM, Blumberg HM.** 2008. Emergence of and risk factors for methicillin-resistant Staphylococcus aureus of community origin in intensive care nurseries. Pediatrics **122:**1039-1046.

36. **Stafford I, Hernandez J, Laibl V, Sheffield J, Roberts S, Wendel G, Jr.** 2008. Community-acquired methicillin-resistant Staphylococcus aureus among patients with puerperal mastitis requiring hospitalization. Obstet Gynecol **112:**533-537.

37. **Top KA, Huard RC, Fox Z, Wu F, Whittier S, Della-Latta P, Saiman L, Ratner AJ.** 2010. Trends in methicillin-resistant Staphylococcus aureus anovaginal colonization in pregnant women in 2005 versus 2009. J Clin Microbiol **48:**3675-3680.

38. **Patras KA, Doran KS.** 2016. A Murine Model of Group B Streptococcus Vaginal Colonization. J Vis Exp doi:10.3791/54708.

39. **Boles BR, Thoendel M, Roth AJ, Horswill AR.** 2010. Identification of genes involved in polysaccharide-independent Staphylococcus aureus biofilm formation. PLoS One **5:**e10146.

40. **Holden MT, Feil EJ, Lindsay JA, Peacock SJ, Day NP, Enright MC, Foster TJ, Moore CE, Hurst L, Atkin R, Barron A, Bason N, Bentley SD, Chillingworth C, Chillingworth T, Churcher C, Clark L, Corton C, Cronin A, Doggett J, Dowd L, Feltwell T, Hance Z, Harris B, Hauser H, Holroyd S, Jagels K, James KD, Lennard N, Line A, Mayes R, Moule S, Mungall K, Ormond D, Quail MA, Rabbinowitsch E,**

Rutherford K, Sanders M, Sharp S, Simmonds M, Stevens K, Whitehead S, Barrell BG, Spratt BG, Parkhill J. 2004. Complete genomes of two clinical Staphylococcus aureus strains: evidence for the rapid evolution of virulence and drug resistance. Proc Natl Acad Sci U S A **101:**9786-9791.

41. **Deng L, Mu R, Weston TA, Spencer BL, Liles RP, Doran KS.** 2018. Characterization of a Two-Component System Transcriptional Regulator, LtdR, That Impacts Group B Streptococcal Colonization and Disease. Infect Immun **86**.

42. **Patras KA, Rosler B, Thoman ML, Doran KS.** 2015. Characterization of host immunity during persistent vaginal colonization by Group B Streptococcus. Mucosal Immunol **8:**1339-1348.

43. **Patras KA, Wang NY, Fletcher EM, Cavaco CK, Jimenez A, Garg M, Fierer J, Sheen TR, Rajagopal L, Doran KS.** 2013. Group B Streptococcus CovR regulation modulates host immune signalling pathways to promote vaginal colonization. Cell Microbiol **15:**1154-1167.

44. **Carey AJ, Weinberg JB, Dawid SR, Venturini C, Lam AK, Nizet V, Caparon MG, Walker MJ, Watson ME, Ulett GC.** 2016. Interleukin-17A Contributes to the Control of Streptococcus pyogenes Colonization and Inflammation of the Female Genital Tract. Sci Rep **6:**26836.

45. **Wang NY, Patras KA, Seo HS, Cavaco CK, Rosler B, Neely MN, Sullam PM, Doran KS.** 2014. Group B streptococcal serine-rich repeat proteins promote interaction with fibrinogen and vaginal colonization. J Infect Dis **210:**982-991.

46. **Crosby HA, Kwiecinski J, Horswill AR.** 2016. Staphylococcus aureus Aggregation and Coagulation Mechanisms, and Their Function in Host-Pathogen Interactions. Adv Appl Microbiol **96:**1-41.

47. **Rhem MN, Lech EM, Patti JM, McDevitt D, Hook M, Jones DB, Wilhelmus KR.** 2000. The collagen-binding adhesin is a virulence factor in Staphylococcus aureus keratitis. Infect Immun **68:**3776-3779.

48. **Josse J, Laurent F, Diot A.** 2017. Staphylococcal Adhesion and Host Cell Invasion: Fibronectin-Binding and Other Mechanisms. Front Microbiol **8:**2433.

49. **Kwiecinski J, Jin T, Josefsson E.** 2014. Surface proteins of Staphylococcus aureus play an important role in experimental skin infection. APMIS **122:**1240-1250.

50. **Foster TJ, Hook M.** 1998. Surface protein adhesins of Staphylococcus aureus. Trends Microbiol **6:**484-488.

51. **Clarke SR, Foster SJ.** 2006. Surface adhesins of Staphylococcus aureus. Adv Microb Physiol **51:**187-224.

52. **Unnikrishnan M, Constantinidou C, Palmer T, Pallen MJ.** 2017. The Enigmatic Esx Proteins: Looking Beyond Mycobacteria. Trends Microbiol **25:**192-204.

53. **Cao Z, Casabona MG, Kneuper H, Chalmers JD, Palmer T.** 2016. The type VII secretion system of Staphylococcus aureus secretes a nuclease toxin that targets competitor bacteria. Nat Microbiol **2:**16183.

54. **Beasley FC, Marolda CL, Cheung J, Buac S, Heinrichs DE.** 2011. Staphylococcus aureus transporters Hts, Sir, and Sst capture iron liberated from human transferrin by Staphyloferrin A, Staphyloferrin B, and catecholamine stress hormones, respectively, and contribute to virulence. Infect Immun **79:**2345-2355.

55. **Hammer ND, Skaar EP.** 2011. Molecular mechanisms of Staphylococcus aureus iron acquisition. Annu Rev Microbiol **65:**129-147.

56. **Stauff DL, Skaar EP.** 2009. The heme sensor system of Staphylococcus aureus. Contrib Microbiol **16:**120-135.

57. **Sheldon JR, Heinrichs DE.** 2015. Recent developments in understanding the iron acquisition strategies of gram positive pathogens. FEMS Microbiol Rev **39:**592-630.

58. **Speziali CD, Dale SE, Henderson JA, Vines ED, Heinrichs DE.** 2006. Requirement of Staphylococcus aureus ATP-binding cassette-ATPase FhuC for iron-restricted growth and evidence that it functions with more than one iron transporter. J Bacteriol **188:**2048-2055.

59. **Zapotoczna M, Jevnikar Z, Miajlovic H, Kos J, Foster TJ.** 2013. Iron-regulated surface determinant B (IsdB) promotes Staphylococcus aureus adherence to and internalization by non-phagocytic human cells. Cell Microbiol **15:**1026-1041.

60. **Tong SY, Davis JS, Eichenberger E, Holland TL, Fowler VG, Jr.** 2015. Staphylococcus aureus infections: epidemiology, pathophysiology, clinical manifestations, and management. Clin Microbiol Rev **28:**603-661.

61. **Wertheim HF, Melles DC, Vos MC, van Leeuwen W, van Belkum A, Verbrugh HA, Nouwen JL.** 2005. The role of nasal carriage in Staphylococcus aureus infections. Lancet Infect Dis **5:**751-762.

62. **Coates R, Moran J, Horsburgh MJ.** 2014. Staphylococci: colonizers and pathogens of human skin. Future Microbiol **9:**75-91.

63. **Andrews JI, Fleener DK, Messer SA, Kroeger JS, Diekema DJ.** 2009. Screening for Staphylococcus aureus carriage in pregnancy: usefulness of novel sampling and culture strategies. Am J Obstet Gynecol **201:**396 e391-395.

64. **Carey AJ, Duchon J, Della-Latta P, Saiman L.** 2010. The epidemiology of methicillin-susceptible and methicillin-resistant Staphylococcus aureus in a neonatal intensive care unit, 2000-2007. J Perinatol **30:**135-139.

65. **Pinter DM, Mandel J, Hulten KG, Minkoff H, Tosi MF.** 2009. Maternal-infant perinatal transmission of methicillin-resistant and methicillin-sensitive Staphylococcus aureus. Am J Perinatol **26:**145-151.

66. **Holtfreter S, Kolata J, Broker BM.** 2010. Towards the immune proteome of Staphylococcus aureus - The anti-S. aureus antibody response. Int J Med Microbiol **300:**176-192.

67. **Krishna S, Miller LS.** 2012. Innate and adaptive immune responses against Staphylococcus aureus skin infections. Semin Immunopathol **34:**261-280.

68. **Segal AW.** 2005. How neutrophils kill microbes. Annu Rev Immunol **23:**197-223.

69. **Kim MH, Granick JL, Kwok C, Walker NJ, Borjesson DL, Curry FR, Miller LS, Simon SI.** 2011. Neutrophil survival and c-kit(+)-progenitor proliferation in Staphylococcus aureus-infected skin wounds promote resolution. Blood **117:**3343-3352.

70. **Brinkmann V, Reichard U, Goosmann C, Fauler B, Uhlemann Y, Weiss DS, Weinrauch Y, Zychlinsky A.** 2004. Neutrophil extracellular traps kill bacteria. Science **303:**1532-1535.

71. **Pilsczek FH, Salina D, Poon KK, Fahey C, Yipp BG, Sibley CD, Robbins SM, Green FH, Surette MG, Sugai M, Bowden MG, Hussain M, Zhang K, Kubes P.** 2010. A novel

mechanism of rapid nuclear neutrophil extracellular trap formation in response to Staphylococcus aureus. J Immunol **185:**7413-7425.

72. **Parlet CP, Kavanaugh JS, Crosby HA, Raja HA, El-Elimat T, Todd DA, Pearce CJ, Cech NB, Oberlies NH, Horswill AR.** 2019. Apicidin Attenuates MRSA Virulence through Quorum-Sensing Inhibition and Enhanced Host Defense. Cell Rep **27:**187-198 e186.

73. **Anderson LS, Reynolds MB, Rivara KR, Miller LS, Simon SI.** 2019. A Mouse Model to Assess Innate Immune Response to Staphylococcus aureus Infection. J Vis Exp doi:10.3791/59015.

74. **Miller LS, Simon SI.** 2018. Neutrophils in hot pursuit of MRSA in the lymph nodes. Proc Natl Acad Sci U S A **115:**2272-2274.

75. **Molne L, Verdrengh M, Tarkowski A.** 2000. Role of neutrophil leukocytes in cutaneous infection caused by Staphylococcus aureus. Infect Immun **68:**6162-6167.

76. **Carey AJ, Tan CK, Mirza S, Irving-Rodgers H, Webb RI, Lam A, Ulett GC.** 2014. Infection and cellular defense dynamics in a novel 17beta-estradiol murine model of chronic human group B streptococcus genital tract colonization reveal a role for hemolysin in persistence and neutrophil accumulation. J Immunol **192:**1718-1731.

77. **Richardson JP, Willems HME, Moyes DL, Shoaie S, Barker KS, Tan SL, Palmer GE, Hube B, Naglik JR, Peters BM.** 2018. Candidalysin Drives Epithelial Signaling, Neutrophil Recruitment, and Immunopathology at the Vaginal Mucosa. Infect Immun **86**.

78. **Yano J, Noverr MC, Fidel PL, Jr.** 2017. Vaginal Heparan Sulfate Linked to Neutrophil Dysfunction in the Acute Inflammatory Response Associated with Experimental Vulvovaginal Candidiasis. MBio **8**.

79. **Soler-Garcia AA, Jerse AE.** 2007. Neisseria gonorrhoeae catalase is not required for experimental genital tract infection despite the induction of a localized neutrophil response. Infect Immun **75:**2225-2233.

80. **Dunn DL, Simmons RL.** 1982. Fibrin in peritonitis. III. The mechanism of bacterial trapping by polymerizing fibrin. Surgery **92:**513-519.

81. **Kapral FA.** 1966. Clumping of Staphylococcus aureus in the peritoneal cavity of mice. J Bacteriol **92:**1188-1195.

82. **Hsieh JY, Smith TD, Meli VS, Tran TN, Botvinick EL, Liu WF.** 2017. Differential regulation of macrophage inflammatory activation by fibrin and fibrinogen. Acta Biomater **47:**14-24.

83. **Rubel C, Fernandez GC, Dran G, Bompadre MB, Isturiz MA, Palermo MS.** 2001. Fibrinogen promotes neutrophil activation and delays apoptosis. J Immunol **166:**2002-2010.

84. **Rubel C, Fernandez GC, Rosa FA, Gomez S, Bompadre MB, Coso OA, Isturiz MA, Palermo MS.** 2002. Soluble fibrinogen modulates neutrophil functionality through the activation of an extracellular signal-regulated kinase-dependent pathway. J Immunol **168:**3527-3535.

85. **Kwiecinski JM, Crosby HA, Valotteau C, Hippensteel JA, Nayak MK, Chauhan AK, Schmidt EP, Dufrene YF, Horswill AR.** 2019. Staphylococcus aureus adhesion in endovascular infections is controlled by the ArlRS-MgrA signaling cascade. PLoS Pathog **15:**e1007800.

86. **Walker JN, Crosby HA, Spaulding AR, Salgado-Pabon W, Malone CL, Rosenthal CB, Schlievert PM, Boyd JM, Horswill AR.** 2013. The Staphylococcus aureus ArlRS two-component system is a novel regulator of agglutination and pathogenesis. PLoS Pathog **9:**e1003819.

87. **Crosby HA, Schlievert PM, Merriman JA, King JM, Salgado-Pabon W, Horswill AR.** 2016. The Staphylococcus aureus Global Regulator MgrA Modulates Clumping and Virulence by Controlling Surface Protein Expression. PLoS Pathog **12:**e1005604.

88. **Cheng AG, McAdow M, Kim HK, Bae T, Missiakas DM, Schneewind O.** 2010. Contribution of coagulases towards Staphylococcus aureus disease and protective immunity. PLoS Pathog **6:**e1001036.

89. **Rothfork JM, Dessus-Babus S, Van Wamel WJ, Cheung AL, Gresham HD.** 2003. Fibrinogen depletion attenuates Staphyloccocus aureus infection by preventing density-dependent virulence gene up-regulation. J Immunol **171:**5389-5395.

90. **Kwiecinski J, Peetermans M, Liesenborghs L, Na M, Bjornsdottir H, Zhu X, Jacobsson G, Johansson BR, Geoghegan JA, Foster TJ, Josefsson E, Bylund J,**

Verhamme P, Jin T. 2016. Staphylokinase Control of Staphylococcus aureus Biofilm Formation and Detachment Through Host Plasminogen Activation. J Infect Dis **213:**139-148.

91. **Cheng AG, Kim HK, Burts ML, Krausz T, Schneewind O, Missiakas DM.** 2009. Genetic requirements for Staphylococcus aureus abscess formation and persistence in host tissues. FASEB J **23:**3393-3404.

92. **Skaar EP, Humayun M, Bae T, DeBord KL, Schneewind O.** 2004. Iron-source preference of Staphylococcus aureus infections. Science **305:**1626-1628.

93. **Sebulsky MT, Hohnstein D, Hunter MD, Heinrichs DE.** 2000. Identification and characterization of a membrane permease involved in iron-hydroxamate transport in Staphylococcus aureus. J Bacteriol **182:**4394-4400.

94. **Nairz M, Haschka D, Demetz E, Weiss G.** 2014. Iron at the interface of immunity and infection. Front Pharmacol **5:**152.

95. **Nairz M, Dichtl S, Schroll A, Haschka D, Tymoszuk P, Theurl I, Weiss G.** 2018. Iron and innate antimicrobial immunity-Depriving the pathogen, defending the host. J Trace Elem Med Biol **48:**118-133.

96. **Szafranska AK, Oxley AP, Chaves-Moreno D, Horst SA, Rosslenbroich S, Peters G, Goldmann O, Rohde M, Sinha B, Pieper DH, Loffler B, Jauregui R, Wos-Oxley ML, Medina E.** 2014. High-resolution transcriptomic analysis of the adaptive response of Staphylococcus aureus during acute and chronic phases of osteomyelitis. MBio **5**.

97. **Date SV, Modrusan Z, Lawrence M, Morisaki JH, Toy K, Shah IM, Kim J, Park S, Xu M, Basuino L, Chan L, Zeitschel D, Chambers HF, Tan MW, Brown EJ, Diep BA, Hazenbos WL.** 2014. Global gene expression of methicillin-resistant Staphylococcus aureus USA300 during human and mouse infection. J Infect Dis **209:**1542-1550.

98. **Kothary V, Doster RS, Rogers LM, Kirk LA, Boyd KL, Romano-Keeler J, Haley KP, Manning SD, Aronoff DM, Gaddy JA.** 2017. Group B Streptococcus Induces Neutrophil Recruitment to Gestational Tissues and Elaboration of Extracellular Traps and Nutritional Immunity. Front Cell Infect Microbiol **7:**19.

99. **Zygiel EM, Nolan EM.** 2018. Transition Metal Sequestration by the Host-Defense Protein Calprotectin. Annu Rev Biochem **87:**621-643.

100. **Jean S, Juneau RA, Criss AK, Cornelissen CN.** 2016. Neisseria gonorrhoeae Evades Calprotectin-Mediated Nutritional Immunity and Survives Neutrophil Extracellular Traps by Production of TdfH. Infect Immun **84:**2982-2994.

101. **Diaz-Ochoa VE, Jellbauer S, Klaus S, Raffatellu M.** 2014. Transition metal ions at the crossroads of mucosal immunity and microbial pathogenesis. Front Cell Infect Microbiol **4:**2.

102. **Novick RP.** 1991. Genetic systems in staphylococci. Methods Enzymol **204:**587-636.

103. **Wormann ME, Reichmann NT, Malone CL, Horswill AR, Grundling A.** 2011. Proteolytic cleavage inactivates the Staphylococcus aureus lipoteichoic acid synthase. J Bacteriol **193:**5279-5291.

104. **Nair D, Memmi G, Hernandez D, Bard J, Beaume M, Gill S, Francois P, Cheung AL.** 2011. Whole-genome sequencing of Staphylococcus aureus strain RN4220, a key laboratory strain used in virulence research, identifies mutations that affect not only virulence factors but also the fitness of the strain. J Bacteriol **193:**2332-2335.

105. **Fey PD, Endres JL, Yajjala VK, Widhelm TJ, Boissy RJ, Bose JL, Bayles KW.** 2013. A genetic resource for rapid and comprehensive phenotype screening of nonessential Staphylococcus aureus genes. MBio **4:**e00537-00512.

106. **Olson ME.** 2016. Bacteriophage Transduction in Staphylococcus aureus. Methods Mol Biol **1373:**69-74.

107. **Ibberson CB, Parlet CP, Kwiecinski J, Crosby HA, Meyerholz DK, Horswill AR.** 2016. Hyaluronan Modulation Impacts Staphylococcus aureus Biofilm Infection. Infect Immun **84:**1917-1929.

108. **Livak KJ, Schmittgen TD.** 2001. Analysis of relative gene expression data using real-time quantitative PCR and the 2(-Delta Delta C(T)) Method. Methods **25:**402-408.

Chapter 5

CONCLUSIONS

Streptococcus agalactiae (Group B *Streptococcus* [GBS]) colonizes the vaginal tract of up to 22% of women. GBS can cause serious complications during pregnancy such as chorioamnionitis, preterm birth, and stillbirth. Women who are colonized by GBS can transmit the pathogen to the newborn during birth and, currently, GBS is a leading cause of neonatal pneumonia, sepsis, and meningitis (1-3). Also, epidemiological studies have indicated that vaginal carriage of GBS is associated with colonization by other pathogens such as *Staphylcococcus aureus* (4, 5). Intrapartum antibiotic prophylaxis (IAP) has lowered the incidence of GBS pneumonia and sepsis, but has so far been ineffective at reducing the rates of meningitis in newborns (6). Moreover, IAP may not be effective at preventing transmission of other pathogens that co-colonize the vaginal tract along with GBS. Additionally, the screening and IAP approach to preventing GBS disease comes with several caveats. GBS vaginal colonization can be constant or intermittent, making culture-based screening strategies incapable of identifying all women colonized by GBS during labor as some may have acquired the pathogen after 37 weeks of pregnancy (7). Rapid test screening strategies that rely on PCR based technologies are meant to address this limitation of culture-based screening, however, these are not 100% sensitive and are logistically challenging to implement in the clinical setting (8, 9). Furthermore, the increasing prevalence of antibiotic resistance is a world-wide public health concern (10). While resistance to penicillin is rare for GBS, resistance to other antibiotics is becoming increasingly common, which is a problem for women who are allergic to β-lactams (11, 12). All of these problems highlight the need for better therapeutics to combat neonatal GBS infections and the importance of continued investigation into factors that govern GBS colonization and disease. This final chapter summarizes

the key findings of the dissertation and highlights avenues for future research into GBS pathogenesis.

SUMMARY OF RESULTS

Discovery of a direct interaction between the GBS adhesin, BspC, and the host endothelial surface factor, vimentin, which promotes the pathogenesis of meningitis.

While a previous study had examined the importance of BspC in the context of polymicrobial interactions during vaginal colonization, no one had investigated whether BspC impacts meningitis before this dissertation work (13). Because meningitis is an inflammatory condition that occurs when bacteria have infiltrated brain endothelial barriers, we hypothesized that BspC, an inflammatory adhesin, could play a very important role in the progression of this disease. We determined that BspC impacts bacterial attachment to hCMEC, and that Δ*bspC* mutants were severely attenuated in our *in vivo* meningitis model (Chapter 2. Figures 2.2 and 2.3). Examination of brain tissue from GBS infected mice showed that those challenged with the Δ*bspC* mutant had lower bacterial loads, fewer inflammatory infiltrates, and lower KC and IL-6 cytokine levels compared to the brains of WT infected mice (Chapter 2. Figure 2.3). We further determined that BspC protein was both necessary and sufficient to stimulate the production of the neutrophil recruiting chemokines IL-8 and CXCL-1, likely through the NF-κB inflammatory signaling pathway (Chapter 2. Figure 2.4).

In a previous study, BspC was shown to mediate bacterial interactions with the extracellular matrix component fibrinogen (14). However, a main goal of this dissertation was to identify a receptor for BspC that is expressed on the endothelial cell membrane. To accomplish this, we performed far western blot analysis of hCMEC membrane proteins, probing with purified

BspC. We observed that BspC interacted specifically with one hCMEC membrane protein, and mass spectrometry analysis identified this protein to be vimentin. We further confirmed a direct interaction between BspC and vimentin using a bacterial two-hybrid assay, microscale thermophoresis, immunofluorescent staining, and imaging flow cytometry (Chapter 2. Figures 2.5 and 2.6). Experiments utilizing specific monoclonal antibodies that recognize either the N-terminal or C-terminal of vimentin revealed that the interaction between BspC and vimentin was dependent on the C-terminal "tail" domain of vimentin (Chapter 2. Figure 2.7). Lastly, we showed that vimentin KO mice were less susceptible to GBS infection and had increased survival, lower brain bacterial load, and lower brain cytokine levels compared to WT mice (Chapter 2. Figure 2.8). These findings are the first to show that an interaction between a GBS adhesin and an endothelial protein influences the progression of meningitis disease by affecting bacterial dissemination into the brain as well as host immune signaling.

LtdR regulation impacts GBS meningitis and colonization states by affecting bacterial invasion and immune stimulation.

The role of the LtdR two-component transcriptional regulator in influencing GBS disease progression was unknown prior to this dissertation. LtdR contains the LytTR non-HTH DNA-binding domain which is predominantly found in regulators of bacterial virulence mechanisms, therefore we chose to investigate the impact of LtdR on GBS pathogenesis (15). In our murine model of hematogenous meningitis, we observed that the Δ*ltdR* mutant was hypervirulent compared to WT GBS; mice infected with the Δ*ltdR* mutant had higher brain bacterial loads as well as increased neutrophil presence in the meninges (Chapter 3. Figure 3.3). In contrast, we saw that the Δ*ltdR* mutant was much less persistent compared to WT GBS in our mouse vaginal

colonization model (Chapter 3. Figure 3.6). Using human cerebral microvascular endothelial cells (hCMEC) and human vaginal epithelial cells (hVEC), we determined that the Δ*ltdR* mutant was more invasive and more inflammatory than WT GBS and induced significantly higher production of IL-8, CXCL-1, and IL-6 (Chapter 3. Figures 3.4, 3.5, and 3.6). The increased capacity of the Δ*ltdR* mutant to cause inflammation likely accounts for the seemingly contradictory phenotypes that we observed in our *in vivo* models of GBS invasive disease and asymptomatic colonization. Previous work has shown that hyper-inflammatory GBS strains are more virulent in models of meningitis disease because the host immune response can exacerbate neuronal injury and tissue damage (16, 17). However, in the context of asymptomatic colonization, hyper-inflammatory strains are less persistent because stimulation of host immune defenses results in bacterial clearance (18).

To identify potential LtdR regulated factors that might contribute to the hyper-invasive and hyper-inflammatory phenotypes observed for the Δ*ltdR* mutant, we compared the transcriptional profiles of WT GBS and the isogenic Δ*ltdR* mutant by performing RNA sequencing. We analyzed samples collected during early-log, mid-log, and stationary culture growth phases, and observed global transcriptional changes between the two strains at all three time points, with the majority of the significant transcriptional changes occurring during stationary phase (Chapter 3. Figure 237). A total of 135 genes were upregulated and 109 genes were downregulated in the Δ*ltdR* mutant compared to WT. Interestingly, there was not much overlap in up-regulated or down-regulated genes between the three time points; there was only one hit which was more abundant in WT cultures and also only one hit which was more abundant in Δ*ltdR* mutant cultures for all three growth phases (Chapter 3. Figure 3.7). Both of those genes encode proteins involved in methionine metabolism. The transcript increased in WT GBS at all time points encodes a bifunctional

homocysteine *S*-methyltransferase/methylenetetrahydrofolate reductase, which is the rate-limiting enzyme in the methyl cycle where homocysteine is remethylated to produce methionine (19). The transcript increased in the Δ*ltdR* mutant at all time points encodes the MtaR transcriptional regulator, which increases the expression of methionine uptake genes (20, 21). We also observed that gene encoding the pore-forming toxin hemolysin III was one of the most highly upregulated by the Δ*ltdR* mutant at the first two time points. The results of our studies using *in vivo* and *in vitro* infection models and the RNA sequencing analysis suggest that LtdR may regulate diverse cellular pathways, including those involved in methionine metabolism and uptake as well as virulence.

Development of a MRSA murine model of vaginal colonization.

Staphylococcus aureus is another common inhabitant of the vaginal tract, and has been reported to colonize up to 22% of pregnant women. Compared to antibiotic sensitive strains, methicillin-resistant *S. aureus* (MRSA) strains are especially problematic because they cause infections that are harder and more expensive to treat, and about 4% of pregnant women are colonized by MRSA (22-24). Epidemiological reports suggest that there may an increased rate of *S. aureus*, including MRSA, colonization in GBS-positive women (23, 25, 26). Similar to GBS, vertical transmission of the pathogen from the colonized mother is a likely route of neonatal MRSA acquisition (24, 25). Characterizing the interaction between GBS and *S. aureus* in the vaginal environment would be of interest as these two microbes co-exist in the vagina and can be transmitted to the newborn with devastating consequences. While a lot of research has focused on vaginal colonization by GBS, essentially nothing was known about vaginal colonization by *S. aureus* prior to the work in this dissertation. The necessary first step to performing these studies is the development of methods for investigating MRSA vaginal colonization.

This dissertation describes for the first time an *in vivo* mammalian model for MRSA vaginal colonization. We adapted our murine model of GBS vaginal carriage and showed that different MRSA strains can persist within the mouse vagina and that MRSA can be detected in the vaginal lumen as well as the cervical and uterine tissues (Chapter 4. Figure 4.1). We found that neutrophils are recruited to the vaginal tissue during MRSA colonization, appearing in the vaginal lamina propria just one-day post-inoculation and infiltrating into the lumen by three-days post-inoculation (Chapter 4. Figure 4.2). It has been previously shown that GBS interacts with fibrinogen (Fg) to promote persistence in the vagina (27). Using our new model, we demonstrated that the same is true for MRSA; a mutant lacking all Fg-binding adhesins was cleared from the mouse vagina significantly faster than WT MRSA (Chapter 4. Figure 4.3). In order to identify other determinants of MRSA vaginal colonization, we performed RNA-sequencing on MRSA growing *in vivo* that we recovered from the mouse 5 hours, 1-day, and 3-days post-inoculation and observed a lot of overlap in the differentially expressed genes for these three time points (Chapter 4. Figure 4.4). Because the most highly significantly differentially expressed transcripts were in iron-homeostasis pathways, we followed up specifically with those. We utilized our *in vivo* colonization model to confirm that MRSA mutants deficient in siderophore transport or heme uptake were less able to colonize the vagina compared to WT MRSA (Chapter 4. Figure 4.5). These findings are novel because we are the first to show that the proper response to iron-limitation is necessary for bacterial persistence in the vagina. Additionally, we have established and characterized an *in vivo* model of MRSA vaginal colonization which can be utilized for future investigations into MRSA-GBS interactions within this environment.

FUTURE STUDIES

Follow-up studies based on discoveries from this dissertation.

There are several key discoveries made in this dissertation that warrant further investigation. One of the major findings of this dissertation work is that the GBS adhesin BspC and the host endothelial receptor vimentin interact directly during the pathogenesis of meningitis. Additionally, our RNA-sequencing analysis of the hyper-invasive, hyper-inflammatory Δ*ltdR* GBS mutant has identified potential novel virulence factors that have not been studied in the context of GBS disease before. Lastly, we have developed a mouse model for MRSA vaginal colonization which can be utilized to investigate general mechanisms of *S. aureus* interactions with the host in a mucosal environment. In our characterization MRSA transcriptional changes during colonization, we identified numerous significantly upregulated transcripts which warrant further investigation. Finally, now that we have established a protocol for examining MRSA vaginal colonization, an obvious next step is to study GBS and MRSA co-colonization using the *in vivo* mouse model.

Further characterize the impact of the BspC-vimentin interaction on immune signaling.

The findings of this dissertation demonstrate that the inflammatory impact of BspC is mediated, at least in part, through the NF-κB signaling pathway. However, the exact mechanisms of how this occurs are still unclear. We found that vimentin KO mice have lower brain cytokine levels than WT mice during GBS infection, but this may be due to decreased bacterial dissemination into tissues. Our data shows that the interaction between BspC and vimentin contribute to bacterial adherence to brain endothelial cells, but it is still unknown if vimentin is also necessary for inflammatory signaling. Vimentin can bind to NOD2 at the surface of cells, and

it has been hypothesized that vimentin can mediate an interaction between NOD2 and bacterial pathogens to activate NF-κB signaling (28-30). Detailed *in vitro* experiments dissecting the mechanisms of NF-κB activation are necessary to confirm whether vimentin is involved in BspC-mediated inflammatory signaling and what its role may be. One useful tool to develop for these assays is a vimentin knock out hCMEC line. Additionally, the NF-κB luciferase reporter construct can be transfected into that cell line. Using these tools, we can assess whether hCMEC that lack vimentin still respond to GBS infection by signaling through the NF-κB pathway or if only bacterial attachment is affected by the loss of vimentin.

Determine if BspC interacts with vimentin during GBS vaginal colonization.

Vimentin is typically expressed by endothelial and other mesenchymal cells, and is not normally found in epithelial cells (31). However, vimentin can be expressed by epithelial cells under some conditions, and the presence of vimentin in epithelium is regarded as a canonical marker of the cellular process known as epithelial to mesenchymal transition (EMT) (32). This is a fundamental process for proper development in multicellular organisms, but it can also be pathogenic. The role of EMT in the progression of cancer has been well studied and it is known to contribute to the dissemination of carcinoma cells from the primary tumor (33). Recently, GBS was found to induce EMT during vaginal colonization and this process caused breakdown of the endothelial barrier which led to bacterial infiltration and infection of the upper reproductive tract tissues (34). As this work indicates that the vaginal epithelium upregulates vimentin expression during exposure to GBS, it is therefore possible that the BspC adhesin could interact with vimentin to promote vaginal persistence and ascending infection. Continued investigation into whether BspC contributes to adherence to vaginal epithelium is warranted. Additionally, it would be

interesting to determine whether blocking the interaction between BspC and vimentin can reduce vaginal colonization or ascending GBS infection into the cervical and uterine tissues.

Identify the domain of BspC that mediates the interaction with vimentin.

For this dissertation, full-length BspC protein was utilized to show an interaction with vimentin. While we predict that binding to vimentin is mediated by the V-domain of BspC, as that region is projected furthest away from the bacterial cell surface, we have not examined this experimentally. Also, other domains of Streptococcal AgI/II proteins have been demonstrated to mediate the interaction with their binding partners. For example, the A-region (alanine-rich repeats) of *S. mutans* SpaP binds to collagen and the C-terminal of *S. gordonni* SspB interacts with *Porphyromonas ginigivalis* (35). To show that the V-domain of BspC binds to vimentin, we can express and purify just the V-domain and measure the binding affinity of BspC V-domain and vimentin using microscale thermophoresis (MST). If the V-domain does indeed bind to vimentin, the next step in this research would be to identify the binding site. We can predict potential V-domain binding sites based on sequence homologies with other AgI/II proteins and make point mutations to determine the regions that are essential for the interaction with vimentin. These experiments would expand our understanding of how BspC engages cell-surface vimentin.

Intravital imaging to visualize WT and Δ*bspC* mutant attachment to cerebral endothelial cells *in vivo.*

In recent years, state-of-the-art microscopy techniques to image mouse meningeal blood vessels have been developed. However, these imaging methods have never been utilized in combination with a mouse hematogenous meningitis model. In this dissertation we have shown

that BspC and vimentin impact the ultimate outcome of meningitis disease, but have not examined earlier time points during *in vivo* infection. Intravital imaging can be utilized to study disease progression from the initiation of infection until the endpoint. For intravital imaging of meningeal blood vessels, first a craniotomy is performed and a coverslip is placed over the exposed meninges to create a cranial window. This cranial window is stable and the meningeal microcirculation can be imaged for many days after it is implanted (36, 37). After the placement of the brain windows, we can infect mice with fluorescently labeled WT or Δ*bspC* GBS and visualize their interaction with the meningeal blood vessels in real-time. Additionally, we can also perform this procedure with vimentin knock out mice. The results of these experiments would further our understanding of the dynamics of meningitis disease progression.

Examine the importance of the LtdR regulated factors hemolysin III and MtaR in GBS meningitis and vaginal colonization.

One of the noteworthy hits that came out of our LtdR RNA sequencing analysis was hemolysin III. Both the gene which encodes hemolysin III (*hlyIII*, GBSCOH1_1179) and its putative regulator (GBSCOH1_1178) where upregulated in the Δ*ltdR* mutant compared to WT GBS. Interestingly, a recent study from our group where we assessed the role of Cas9 in GBS virulence showed that hemolysin III expression was also highly dysregulated in a Δ*cas9* mutant (38). Hemolysin III has been studied in *Virbrio vulnificus* and *Bacillus cereus*, and in those bacteria it has been characterized as a pore-forming toxin with specificity for human erythrocytes (39, 40). The protozoan parasite *Plasmodium falciparum*, which is the causative agent of malaria, also has a hemolysin III homolog that possesses red blood cell lysis activity (41). It would be interesting to determine if hemolysin III could be responsible for the hyper-invasive and hyper-inflammatory

phenotype that we observed in the Δ*ltdR* mutant GBS strain. We reported that the Δ*ltdR* mutant was not more hemolytic than WT GBS, but those assays were performed using sheep blood. One experiment that may yield informative results is deleting the *hlyIII* gene in the Δ*ltdR* mutant strain and assessing whether its hyper-virulence is attenuated.

Another interesting finding from our LtdR RNA sequencing study was that methionine uptake pathways were differentially regulated in the Δ*ltdR* mutant GBS strain. While WT GBS had increased expression of an enzyme that is critical for methionine synthesis, the Δ*ltdR* mutant upregulated expression of MtaR. MtaR is a regulator that increases the expression of methionine uptake pathways, and it has been shown to contribute to GBS survival in a neonatal-rat sepsis model (20, 42). As with hemolysin III, it would be interesting to delete the *mtaR* gene in the Δ*ltdR* mutant GBS background to determine if the Δ*ltdR* mutant is rendered less virulent. These investigations would further define the mechanisms of how LtdR regulation influences colonization and meningitis.

Investigate the impact of nutritional immunity on vaginal colonization by GBS and MRSA.

Nutritional immunity is a host defense mechanism where pathogens are deprived of necessary nutrients. The term was originally applied to iron limitation, which the host accomplishes with iron-binding complexes such as lactoferrin, transferrrin, hemoglobin, and haptoglobin (43-46). Currently the definition of nutritional immunity has been expanded to include the restriction of other transition metals, such as manganese and zinc, as well as nonmetal nutrients, like amino acids (47). Our MRSA RNA sequencing results show that *S. aureus* experiences iron-limitation during vaginal colonization and responds by upregulating iron-acquisition pathways. Additionally, we performed ICP-MS to verify that vaginal lavage fluid contains much less iron

than culture medium that is used to grow bacteria under laboratory conditions. Quantification of manganese and zinc levels in vaginal lavage fluid by ICP-MS would reveal whether those metals are also limited in the vaginal environment.

This dissertation includes RT-qPCR data showing differential expression of iron-homeostasis genes in MRSA incubated in vaginal lavage fluid compared to bacteria cultured in tryptic soy broth. Similar analyses can be performed to examine genes involved in the uptake of other transition metals and the results from those experiments would also uncover which metals are restricted to MRSA in the vaginal environment. Lastly, these same methods can be used to investigate how GBS alters its gene expression in response to nutritional limitation during vaginal colonization. It would be interesting to compare how nutritional immunity impacts MRSA and GBS as there is potential to find common pathways to target for therapeutic interventions.

Characterize GBS and MRSA co-colonization.

The mouse model for MRSA vaginal colonization that was developed for this dissertation work was utilized successfully to identify key determinants of MRSA persistence in the vagina. The next step in this research is to examine GBS and MRSA co-colonization. To investigate whether the presence of GBS can promote MRSA persistence in the vagina, mice can be inoculated with MRSA or a mix of both GBS and MRSA and monitored for clearance of MRSA over time.

In this dissertation, it was determined that MRSA binding to fibrinogen is important for persistent colonization using both *in vitro* and *in vivo* methods. This is an interesting observation because GBS also interacts with fibrinogen to promote colonization of the vagina (27). Fibrinogen is a large, linear protein composed of two identical end nodules that are joined by a central domain (48). Previous work has shown that *S. aureus* can interact with the end nodules of fibrinogen to

form clumps (49-51). Therefore, it is worth investigating whether fibrinogen can act as a molecular bridge to facilitate interactions between MRSA and GBS during vaginal colonization. This question can be answered with a microscopy based approach where mice are co-inoculated with GBS and MRSA strains expressing different fluorescent proteins (e.g. GFP and DsRed). We can then collect the vaginal tissues for histological processing and perform fluorescence microscopy to visualize GBS and MRSA. To assess whether GBS and MRSA only co-aggregate in the presence of fibrinogen, the same procedure can be repeated with fibrinogen deficient mice.

In conclusion, the focus of this dissertation was to investigate how GBS is able to successfully colonize the healthy host asymptomatically as well as transition to an invasive pathogen in the susceptible newborn. I have characterized the interaction between BspC and its endothelial receptor vimentin, demonstrating that this interaction is important for both GBS attachment to endothelial cells and stimulation of host immune responses during meningitis. I have shown that LtdR regulates numerous bacterial processes and this regulation can impact both vaginal colonization and meningitis disease. Finally, I have established an *in vivo* model of MRSA vaginal colonization which will be essential to future investigations into GBS and MRSA co-colonization of the vaginal tract. The discoveries in this dissertation contribute to our current understanding of GBS pathogenesis and provide new avenues for research which will ultimately inform the development of more successfully therapies to prevent GBS disease.

REFERENCES

1. **Doran KS, Nizet V.** 2004. Molecular pathogenesis of neonatal group B streptococcal infection: no longer in its infancy. Mol Microbiol **54:**23-31.

2. **Vornhagen J, Adams Waldorf KM, Rajagopal L.** 2017. Perinatal Group B Streptococcal Infections: Virulence Factors, Immunity, and Prevention Strategies. Trends Microbiol doi:10.1016/j.tim.2017.05.013.

3. **Davies HG, Carreras-Abad C, Le Doare K, Heath PT.** 2019. Group B Streptococcus: Trials and Tribulations. Pediatr Infect Dis J **38:**S72-S76.

4. **Chen KT, Huard RC, Della-Latta P, Saiman L.** 2006. Prevalence of methicillin-sensitive and methicillin-resistant Staphylococcus aureus in pregnant women. Obstet Gynecol **108:**482-487.

5. **Kubota T, Nojima M, Itoh S.** 2002. Vaginal bacterial flora of pregnant women colonized with group B streptococcus. J Infect Chemother **8:**326-330.

6. **Nanduri SA, Petit S, Smelser C, Apostol M, Alden NB, Harrison LH, Lynfield R, Vagnone PS, Burzlaff K, Spina NL, Dufort EM, Schaffner W, Thomas AR, Farley MM, Jain JH, Pondo T, McGee L, Beall BW, Schrag SJ.** 2019. Epidemiology of Invasive Early-Onset and Late-Onset Group B Streptococcal Disease in the United States, 2006 to 2015: Multistate Laboratory and Population-Based Surveillance. JAMA Pediatr **173:**224-233.

7. **Kwatra G, Adrian PV, Shiri T, Buchmann EJ, Cutland CL, Madhi SA.** 2014. Serotype-specific acquisition and loss of group B streptococcus recto-vaginal colonization in late pregnancy. PLoS One **9:**e98778.

8. **Akker-van Marle ME, Rijnders ME, Dommelen P, Fekkes M, Wouwe JP, Amelink-Verburg MP, Verkerk PH.** 2005. Cost-effectiveness of different treatment strategies with intrapartum antibiotic prophylaxis to prevent early-onset group B streptococcal disease. BJOG **112:**820-826.

9. **Hakansson S, Kallen K, Bullarbo M, Holmgren PA, Bremme K, Larsson A, Norman M, Noren H, Ortmark-Wrede C, Pettersson K, Saltvedt S, Sondell B, Tokarska M, von Vultee A, Jacobsson B.** 2014. Real-time PCR-assay in the delivery suite for determination of group B streptococcal colonization in a setting with risk-based antibiotic prophylaxis. J Matern Fetal Neonatal Med **27:**328-332.

10. **Munita JM, Arias CA.** 2016. Mechanisms of Antibiotic Resistance. Microbiol Spectr **4**.

11. **Kimura K, Suzuki S, Wachino J, Kurokawa H, Yamane K, Shibata N, Nagano N, Kato H, Shibayama K, Arakawa Y.** 2008. First molecular characterization of group B streptococci with reduced penicillin susceptibility. Antimicrob Agents Chemother **52:**2890-2897.

12. **Mulla ZD, Ebrahim MS, Gonzalez JL.** 2010. Anaphylaxis in the obstetric patient: analysis of a statewide hospital discharge database. Ann Allergy Asthma Immunol **104:**55-59.

13. **Pidwill GR, Rego S, Jenkinson HF, Lamont RJ, Nobbs AH.** 2018. Coassociation between Group B Streptococcus and Candida albicans Promotes Interactions with Vaginal Epithelium. Infect Immun **86**.

14. **Chuzeville S, Dramsi S, Madec JY, Haenni M, Payot S.** 2015. Antigen I/II encoded by integrative and conjugative elements of Streptococcus agalactiae and role in biofilm formation. Microb Pathog **88:**1-9.

15. **Galperin MY.** 2008. Telling bacteria: do not LytTR. Structure **16:**657-659.

16. **Doran KS, Chang JC, Benoit VM, Eckmann L, Nizet V.** 2002. Group B streptococcal beta-hemolysin/cytolysin promotes invasion of human lung epithelial cells and the release of interleukin-8. J Infect Dis **185:**196-203.

17. **Kim KS.** 2003. Pathogenesis of bacterial meningitis: from bacteraemia to neuronal injury. Nat Rev Neurosci **4:**376-385.

18. **Patras KA, Wang NY, Fletcher EM, Cavaco CK, Jimenez A, Garg M, Fierer J, Sheen TR, Rajagopal L, Doran KS.** 2013. Group B Streptococcus CovR regulation modulates host immune signalling pathways to promote vaginal colonization. Cell Microbiol **15:**1154-1167.

19. **Miller AL.** 2003. The methionine-homocysteine cycle and its effects on cognitive diseases. Altern Med Rev **8:**7-19.

20. **Bryan JD, Liles R, Cvek U, Trutschl M, Shelver D.** 2008. Global transcriptional profiling reveals Streptococcus agalactiae genes controlled by the MtaR transcription factor. BMC Genomics **9:**607.

21. **Kovaleva GY, Gelfand MS.** 2007. Transcriptional regulation of the methionine and cysteine transport and metabolism in streptococci. FEMS Microbiol Lett **276:**207-215.

22. **Lee BY, Singh A, David MZ, Bartsch SM, Slayton RB, Huang SS, Zimmer SM, Potter MA, Macal CM, Lauderdale DS, Miller LG, Daum RS.** 2013. The economic burden of community-associated methicillin-resistant Staphylococcus aureus (CA-MRSA). Clin Microbiol Infect **19:**528-536.

23. **Andrews WW, Schelonka R, Waites K, Stamm A, Cliver SP, Moser S.** 2008. Genital tract methicillin-resistant Staphylococcus aureus: risk of vertical transmission in pregnant women. Obstet Gynecol **111:**113-118.

24. **Lin J, Yao Z.** 2018. Maternal-Infant Correlation of Multidrug-Resistant Staphylococcus aureus Carriage: A Prospective Cohort Study. Front Pediatr **6:**384.

25. **Top KA, Huard RC, Fox Z, Wu F, Whittier S, Della-Latta P, Saiman L, Ratner AJ.** 2010. Trends in methicillin-resistant Staphylococcus aureus anovaginal colonization in pregnant women in 2005 versus 2009. J Clin Microbiol **48:**3675-3680.

26. **Chen KT, Campbell H, Borrell LN, Huard RC, Saiman L, Della-Latta P.** 2007. Predictors and outcomes for pregnant women with vaginal-rectal carriage of community-associated methicillin-resistant Staphylococcus aureus. Am J Perinatol **24:**235-240.

27. **Wang NY, Patras KA, Seo HS, Cavaco CK, Rosler B, Neely MN, Sullam PM, Doran KS.** 2014. Group B streptococcal serine-rich repeat proteins promote interaction with fibrinogen and vaginal colonization. J Infect Dis **210:**982-991.

28. **Stevens C, Henderson P, Nimmo ER, Soares DC, Dogan B, Simpson KW, Barrett JC, International Inflammatory Bowel Disease Genetics C, Wilson DC, Satsangi J.** 2013. The intermediate filament protein, vimentin, is a regulator of NOD2 activity. Gut **62:**695-707.

29. **Chi F, Bo T, Wu CH, Jong A, Huang SH.** 2012. Vimentin and PSF act in concert to regulate IbeA+ E. coli K1 induced activation and nuclear translocation of NF-kappaB in human brain endothelial cells. PLoS One **7:**e35862.

30. **Mak TN, Bruggemann H.** 2016. Vimentin in Bacterial Infections. Cells **5**.

31. **Eriksson JE, Dechat T, Grin B, Helfand B, Mendez M, Pallari HM, Goldman RD.** 2009. Introducing intermediate filaments: from discovery to disease. J Clin Invest **119:**1763-1771.

32. **Satelli A, Li S.** 2011. Vimentin in cancer and its potential as a molecular target for cancer therapy. Cell Mol Life Sci **68:**3033-3046.

33. **Thiery JP.** 2002. Epithelial-mesenchymal transitions in tumour progression. Nat Rev Cancer **2:**442-454.

34. **Vornhagen J, Armistead B, Santana-Ufret V, Gendrin C, Merillat S, Coleman M, Quach P, Boldenow E, Alishetti V, Leonhard-Melief C, Ngo LY, Whidbey C, Doran KS, Curtis C, Waldorf KMA, Nance E, Rajagopal L.** 2018. Group B streptococcus exploits vaginal epithelial exfoliation for ascending infection. J Clin Invest **128:**1985-1999.

35. **Brady LJ, Maddocks SE, Larson MR, Forsgren N, Persson K, Deivanayagam CC, Jenkinson HF.** 2010. The changing faces of Streptococcus antigen I/II polypeptide family adhesins. Mol Microbiol **77:**276-286.

36. **Cabrales P, Carvalho LJ.** 2010. Intravital microscopy of the mouse brain microcirculation using a closed cranial window. J Vis Exp doi:10.3791/2184.

37. **Mostany R, Portera-Cailliau C.** 2008. A craniotomy surgery procedure for chronic brain imaging. J Vis Exp doi:10.3791/680.

38. **Spencer BL, Deng L, Patras KA, Burcham ZM, Sanches GF, Nagao PE, Doran KS.** 2019. Cas9 Contributes to Group B Streptococcal Colonization and Disease. Front Microbiol **10:**1930.

39. **Chen YC, Chang MC, Chuang YC, Jeang CL.** 2004. Characterization and virulence of hemolysin III from Vibrio vulnificus. Curr Microbiol **49:**175-179.

40. **Baida GE, Kuzmin NP.** 1996. Mechanism of action of hemolysin III from Bacillus cereus. Biochim Biophys Acta **1284:**122-124.

41. **Moonah S, Sanders NG, Persichetti JK, Sullivan DJ, Jr.** 2014. Erythrocyte lysis and Xenopus laevis oocyte rupture by recombinant Plasmodium falciparum hemolysin III. Eukaryot Cell **13:**1337-1345.

42. **Shelver D, Rajagopal L, Harris TO, Rubens CE.** 2003. MtaR, a regulator of methionine transport, is critical for survival of group B streptococcus in vivo. J Bacteriol **185:**6592-6599.

43. **Kochan I.** 1973. The role of iron in bacterial infections, with special consideration of host-tubercle bacillus interaction. Curr Top Microbiol Immunol **60:**1-30.

44. **Weinberg ED.** 1977. Infection and iron metabolism. Am J Clin Nutr **30:**1485-1490.

45. **Weinberg ED.** 1978. Iron and infection. Microbiol Rev **42:**45-66.

46. **Hammer ND, Skaar EP.** 2011. Molecular mechanisms of Staphylococcus aureus iron acquisition. Annu Rev Microbiol **65:**129-147.

47. **Palmer LD, Skaar EP.** 2016. Transition Metals and Virulence in Bacteria. Annu Rev Genet **50:**67-91.

48. **Mosesson MW.** 2005. Fibrinogen and fibrin structure and functions. J Thromb Haemost **3:**1894-1904.

49. **Walker JN, Crosby HA, Spaulding AR, Salgado-Pabon W, Malone CL, Rosenthal CB, Schlievert PM, Boyd JM, Horswill AR.** 2013. The Staphylococcus aureus ArlRS two-component system is a novel regulator of agglutination and pathogenesis. PLoS Pathog **9:**e1003819.

50. **Crosby HA, Schlievert PM, Merriman JA, King JM, Salgado-Pabon W, Horswill AR.** 2016. The Staphylococcus aureus Global Regulator MgrA Modulates Clumping and Virulence by Controlling Surface Protein Expression. PLoS Pathog **12:**e1005604.

51. **Crosby HA, Kwiecinski J, Horswill AR.** 2016. Staphylococcus aureus Aggregation and Coagulation Mechanisms, and Their Function in Host-Pathogen Interactions. Adv Appl Microbiol **96:**1-41.